6-2001

Evaluation of Some Organic Inhibitors for Stainless Steel Corrosion Using Different Electrochemical and Surface Techniques

Maryam Hassan Saeed Al-Hassan

Evaluation of Some Organic Inhibitors for Stainless Steel Corrosion Using Different Electrochemical and Surface Techniques

A Thesis Submitted to

The Deanship of Graduate Studies of the United Arab Emirates University

By

Maryam Hassan Saeed Al-Hassan

In Partial Fulfillment of the degree of

MSc

In

Materials Science and Engineering

June-2001

Supervision Committee Members

Prof. Dr. Rashid A. Al Saeed
Professor of Physical Chemistry
Department of Chemistry,
College of Science,
United Arab Emirates University

Dr. Ahmed Galal Helmy
Assistant Professor of Physical Chemistry
and Materials Chemistry
Department of Chemistry,
College of Science,
United Arab Emirates University

Examination Committee Members

Dr. Ahmed Saeed Al Shamsi
Assistant Professor of Physical Chemistry
and Corrosion Science
Department of Chemistry
College of Science,
United Arab Emirates University

Dr. Ali Noor Moosavi
Senior Corrosion Engineer
Abu Dhabi Company for Onshore
Oil Operations ADCO,
Abu Dhabi
United Arab Emirates

TABLE OF CONTENT

CHAPTER **Page**

AKNOWLEDGMENT----------I

ABSTRACT----------II

LIST OF TABLES----------III

LIST OF FIGURES----------V

LIST OF ABBRAVIATIONS AND SYMPOLS----------VIII

CHAPTER I (INTRODUCTION)

I-1 General introduction----------1

I-2 The electrochemistry of corrosion----------4

I-3 Mechanism of corroson inhibition by organic compounds----------7

I-4 Corrosion inhibition of steels methodologies and techniques--------11

I-5 Pitting corrosion of stainless steel----------18

I-6 Factors affecting the rate of corrosion and efficiency of inhibition--22

I-7 High-Grade steels----------31

I-9 Aim of the study----------33

CHAPTER II (EXPERIMENTAL WORK)

II-1 Materials and reagents----------36

II-1.1 Stainless steel sample----------36

II-1.2 Reagents and solutions preparation----------36

II-1.3 Electrode mounting and electrochemical cells----------38

II-2 Equipments and instruments----------41

II-2.1 Electrochemical equipments----------41

II-2.2 Surface instrumentation----------41

II-3 Solutions preparation and solvents----------42

II-4 Electrochemical measurements----------43

II-4.1 Potentiodynamic polarization measurements----------43

II-4.2 Polarization resistance measurements----------43

II-4.3 Tafel measurements----------44

II-4.4 EIS measurements----------44

II-5 Surface characterization----------45

II-5.1 Scanning electron microscopy----------46

II.5.2 Surface reflectance FT-IR spectroscopy----------46

CHAPTER III (RESULTS AND DISSCUSION)

III.1 Electrochemical measurements----------47

III-1.a Potentiodynamic behavior investigation----------47

III-1.b Effect of adding chloride ions----------51

III-1.c Effect of varying the concentration of inhibitor----------54

III-1.d Effect of varying the concentration of acid----------61

III-2 Effect of molecular structure on inhibition efficiency----------65

III-3 Temperature coefficient of corrosion inhibition----------86

III-4 Electrochemical impedance spectroscopy----------98

III-5 Surface measurements----------108

III-5.a Scanning electron microscopy----------108

III-5-b. Surface reflectance FT-IR----------107

CONCLUSION----------113

REFERENCE----------115

ARABIC SUMMARY

Acknowledgement

To those whom I hold respect, to the people who where behind me and gave me their support. To all of them I would like to say many thanks to you. Because without your help and support I would not been able to finish this study.

With my pleasure I would like to thank Prof. Dr. Rashid A. Alsaeed and Dr. Ahmed Galal Helmy, the supervision committee. Their guidance and support throughout this work is highly appreciable. Deanship and council of Graduate Studies. I extend my thanks and appreciation to the department of chemistry and college of science and United Arab Emirates University for the valuable effort.

Finally, I am grateful to my family and friends for standing with me and for their great support and advices.

Abstract

Stainless steels have been extensively used in automotive, industrial, electronics, etc., applications. Iron (Fe) and chromium (Cr) are the main elements with weight percentage contribution of 60-75% and 10-25% respectively. Other elements, such as Ni, Co, Mo, Mn, C etc. are also present with variable concentrations. The purpose of this work is to use different electrochemical and surface techniques to study the corrosion behavior of stainless steel type 316 (percent composition of different chemical elements are listed in table 1) in acid media in presence and absence of different thiophene derivatives (list of inhibitors in figure1). Moreover, other important goals were to study the effect of adding chloride ion to the acidic media on the corrosion behavior of stainless steel, protection efficiency of ihibitors studied, and to determine the temperature coefficient and the adsorption isotherm of the inhibitor on the stainless steel type 316.

Electrochemical techniques such as potentiodynamic polarization, Tafel experiments, polarization resistance and electrochemical spectroscopy were used to evaluate the effect of the inhibitors on the corrosion of stainless steel type 316. Surface analyses were employed to study the surface morphology and structural analysis of the surface using

scanning electron microscope(SEM), Fourier Transform infrared(FT-IR), and x-ray diffraction techniques EDAX.

The results showed distinct effects for the different inhibitors used that depend on the molecular structure and the electron density on the sulfur atom of the thiophene ring. The order of inhibition efficiency was 2-thiophene carboxylic hydrazide > 2-thiophene carboxylic acid > 3-thiophene caroxaldhyde > 2-acetyl thiophene. It was concluded that the inhibitors studied were of the mixed type.

The adsorption pattern for the inhibitors at the stainless steel surface followed a Langmuir isotherm model. The thermodynamic parameters of adsorption were calculated. It was concluded that a thin layer of inhibitor is formed at the surface of steel preventing the corrosion of the specimen in the acid medium. It was also suggested that anchoring of the sulfur atom of the thiophene ring to the surface of the stainless steel takes place that allowed a blanket of the inhibitor molecule to cover the surface.

Surface reflectance FT-IR proved the adsorption of the inhibitor molecule at the stainless steel surface. Scanning electron microscopy showed that the presence of inhibitor protected the surface of the stainless steel against pitting in chloride-containing sulfuric acid electrolyte.

LIST OF TABLES

Table **Page**

II-1 Percent chemical composition of 316 stainless steel ----------36

II-2 A list of inhibitors and suitable solvents for each inhibitor----------42

II-3 Potentiodynamic polarization experimental conditions---------- 43

II-3 Polarization resistance experimental conditions---------- 44

II-4 Tafel experimental conditions---------- 44

II-5 EIS experimental conditions---------- 44

II-6 Experiemental conditions for the preparation of surface samples--- 45

III-1 Electrochemical parameters for 316 SS in 0.5 M H_2SO_4 M in the absence and presence of TCAL(data derived frompotentiodynamic measurements).----------59

III-2 Electrochemical parameters for 316 SS in 0.5 M H_2SO_4 M in the absence and presence of AcT(data derived frompotentiodynamic measurements).----------59

III-3 Electrochemical parameters for 316 SS in different concentration of sulfuric acid in absence and presence of 1 X 10^{-2} M TCH(data derivedfrompotentiodynamic measurements).----------63

III-4.a Electrochemical parameters for 316 SS in 0.5 M H_2SO_4 in the absence and presence of TCH.----------69

III-4.b Electrochemical parameters for 316 SS in 0.5 M H_2SO_4 in the absence and presence of TCA.----------69

III-4.c Electrochemical parameters for 316 SS in 0.5 M H_2SO_4
in the absence and presence of TCAL.----------70
III-4.d Electrochemical parameters for 316 SS in 0.5 M H_2SO_4
in the absence and presence of AcT.----------70
III-5.a Electrochemical parameters for 316 SS in 0.5 M H_2SO_4
In differenct concentration of TCAL at 25° C.----------88
III-5.b Electrochemical parameters for 316 SS in 0.5 M H_2SO_4
In differenct concentration of TCAL at 30° C.----------88
III-5.c Electrochemical parameters for 316 SS in 0.5 M H_2SO_4
In differenct concentration of TCAL at 35° C.----------88
III-5.d Electrochemical parameters for 316 SS in 0.5 M H_2SO_4
In differenct concentration of TCAL at 40° C.----------88
III-6 Thermodynamic data for TCAL.----------101
III-7 A.C impedance data of 316 SS in 0.5 H_2SO_4 in presence
And absence of of TCA at –0.1 V.----------107
III-8 A.C impedance data of 316 SS in 0.5 H_2SO_4 in presence
And absence of of AcT at –0.1 V.----------108

LIST OF FIGURES

FIGURE **PAGE**

I-1 Compositional and property linkage in the stainless steel family of alloys----------3

II-1 List of compounds used as inhibitors in the present study----------37

II-2.a Conventional one compartment cell----------40

II-1.b Flat cell----------40

III-1 Potentiodynamic polarization curve of stainless steel type 316 in 1.0 M H_2SO_4 in presenc and absence of TCH----------49

III-2 Potentiodynamic polarization curve of stainless steel type 316 in 0.01 M NaCl/ 0.1 MH_2SO_4 in presenc and absence of TCH----------52

III-3 Potentiodynamic polarization curve of stainless steel type 316 in 0.5 M H_2SO_4 in presenc and absence of TCAL---------57

III-4 Potentiodynamic polarization curve of stainless steel type 316 in 1.0 M H_2SO_4 in presenc and absence of AcT----------58

III-5 Potentiodynamic polarization curve of stainless steel type 316 in different acid concentrations in presence of 1 X 10^{-2} M TCH.----------64

III-6 Configuration of inhibitors----------68

III-7.a Tafel curves of 316 stainless steel in 0.5 M H_2SO_4 M In absence and presence of TCH.----------72

III-7.b Polarization resistance curves for 316 stainless steel
in 0.5 M H_2SO_4 M in absence and presence of TCH.----------73
III-8.a Tafel curves of 316 stainless steel in 0.5 M H_2SO_4 M
In absence and presence of TCA.----------75
III-8.b Polarization resistance curves for 316 stainless steel
in 0.5 M H_2SO_4 M in absence and presence of TCA.----------76
III-9.a Tafel curves of 316 stainless steel in 0.5 M H_2SO_4 M
In absence and presence of TCAL.----------79
III-9.b Polarization resistance curves for 316 stainless steel
in 0.5 M H_2SO_4 M in absence and presence of TCAL.----------80
III-10.a Tafel curves of 316 stainless steel in 0.5 M H_2SO_4 M
In absence and presence of AcT.----------81
III-10.b Polarization resistance curves for 316 stainless steel
in 0.5 M H_2SO_4 M in absence and presence of AcT.----------82
III-11 Variation of corrosion rate and % inhibition efficiency
With concentration of inhibitors.----------84
III-12 Inhibition efficiency for differetn concentration of
TCAL at different temperatures----------91
III-13 Plots of log (θ/1- θ) vs. 1/T at different concentrations
Of TACL in 0.5 M H_2SO_4----------95
III-14 Plots of log (θ/1- θ) vs. Log C for 316 stainless steel
In presence of TCAL in 0.5 M H_2SO_4----------96

III-15 Arrhenius plots of inhibited corrosion rate for TCAL----------99

III-16 Effective energy for inhibition corrosion of 316 stainless steel in 0.5 M H_2SO_4 and TCAL.----------100

III-17 Equivalent circuit used in data fitting for the corrosion of 316 stainless steel in 0.5 M H_2SO_4 in presence of of thiophene derivatives inhibitors.----------104

III-18 Nyquist diagram for 316 stainless steel in 0.5 M H_2SO_4 in different concentration of TCA.----------105

III-19 Nyquist diagram for 316 stainless steel in 0.5 M H_2SO_4 in different concentration of AcT.----------106

III-20.a SEM for the surface of 316 SS exposed to 0.5 M H_2SO_4 with and without TCH----------111

III-20.b SEM for the surface of 316 SS exposed to 0.1 M H_2SO_4 with TCH in absence and presence of chloride ions----------112

III-21 EDAX of 316 stainless steel in 0.5 M H_2SO_4 (a) and 0.5 M H_2SO_4 + 0.001 M TCH (b).----------113

III- 22 FT-IR at 316 SS exposed to 0.5 M H_2SO_4 + 0.001 M TCH (red) and transmission spectra of TCH----------114

List of Abbreviations and Sympols

- i_{corr} Corrosion current
- E_{corr} Corrosion potential
- ΔE Change in potential
- Δi Change in current
- PZC Potential of zero charge
- SHAB Soft and hard acids and bases
- UV Ultra-violet
- AISI American Iron and Steel Institute
- C_{dl} Double layer capacitance
- R_t Charge transfer resistance
- AC Alternative current
- E_{pit} Pitting potential
- SCC Stress corrosion cracking
- β_c Cathodic Tafel slope
- β_a Anodic Tafel slope
- E.W Equivalent weight of the corroding species, g.
- TCH 2-Thiophene Caroboxylic Hydrazide
- TCA 2-Thiophene Caroboxylic Acid
- TCAL 3-Thiophene Carboxaldhyde
- AcT 2-Acetyl Thiophene

List of Abbreviations and Sympols

- i_{corr} Corrosion current
- E_{corr} Corrosion potential
- ΔE Change in potential
- Δi Change in current
- PZC Potential of zero charge
- SHAB Soft and hard acids and bases
- UV Ultra-violet
- AISI American Iron and Steel Institute
- C_{dl} Double layer capacitance
- R_t Charge transfer resistance
- AC Alternative current
- E_{pit} Pitting potential
- SCC Stress corrosion cracking
- β_c Cathodic Tafel slope
- β_a Anodic Tafel slope
- E.W Equivalent weight of the corroding species, g.
- TCH 2-Thiophene Caroboxylic Hydrazide
- TCA 2-Thiophene Caroboxylic Acid
- TCAL 3-Thiophene Carboxaldhyde
- AcT 2-Acetyl Thiophene

List of Abbreviations and Sympols

- i_{corr} Corrosion current
- E_{corr} Corrosion potential
- ΔE Change in potential
- Δi Change in current
- PZC Potential of zero charge
- SHAB Soft and hard acids and bases
- UV Ultra-violet
- AISI American Iron and Steel Institute
- C_{dl} Double layer capacitance
- R_t Charge transfer resistance
- AC Alternative current
- E_{pit} Pitting potential
- SCC Stress corrosion cracking
- β_c Cathodic Tafel slope
- β_a Anodic Tafel slope
- E.W Equivalent weight of the corroding species, g.
- TCH 2-Thiophene Caroboxylic Hydrazide
- TCA 2-Thiophene Caroboxylic Acid
- TCAL 3-Thiophene Carboxaldhyde
- AcT 2-Acetyl Thiophene

-	θ	Degree of coverage
-	Q	Heat of adsorption
-	EIS	Electrochemical Impedance Spectroscopy
-	z	charge of the species
-	F	Faraday constant
-	T	Temperature K

INTRODUCTION

INTRODUCTION

1. General Introduction

The field of corrosion has seen a tremendous amount of research and development stimulated by problems related to great advances in technology and facilitated by parallel advances in techniques for investigating corrosion problems.

On the other hand, corrosion is an electrochemical process that, lead to the deterioration of a metal or alloy as a result of exposure to and reaction with its environment [1]. Therefore, the use of electrochemical techniques to study the corrosion behavior of stainless steels has been increased considerably in the last two decades. This has lead to improving the ability to predict, by short-term laboratory tests, the behavior and deterioration of stainless steel in different environments.

Stainless steels have a technological and economic importance [2]. Stainless steels are iron alloys containing a minimum of approximately 11% chromium. This amount of chromium prevents the formation of rust in "unpolluted" atmospheric environments [3]. Nowadays, there are more than 190 different kinds of alloys that can be recognized as belonging to the stainless steel family. In some steels chromium content approaches 30% and many other elements are added to provide specific properties. For example, nickel and molybdenum are added for corrosion resistance, carbon, molybdenum, titanium, aluminum, and copper for strength, sulfur and selenium for machinability, and nickel for formability

and toughness. The austenitic stainless steel type 304 has a predominant ranking among all types of steels in terms of yearly produced amount. From corrosion resistance viewpoint, of interest is the low-carbon grades: types 304L, 316L, and 317L. In these grades, the carbon content is reduced to 0.03% to improve resistance to sensitization. Figure 1 illustrates the compositional and property linkages in the stainless steel family of alloys [4].

Stainless steels are used in a wide variety of services in which primary considerations are long service life (in a given environmental condition), reliability, appearance, and sanitary factors. Stainless steels are also successfully used in many applications such as architecture, aircraft and aerospace, electronics, food and beverage industries, home appliances, medicine, solar heating and transportation. Of recent interest, is the use of metals in the medical field [5]. For instance, stainless steels have replaced the vanadium steel plates and screws used in orthopedic surgery. By 1946, the American College of Surgeons endorsed Types 316 and 317 as the preferred grades of stainless steels and currently the low-carbon grades are employed.

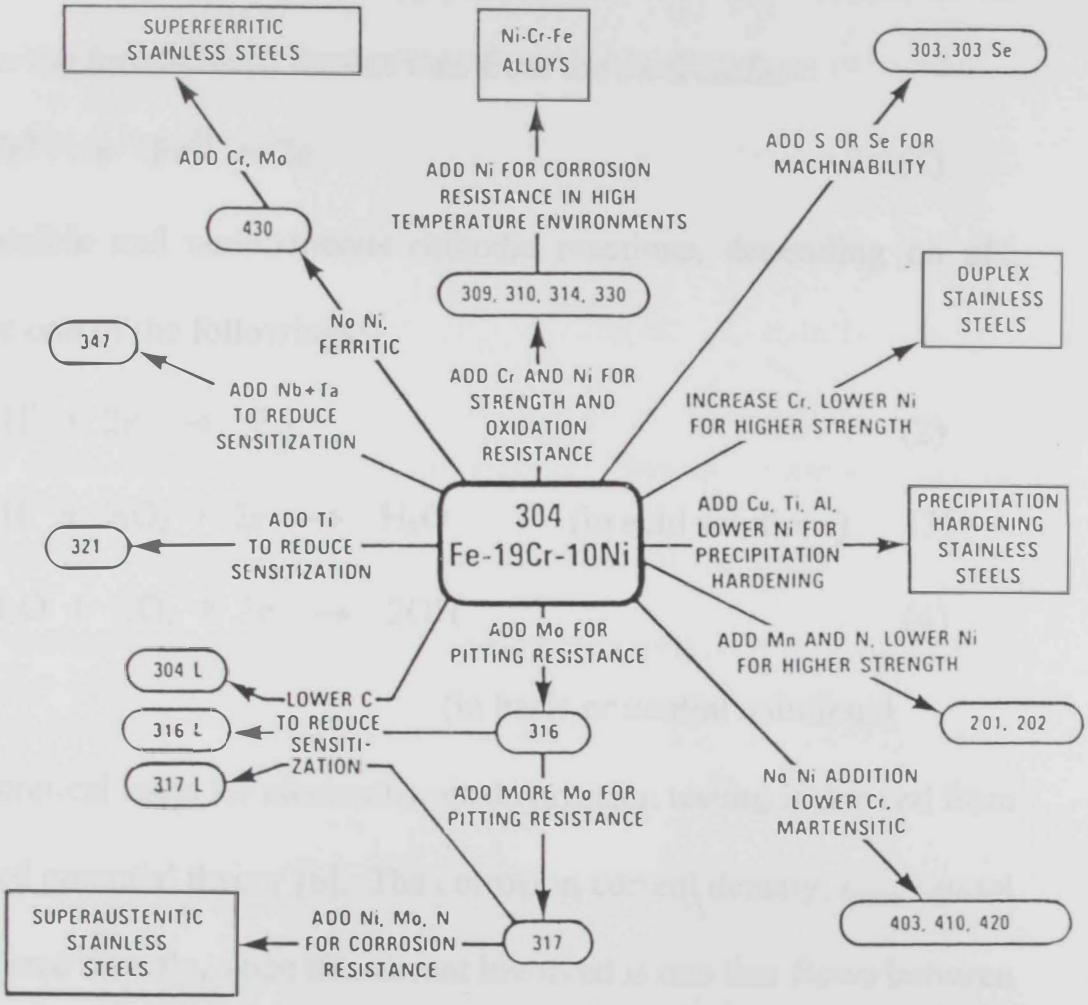

Figure 1. Compositional and property linkages

in the stainless steel family of alloys

2. The electrochemistry of corrosion

As in the case of a battery, the metallic corrosion proceeds by an anodic reaction, a cathodic reaction, electrolytic ion migration and current flow. The anodic reaction, the oxidation of the metal atoms, is for example the formation of ferrous ions from the steel surface:

$$Fe^0 \rightarrow Fe^{2+} + 2e \qquad (1)$$

The possible and simultaneous cathodic reactions, depending on pH, could be one of the followings:

$$2H^+ + 2e \rightarrow H_2 \qquad (2)$$

$$2H^+ + \tfrac{1}{2}O_2 + 2e \rightarrow H_2O \qquad \text{(in acid solutions)} \qquad (3)$$

$$H_2O + \tfrac{1}{2}O_2 + 2e \rightarrow 2OH^- \qquad (4)$$

(in basic or neutral solutions)

The theoretical basis for electrochemical corrosion testing is derived from the mixed potential theory [6]. The corrosion current density, i_{corr}, cannot be measured directly, since the current involved is one that flows between numerous microscopic anodic and cathodic sites on the surface of the corroding metal. The value of i_{corr} can also be measured by another technique, generally known as "linear polarization." This technique is based on the theoretical and practical demonstration that at potentials very close to E_{corr}, $\pm$ 10 mV, the slope of the potential/applied current curve is approximately linear [7]. This slope, $\Delta E/\Delta i$, has the units of

resistance. It has been also shown that the inverse of this slope $\Delta E/\Delta i$, is related to i_{corr} according to the equation [8, 9]:

$$i_{corr} = \left[\frac{\beta_a \beta_c}{2.3(\beta_a + \beta_c)}\right]\frac{\Delta i}{\Delta E} \qquad (1)$$

Where β_a and β_c are the anodic and cathodic Tafel slopes, respectively. It is generally accepted that the quantity $\beta_a \beta_c/2.3\ (\beta_a + \beta_c)$ is a constant C. Therefore, the expression is reduced to the following:

$$i_{corr} = C\left(\frac{\Delta i}{\Delta E}\right) \qquad (2)$$

On the other hand, the corrosion rate of "reactive" metals can be suppressed to a great extent by a modification of the metal surface by organic molecules or polymers. A well-known example is the corrosion protection by lacquers and other organic coatings [10-12]. This approach was used practically to protect, for example, cars against atmospheric corrosion, pipelines against corrosion in humid soil, and ships against corrosion in seawater. It was shown that the corrosion protection is due to the barrier properties of the coating, which prevents the penetration of water and oxygen to the metal/polymer interface [13]. However, many coatings are highly permeable for water and oxygen. Thus, it has been shown by Feser and Stratmann that the corrosion stability caused by coatings which are highly permeable for water and oxygen is due to specific electrochemical properties of the metal/polymer interface

[14,15]. It was suggested that an important example of such electrochemical properties is the extended diffuse double layer. In the presence of defects, such as pores, which may penetrate through the coating, the diffusion barrier is lowered, and the delamination rate of the polymer defect is determined by the formation of galvanic elements. The local anode of this element being the defect and, the local cathode is, in this case the metal/polymer interface at which predominantly oxygen is reduced [16,17]. The stability of the metal/polymer interface is determined by inhibition of the oxygen reduction at the interface. It was shown that the products of the electrochemical reduction of oxygen, namely $^{\bullet}OH$ and OH^{-}, have detrimental effects on the chemical bonding within the polymer film [18]. From the previous discussion we can conclude that the corrosion inhibition of the coating depends to a greater extent on the composition, structure, and chemical bonding at the substrate/polymer interface than on the thickness of the coating. Thus, more attention should be directed towards improving the chemical interaction between the first monolayer of the coating and the substrate in order to improve the metal resistance to the attack of water and other aggressive ions. In this respect, the development of "molecular adhesion promoters" was suggested [19]. The molecular adhesion promoters provide a link between the substrate and the organic coating. In this respect, reactive centers are prepared on top of the substrate, which can

serve as anchor sites for suitable functional groups of the organic molecules [20, 21]. Organic compounds were successfully used as corrosion inhibitors [22]. Organic inhibitors are well known to affect the rate of metallic corrosion by decreasing the rate of either or both the anodic metal dissolution and the cathodic oxygen reduction [23].

3. Mechanisms of Corrosion Inhibition by Organic Compounds:

The inhibition mechanism is generally affected by the chemical changes occurring to the inhibitor and changes to the electrolytic medium. The general possible scenarios are the partial or full dissolution of the inhibitor or its adsorption at the metal surface.

The use of inhibitors to protect metals against corrosion is based on the ability of certain individual chemical compounds, or mixtures of these, to reduce the rated of corrosion process, or to completely supress this process, when they introduce in small concentrations into corrosive medium. Inhibitors can vary the rate of a corrosion process only if they influence the kinetic of electrochemical reactions responsible for this process. Taking this into acount, inhibitors can be classified into anodic, cathodic and mixed in veiw of the fact that the first type predominantly retards the anodic reaction, the second retards the cathodic reaction, while the third retards both reactions simultaneously.

Organic inhibitors, used mainly in acid electrolytes, in which the stability of the phase layer is lower, operate according to a different mechanism. In this case adsorption, and the effect which it has on the kinetic of the cathodic, are of great importance. In acid electrolytes the rate of dissolution can be reduced considerably by lowering the rate of cathodic reaction of hydrogen-ion discharge or discharge of some other depolarizing agent. Another way to reduce the dissolution rate is to remove the intermediate product of the reduction reaction from the reaction sphere. However, some effect of the inhibititors on the the anodic reaction is often observed as well [24].

For example, hydrazinium reduces the oxygen activity and adsorb at the metal/electrolyte interface. The adsorption of hydrazinium at the metal/electrolyte interface leads to the enhancement of passive film formation as in the case of benzotriazol adsorption at the copper surface [25] and benzoates on iron surfaces. On the other hand, monomolecular adsorption layers of inhibitors, known as interfacial inhibitors [26], prevent the dissolution of the substrate and the reduction of oxygen by changing the potential drop across the interface and/or the reaction mechanism thereafter. In this later case, the electric field at the outer Helmholtz plane of the double layer allows for the interaction between organic ions or dipoles and the electrified metal surface. The nature of this interaction is mainly electrostatic, during which a competitive

Organic inhibitors, used mainly in acid electrolytes, in which the stability of the phase layer is lower, operate according to a different mechanism. In this case adsorption, and the effect which it has on the kinetic of the cathodic, are of great importance. In acid electrolytes the rate of dissolution can be reduced considerably by lowering the rate of cathodic reaction of hydrogen-ion discharge or discharge of some other depolarizing agent. Another way to reduce the dissolution rate is to remove the intermediate product of the reduction reaction from the reaction sphere. However, some effect of the inhibititors on the the anodic reaction is often observed as well [24].

For example, hydrazinium reduces the oxygen activity and adsorb at the metal/electrolyte interface. The adsorption of hydrazinium at the metal/electrolyte interface leads to the enhancement of passive film formation as in the case of benzotriazol adsorption at the copper surface [25] and benzoates on iron surfaces. On the other hand, monomolecular adsorption layers of inhibitors, known as interfacial inhibitors [26], prevent the dissolution of the substrate and the reduction of oxygen by changing the potential drop across the interface and/or the reaction mechanism thereafter. In this later case, the electric field at the outer Helmholtz plane of the double layer allows for the interaction between organic ions or dipoles and the electrified metal surface. The nature of this interaction is mainly electrostatic, during which a competitive

adsorption between water dipoles and the organic molecule take place. Bockris and Swinkels [27] showed that when the potential of the electrode is shifted from the potential of zero charge (PZC), at which the surface is highly charged, water adsorption is more prevailing. The organic molecule adsorption at the metal substrate, on the other hand, prevail at the vicinity of the PZC while cations and anions adsorption take place at potentials negative to PZC and positive to PZC, respectively. Specific adsorption can not exclusively be considered because of the adsorption dependence on the charge at the metal surface. It was suggested in the literature [28, 29], that the adsorption valency, the number of electrons exchanged per adsorbed molecule, is typically less than 1. The adsorption which is accompanied by a low activation energy is fast and reversible, and thus called "physisorption." Strong interactions between the electrolytic molecules and the surface are observed in the case of "chemisorption" which is irreversible in nature [30]. The process of chemisorption is specific for certain metals, during which an electron transfer between the substrate and the adsorbed molecule may occur. Thus, the empty electronic bands of the solid substrates overlap with pair of electrons of the adsorbed molecules such as N, S, and P. This explains the slower nature of the "chemisorption" and justifies its need for a high activation energy. The electron transfer process between the molecule a nd the substrate is characteristic for transition metals having vacant low-

energy d-electron orbitals. On the other hand, the higher the polarizability of the heteroatom under consideration (which should possess free electron pairs) the stronger is the adsorption. Based on the Lewis acid-base concept, the inhibitor is considered the electron donor and the metal is the electron acceptor. This rationalization is in good agreement with the principle of soft and hard acids and bases (SHAB). At this stage, it is important to distinguish between the interaction of corrosion inhibitors and molecular adhesion promoters. In the case of corrosion inhibitors, the composition and structure of the metal surface are defined by the corrosive medium. On the other hand, the surface properties can be changed and adjusted to the structure of the adhesion promoter. Moreover, while inhibitors must be soluble in the electrolytic medium and applied only for well-defined reaction conditions, adhesion promoters, however, may be applied from aqueous, nonaqueous solvents, or the gas phase and the reaction conditions can be optimized for the given substrate.

Adsorption inhibitors may be anions, cations, or neutral molecules e.g. organic molecules having an electric dipole. The protection action of adsorption inhibitors is due to a blanking effect over the entire surface.

It is very important to consider the relation between the structure of organic inhibitors, their chemical stability, and their inhibiting properties. Dealing with this relation, it was realized that the chemical

change in the nature of the organic inhibitors may occur as a result of interaction with cathodic hydrogen, corrosive medium, or dissolved metal ions. These interactions may lead to protonation, reduction, hydrolysis, decomposition, or even polymerization of the organic inhibitor. This, in turn, may lead to decrease or increase in the corrosion rate which is caused by the transformation products.

The inhibition mechanism is generally affected by thermochemical changes occurring to the inhibitor and changes to the electrolytic medium. The general possible scenarios are the partial or full dissolution of the inhibitor or its adsorption at the metal surface

3. Corrosion inhibition of stainless steel - Methodologies and Techniques

The protection of iron and steel can be achieved in several approaches. Thus, *the cathodic protection*, in which the electrode potential is depressed to the region of immunity. This is carried out by carefully employing a reducing action on the metal surface. The sacrificial anodes of zinc or magnesium are extensively used in this context. The protection of iron and steel by *passivation or oxidizing inhibitors* is another alternative. In this later case, the electrode potential of the metal can be raised to the region of passivity by adding oxidizing inhibitors (such as chromates), by anodic polarization of the metal substrate in a given electrolyte, or by alkalization of the solution. The

other major means of protection of iron and steel against corrosion are the adsorption of inhibitors to the metal surface(as discussed in the previous section), the use of impermeable coatings (such as paints, metallic coatings, plastic coatings, etc.) and rubber.

In the following section, the candidate will survey some of the recent literature concerning the methodologies and techniques for the corrosion inhibition of steels. Fujimoto et al. showed recently that the pitting corrosion resistance of type 304 stainless steel can be improved by modification of the steel passive film with ultraviolet light irradiation [31]. They showed that the pitting potential shifts to the positive direction by exposing the surface of the steel to UV light during the passivation step. Moreover, the pit generation rate, was lowered by half an order of magnitude following UV light exposure during passivation, while the repassivation rate, was unaffected. X-ray photo-electron spectroscopy revealed additional chromium enrichment in the passive film after exposure to UV light during passivation, and this is thought to be related to the suppression of the pit generation rate. Specific types of corrosion can be also inhibited using specific cations or anions. Thus, Aballe et al. [32] mentioned that lanthanum, cerium and samarium chlorides can be used as uniform and pitting corrosion inhibitors of AISI 434 and AISI 304 stainless steels in 3.5% NaCl aerated aqueous solutions. The inhibition efficiency was evaluated by using

electrochemical techniques such as linear and cyclic polarization which was cathodic in nature and confirmed by SEM and energy dispersive spectroscopic techniques. In a similar study, the influence of sulfate ions on the stress corrosion cracking for stainless steel AISI 321 with constant strain rate in aqueous chloride solution at relatively high temperatures was examined [33]. In this work the steel specimens were tested in solutions with 10^{-2} M Na_2SO_4 and 10^{-3} M NaCl and 5 10^{-3} M NaCl at 150 and 280 °C. The presence of SO_4^{-2} in Cl^- solutions increases the time to fracture and the reduction of area in comparison to pure Cl^- solution. The authors explained their observation in terms of the lower concentration of corrosive hydrogen near the fracture surface in comparison with tests in Cl^- solutions.

Corrosion inhibition of mild steel in acid solution by alkylamines (ALK-AM) and aniline hydrochloric (ANL-HCl) salts was investigated in the presence of sodium sulfate and sodium chloride using a potentiostatic, scaning electron microscope and fourier transform infrared techniques [34]. Results showed chloride ions have a pronounced effect on inhibition of amines and ANL-HCl for corrosion of mild steel. In the presence of Cl^- ions, cationic type surfactants were attached to the surface through formation of chloride precipitate at the surface. In the absence of the organic inhibitor, corrosion initiated along the grain boundaries of ferrite and pearlite structures. In the presence of organic inhibitor,

however, the steel surface was covered by an organic salt precipitation and corrosion was reduced. In another study, sulphamethoxazole was tested as corrosion inhibitor for mild steel in HCl solution using potentiodynamic polarization and weight loss techniques [35]. Results showed that the sulphamethoxazole is an effective inhibitor for mild steel in this medium. The inhibition was assumed to occur via adsorption of the inhibitor molecule on the metal surface. The protection efficiency increases with increasing inhibitor concentration but decreases with increasing temperature. On the other hand, the effect of changing functional groups of some amides and thiosemicarbazone derivatives on their inhibition efficiency has been studied on mild steel [36]. Results showed the mechanism of corrosion inhibition and considered the total molecular structure of the inhibitor that relates to the nature and spatial relationship of the different functional group. All the compounds studied inhibited the corrosion to varying degrees. However, molecules that possessed a thiocarbonyl group, such as thiourea, thioacetamide, and thiosemicarbazide have higher inhibition efficiency than the corresponding compounds that do not, such as urea, acetamide and semicarbazide. In another study, the effect of a 2,5-disubstituted 1,3,4-oxadizoles, on corrosion of mild steel in 1 M HCl and 0.5 M H_2SO_4 have been investigated [37]. The results revealed that these compounds are very good inhibitors and behave better in 1 M HCl than 0.5 M H_2SO_4.

These compounds acted on the cathodic reaction without changing the mechanism of the hydrogen evolution reaction. The changes in impedance parameters, namely the charge transfer resistance (R_t) and the double layer capacitance (C_{dl}) indicated the adsorption of the inhibitor at the surface of the steel. It was shown that the adsorption mechanism of these derivatives in acidic media followed a Langmuir adsorption isotherm. In another publication [38], the objective was to evaluate the effect of changing functional and structural groups on the protection efficiency imparted by various inhibitor molecules. It was found that the molecules that possessed a thiocarbonyl group exhibited much higher protection efficiencies than corresponding compounds that did not. Furthermore, it made only little difference whether the thiocarbonyl group was attached to two amino or methyl groups. However, above certain concentrations they lose their efficiency and eventually become corrosion promotors. These results are in good agreement with those obtained recently by Lagrenee et al.

Thiourea and derivatives have been studied as inhibitors for mild steel [39]. Results showed that the inhibitor efficiency increased with molecular weight and inhibitor concentration. Higher inhibitor concentrations decreased hydrogen pickup. Thiourea accelerated corrosion reaction and hydrogen pickup at higher concentrations. Potential studies showed that cathodic reaction was inhibited at lower

concentrations of inhibitor. Moreover, anodic reactions were inhibited at higher concentrations and results were based on the Langmuir adsorption isotherm. In other study, the inhibiting action of linear and cyclic thiocarbamides on mild steel corrosion in 1 M HCl was examined [40]. It was found that the inhibiting effect of these compounds increased with the temperature of the corrosion medium. The presence of inhibitor in the solution decreases the apparent activation energy of the hydrogen evolution reaction. Inhibitor chemisorption on the metal surface was described by the Temkin adsorption isotherm. The thiocarbamides studied are adsorbed through the sulfur atom that is the adsorption center, forming a donor-acceptor between the unpaired electrons of the sulfur atom and the positive center of the metal surface. Ita and Offiong [41] indicated from weight loss and hydrogen evolution measurements that 4-phenylsemicarbazide and semicarbazide actually have very significant effect on corrosion of mild steel in HCl acid. Generally, the inhibition was found to increase with increase in inhibitor concentration and in half-life, but with a decrease in temperature and decrease in the first-order rate constants obtained at 30 °C and 40 °C. The results showed that a physisorption mechanism was obeyed and the inhibitors followed the Freundlich adsorption isotherm.

The influence of the organic sulfur-containing compounds on the corrosion of ferritic and austenitic stainless steel in sulfuric acid was

studied [42]. The results showed that the anodic dissolution and self-corrosion of stainless steel were remarkably accelerated in solution in presence of a low amount of the organic sulfur-containing compounds, ca. 0.02 mmol.dm^{-3}. With an increase of the inhibitor concentration the molecules adsorbed on the surface and segregated the metal surface from the solution, that decreases the anodic dissolution and hydrogen evolution current of the stainless steel. On the other hand, 2-aminobenzothiazole and its derivatives were synthesized, and their inhibitive-action on the corrosion of mild steel in 1 M HCl acid was investigated [43]. All these compounds were found to reduce the permeation of hydrogen through mild steel in HCl solution. The determination of the inhibition efficiency of these compounds at different temperatures indicated that 2-amino-6-chlorobenzothiazole showed the best performance over 2-aminobenzothiazole, 2-amino-6-methyl benzothiazole, and 2-amino-6-methoxy benzothiazole. Moreover, the study showed that this class of inhibitors acted as a cathodic type, and the adsorption of these compounds obeys Temkin adsorption isotherm. The inhibitive action of thiourea and its derivatives was investigated on corrosion of AISI 410 stainless steel using weight loss measurements, potentiodynamic polarization and scanning electron microscopy technique [44]. Results showed that they are effective inhibitors and they obey Langmuir adsorption isotherm. In this investigation, thiourea, alkylthiourea, and n-

)henylthiourea were studied, with n-phenylthiourea showing the highest ;urface coverage and hence being the most efficient inhibitor.

The effect of chloride concentration on early stages of pitting for Type 304 stainless steel has been studied using an AC impedance method. The Warburg impedance coefficient, which is calculated from Bode plots, increases with increasing chloride concentration at low potentials in the passive region when the diffusion process begins to occur at the surface. In their study, Hong and Magumo [45] found that for a pit which is nucleated under a given potential, there exists a minimum chloride concentration above which the pit on the surface of the steel can be activated into metastable propagation, and below which it cannot. Moreover, it was found that the value of pitting potential increases linearly with the logarithm of chloride concentration of solution. The influence of propargyl alcohol and some ethoxylated fatty acids on the corrosion behavior of mild steel in H_3PO_4 and sulfuric acid were investigated over a range of acid concentrations and solution temperature by using electrochemical measurements [46]. Propargyl alcohol was found to inhibit the cathodic reaction at temperatures ≥ 40 °C by adsorption at the steel surface. It was also found that the adsorption is most favorable at a surface partially covered by adsorbed hydrogen. For the uninhibited H_3PO_4 solutions, a straight-line relationship was found between the corrosion rate and the logarithm of acid concentration. On

ıe other hand, the inhibition efficiency increases with increasing the oncentration and chain length of the fatty acids for mild steel in 1.0 M ulfuric acid and decreased by temperature [47]. In another study by .emaitre, the presence of halide ions in an electrolyte can provoke local ›reakdown of the passive film of stainless steel in initiate the localized :orrosion by different exposed mechanisms, resulting in stress corrosion :racking crevice corrosion or pitting. The efficiency of the presence of ›ther oxyanions with chloride to prevent the risk of pitting corrosion is shown by the use of polarization curves or impedance measurements and :alculated by the statistical studies of the pitting potential values [48]. The chemical etching, the determination of pitting potential and I-t curves, the test of simulated occluded cell and electrochemical impedance spectra were used in this work. Both sodium dodecyl benzene sulfonate and monoethanolamine were proved to act as inhibitors for stainless steel in solution of chloride to prevent pitting corrosion during the periods of initiation and propagation, and that the mixture shows synergetic inhibition, especially during the propagation of the pitting [49]. The pit generation rate was measured on Type AISI stainless steel 304 in chloride and chromate containing media by a statistical method [50]. Inhibition efficiency was calculated, and an inhibition diagram was constructed from the parameters obtained, showing a competitive phenomenon between the two species in solution. An experimental equation for the

between the two species in solution. An experimental equation for the decrease of the pit generation rate was obtained in the pitting domain of the diagram, indicating that adsorption was the limiting stage of the inhibition mechanism. It was suggested that the ion playing the role of the inhibitor species was not CrO_4^{2-} but $HCr_2O_7^-$. The presence of chromate allowed the pH value to stabilize near the active site. A diffusion process occurred with an increase of the thickness of the passive film due to inhibitor presence. When all sites were covered by the inhibiting species in the inhibition domain, adsorption was stopped and diffusion was the limiting process. A study published by Dhirendra [51], showed the effect of Cl^- content (0.007 –0.12 g/100 ml) at 100% relative humidity in air on the corrosion of austenitic stainless steel in 24 hours was evaluated by weight loss. The corrosion increased with increasing Cl^- to 0.05g/100 ml but practically no increase in corrosion was observed at higher Cl^- content. The efficiency of protection by treatment with 1% solution of a newly developed corrosion inhibitor DX-A increased to 85%. The corrosion resistance of 13Cr stainless steel tubing in CO_2 offshore wells was evaluated [52]. Based on uniform and pitting corrosion NaCl solutions in down-hole corrosion, the sensitization is prevented by stress-relief heat treatment at < 300 °C or annealing at > 650 °C. In the same study, crevice corrosion of pipe-thread coupling was reduced by tight metal-to-metal seals, greased copiously and by surface

treatment by oxalate. However, galvanic corrosion of carbon steel occurs in contact with the stainless steel. The corrosion of stainless steel was limited at 30 bar CO_2 and 120° C and no need arised for inhibition treatment.

The electrochemical and corrosion behavior of mild steel in 1 M H_2SO_4 solution containing some selected thiols namely, 2-mercaptobenzothiazol, 2-mercaptobenzimidazol, and 2-mercapto-benzoxazol together with halide ions have been studied by galvanostatic polarization technique, at temperatures ranging from 30 to 60 °C [53]. The effect of temperature on the inhibition efficeincy of both investigated thiols and halide ions was studied. The presence of halide ions together with thiols caused a shift in the corrosion potential as well as the linear part of the cathodic Tafel line to the anodic direction. The corrosion process was found to be under activation control. Moreover, the inhibitors did not change the mechanism of the corrosion process. The thermodynamic parameters for adsorption of thiols were also calculated.

Electrochemical techniques were employed to compare and contrast the roles of alloyed Mo and aqueous MoO_4^{2-} in enhancing pitting resistance of ferritic stainless steel in neutral chloride solutions at 80 °C [54]. Alloyed Mo inhibits pitting in 0.14 N and 1 N chloride solutions while aqueous MoO_4^{2-} inhibits in the diluted Cl^- solutions only. Prepassivation experiments show that the major role of high Cl^-

concentrations is to prevent MoO_4^{2-} from forming a passive film rather than in attacking the film after it has formed. Alloyed Mo and aqueous MoO_4^{2-} inhibit through incorporation into the passive film but incorporation from the solution is easily influenced by solution variables such as chloride concentration.

6. Factors affecting the rate of corrosion and efficiency of inhibition

The influence of factors which can increase or decrease the rate of pH reduction and halide ion build up in a developing pit solution were evaluated for pits nucleated on the surface of a commercial grade 316L [55]. Temperature and applied potential were shown to have a significant influence on these processes for the steel immersed in Cl^- and Br^- solutions and not in F^-. Additions of appropriate buffers to chloride test solutions was shown to alter quite considerably the extent of pH reduction in growing pits and in a number of cases to increase the pitting potential also. Moreover, in chloride solutions containing suitable amounts of sodium dichromate the passivation behavior of 316L was shown to alter considerably with the almost total elimination of activation-repassivation events on the oxide surface as evidenced by the absence of current peaks or fluctuations on potentiostatic current time plots. On the other hand, inhibition efficiencies of different concentrations BMAT (benzoimidazole compound) on 316L ss in 5%

HCl were tested by weight loss measurements [56]. BMAT sorption obeyed the Frumkin isotherm adsorption model. The corrosion inhibition was considered to be chemisorption by studying the influence of temperature on 316L SS. Testing of polarization curve showed that BMAT was mainly cathodic inhibitor.

The effects of alloying elements on the localized corrosion resistance of austenitic SS are considered in terms of anodic and cathodic reaction inhibition [57]. Surface analysis has confirmed that when local attack takes place nitrogen enhances the anodic segregation of beneficial alloying elements, such as Cr and significantly prevents the transpassive dissolution of Mo. Alloyed chromium, molybdenum and nitrogen, all improve the localized corrosion resistance of stainless steel by inhibiting the anodic process. However, in order to further increase localized corrosion resistance, it was also necessary to constrain the cathodic reaction. It was shown that cerium ion implantation of UNSS 31603 stainless steel was very effective in inhibiting the cathodic electrode reaction involved in metallic corrosion. As a result of the inhibition of the kinetics of electrode processes, cerium treatment improved the localized corrosion resistance, and especially crevice corrosion resistance. This was supported by the results of electrochemical measurements in aerated 0.6 M NaCl + 0.1 M Na_2SO_4, and by accelerated corrosion tests.

Pitting corrosion behavior of commercial stainless steels type 904L and 316L was investigated in pure sodium chloride solutions of different pH values and at different temperature [58]. In this study, potentiodynamic polarization technique and SEM were utilized. Pitting corrosion of 316L stainless steel occurred readily at 30 °C and in all chloride solutions of concentrations ranging between 10-3 mol/m^3 while 904L stainless steel did not pit at temperatures lower than 40°C and 0.6 mol/m^3 NaCl, respectively. Pitting potential for 904L stainless steel was much more noble than that obtained for 316L stainless steel while the protection potential values were almost the same for both alloys. The pitting corrosion inhibition by OH^- ions was more pronounced for 316L SS and E(pit) approached that obtained for 904L SS in alkaline solutions. The alloy with higher Cr, Ni and Mo content 904L SS was more sensitive to the temperature effect as compared to 316L. E(pit) was dependent on the alloy composition while the protection potential, E(prot), was not affected by the alloy composition. Another study describes the temperature dependent pitting potential behavior of austenitic stainless steel in neutral chloride solutions between 10 and 70 °C [59]. Two chloride ion concentrations 0.1 and 0.5 M were chosen in this study. Molybdate ion additions were between 0.01 and 0.1M. While the pitting potential of AISI 304 stainless steel decreased continuously with temperature, AISI 316 stainless steel had a temperature independent

region after 50 °C. When molybdate ions were added into the solution the pitting potential of AISI 304 SS also became temperature independent after 50 °C. The pitting potential change the by the addition of molybdate ions, defined as inhibition efficiency, increased with increased molybdate/chloride ratio and temperature. The pitting inhibition efficiency obtained by the addition of sulfate ions decreased with the increase of temperature. The addition of molybdate ions after initiation of pitting in AISI 304 SS, repassivated the pits and shifted the pitting potential. The pronounced beneficial effects of molybdate ions on the propagation of pitting, was attributed to the conditions favoring the reduction and precipitation of the reduction products of molybdate ions. Another comparison was mentioned, that is the effect of dissolved oxygen on the corrosion of carbon steel and stainless steel SUS 304 and 316L in pure water containing < 5-1000 ppb dissolved oxygen by a recirculating plant simulating BWR conditions at 288 °C for 1000 hours [60]. The corrosion weight loss and metal release amount decreased in the order of carbon steel > SUS 304 > SUS 316L. The corrosion of carbon steel decreased with increasing dissolved oxygen concentration. At < 5 ppb dissolved oxygen, the corrosion of SUS 304 was inhibited by a Cr-rich film and that of SUS 316L by an oxide film containing Mo, Ni, and Cr. The corrosion resistance of SUS 304 and 316L increased by Fe and Ni ferrite films at >100 ppb dissolved oxygen. The metal distribution

in the oxide films varied with immersion time and dissolved oxygen concentration.

The anodic behavior of high purity stainless steels based on 316L-composition, was studied at room temperature in HCl solutions from 1 to 6 M [61]. For all acid concentrations, the presence of 0.22% N had little or no effect on the active dissolution kinetics at low overpotentials. The effect on the critical current density for passivation was small for low HCl concentrations (< 3 M). At high HCl concentration (> 4.5 M), no passivation occured and again N had a little effect. For HCl concentration approximately 4 M, N reversibly impedes active dissolution at a few hundreds mA/cm^2. The effect did not appear to be an oxide passivation, but was more likely due to surface enrichment of N atoms. Implications for localized localized corrosion were discussed. Moreover, an effect similar to that of N alloying is reproduced on a N free alloy by adding 2 M $NaNO_3$ to a 4 M HCl solution. This effect was distinct from the passivation of salt-covered surfaces and may be preferable to the later as an explanation of the increase in pitting potential by NO_3^- addition to NaCl solutions. Passivation under a salt film was suggested to explain the passivation of growing pits above the inhibitions potential. In another study, The kinetic of the electrochemical reactions occurring during the initiation and propagation of crevice corrosion were investigated using electrochemical impedance measurement [62]. Two

types of crevice formed were used and comparable results were obtained. The initial stage of crevice corrosion is similar to that previously observed for the initiation of pitting corrosion of 316L SS but at lower potentials. The crevice would appear to encourage the build up of a local environment suitable for the acceleration of the metal dissolution or inhibition of the film repassivation processes. A stochastic process of film rupture and chloride adsorption was proposed based on the observed changes of capacitance, potential and charge transfer. The initial corrosion follows a rate law that reached a maximum some 10-20 h after immersion and then decreased to a relatively steady value. Higher frequency capacitance values indicated a change from passive film condition to active electrochemical dissolution whereas the lower frequency response indicated the increasing role of an adsorption during initiation that then changed to diffusion as the crevice corrosion propagated. Habeeb et al. [63] explained the inhibition efficiency of two mixtures of organic substances, ca. quinoline + thiourea and quinoline + methyl methylacrylate (stabilized with 5% hydroquinone) using a potentiodynamic polarization technique. Tests were made on stainless steel 316L and 316MA in 5% H_2SO_4 at 25-65 °C. The inhibition efficiency was calculated from the corrosion current density. The mixture of 0.05 N quinoline with 0.05 N methylmethacrylate gave good protection of the steels, and the inhibition efficiency was better at 25 than

at 65 °C. The protection degree was much less by using each inhibitor separately.

Different types of organic susbstances, namely an acetylenic derivative, and sulfur or nitrogen-containing additives, were tested as inhibitors for intergranular corrosion of sensitized AISI 304 stainless steel, in diluted sulfuric or sulfamic acid solutions at 70 °C [64]. Among the different organic substances examined, the sole compounds able to stop the intergranular attack are those containing sulfur atom with its electronic lone pair free. These inhibitors accomplish their action by reducing the differences of the corrosion rate between the chromium-depleted grain-boundaries and the matrix. As some of the tested inhibitors could decompose with the formation of HS^- or H_2S, the influence exerted by HS^- ion on the corrosion process is evaluated.

Corrosion of iron in 2 M HNO_3 has been studied by the electrochemical polarization and weight-loss measurements [65]. The effect of some thiophene derivatives has been invistigated. The results showed that the inhibitors influence both the cathodic and anodic processes, and are adsorbed on the metal surface in molecular form. They do not change the mechanism of reaction between the iron and nitric acid but decrease its rate. This effect is controlled by the values of their dipole moments. In another study, the adsoption from solution of chloroacetic acid at low carbon steel surface has been measured using

Langmuir and Bockris-Swinkels isotherm [66]. The coverage has been determined and the standard free energy of adsorption was about 4 KJ/mol. The adsorption arises largely from metal-adsorbate dispersion interface differences between water and organic acid. A knowledge of the adsorption of organic acids at the electrode–solution interface is needed for understanding of organic electrode reactions and the inhibitive action of organic acid on corrosion.

The corrosion inhibition effect of glycol-ether-diamine-tetra-acetic acid on stainless steel SUS 304 was electrochemically examined in deaerated 2% NaCl solution at 30 °C [67]. Glycol-ether-diamine-tetra-acetic acid was chemically adsorbed on the steel surface and the film had a good thickness, strong binding energy, and uniformity. The film had high corrosion inhibition effect at pH 2-9 and high concentration of Cl^- but was unsuitable against oxidizing agents. The aniticorrosive efficiency was 16.01% in 6 % $FeCl_3$ solution at 35° C. In another study, a series of compounds having N-acylamino acid or related structure were investigated as potential inhibitors or localized corrosion of AISI 304L stainless steel [68]. The effect of these compounds on the breakdown potential was measured using the linear current scan method. Interaction of the inhibitors with electrode surface was studied using capacitance measurements and correlated with solution surface tension measurements. Successful inhibitors interact strongly with the AISI 304L surface, but the

inhibition effect appears to involve more than just adsorption of a hemimicellar inhibitor layer, which could exclude Cl^- from the surface or provide surface pH buffering. Formation of such a layer is sensitive to the structure of the compound. Trabanelli et al. tested different types of organic containing additives (N-containing, S-containing, and acetylenic derivatives) as inhibitors for the intergranular corrosion of a sensitized AISI 304 stainless steel in 1 N sulfamic acid solution at 70 °C [69]. Only S-containing additives inhibit intergranular in sulfamic acid solution. Among the organic additives tested (without sulfur) only benzotriazole and the N-containing inihibitor decrease the severity of the localized attack in hot, diluted sulfamic acid solutions. In the presence of the S-containing additives, the corrosion rate of senstized SS specimen is equal to that of a non-sensitized specimen.

A slow strain rate (10^{-6} s^{-1}) was used to study the possibility of inhibiting or delaying the stress corrosion cracking (SCC) of AISI 304 stainless steel wires in 1 M HCl solutions at room temperature by using organic additives [70]. Some of the tested organic substances (phenylthiourea, benzimidazole-2-thiol, and benzothiazole-2-thiol) inhibit SCC in the quoted environment. The results obtained in tests of long duration on U-bent specimens. The efficient SCC inhibitors manifest their action on either the incubation stage or the propagation stage of the

SCC process. The action of the inhibitors cannot be directly correlated with the corrosion potential of stainless steel wires tested.

7. High-Grade steels

A review on the corrosion mechanism of high-Cr stainless steel was presented in the literature [71]. Good adhesive, corrosion-inhibiting-Cr_2O_3 coatings (some nm-thick), were formed on the steel surface. A local depletion of Cr (< 10%) leads to a loss of the corrosion inhibiting layer, and therefore to an accelarated metal dissolution. Simultaneously, the carbide (Cr, Fe) 23C6 is formed at the grain boundries. Intergranular corrosion starts at the Cr-depleted grain boundaries. In another study, weight loss measurements were performed in 20% and 28% HCl at 90 °C on C steel X65, 22Cr5Ni duplex stainless steel, and 2 superaustenitic steels in presence of organic subastance [72]. The organic substances tested were quaternary ammonium salts. The synergistic effect of KI on the inhibitive efficiency of the organic substance was studied. The variation of corrosion rate during the test time, normally 6 hours were recorded. The corrosion rates of the four steels examined were reduced to < 1 mg/cm^2 using ternary inhibitor mixtures containing quaternary ammonia salts, trans-cinnamaldehyde and 0.2% of each component. On the other hand, corrosion of stainless steel reactors in the manufacture of nitrogen containing organic phosophonic acids, was prevented by contracting the reactor with HNOx (x= undefined), to form a layer of

MNO_3 (M= metal), such that the reactor product stream contains corrosion products content of Ni 10.1-2, Mo 0-0.3, and Fe 0.2-3 ppm [73]. Thus, a stainless steel reactor was treated with 98% HNO_3, then a mixture of ammonium sulfate, 37% HCHO, and phosphorous acid passed through the reactor at 105 °C producing 97% conversion to N-[-$CH_2PO(OH)_2]_3$, with the product stream containing Ni 0.5, Mo and F_2 2 ppm, vs. 90.5, 70, 20 and 300, respectively for a stainless steel reactor not treated with HNO_3.

AIM OF THE THESIS

The corrosion of stainless steels in acidic and in aggressive media such as those containing-chloride is of great importance to the industrial processes. The goals of the present thesis is to investigate the effect of using a new class of organic inhibitors on the corrosion behavior of stainless steel type 316 in sulfuric acid. The candidate will attempt to clarify important issues, among them:

- To study the electrochemical behavior of stainless steel type 316 in sulfuric acid medium.
- To study and compare the electrochemical characteristics of the stainless steel in sulfuric acid solution of different concentrations.
- To apply and compare the effect of some thiophene derivatives on the corrosion behavior of stainless steel in acidic and in chloride-containing acidic media.
- To correlate the geometrical factor imparted by the different inhibitors on the experimental results obtained.
- To investigate the effect of temperature on the adsorption characteristics of the inhibitors at the stainless steel surface.
- To estimate the thermodynamic parameters of the adsorbed organic layers of the inhibitor at the stainless steel surface, such as ΔH°, ΔS°, ΔG° for the adsorption process.

EXPERIMENTAL WORK

1. Materials and reagents

1.1 stainless steel sample

AISI 316 stainless steel was used in this study, with the percentage chemical composition listed in table 1. The stainless steel sample was purchased from Goodfellow (Huntingdon, England).

Table 1: Percent chemical composition of stainless steel 316 used in this study.

Element	% composition
Cr	16.9
Ni	10.9
Si	0.75
Mn	1.24
N	0.025
S	0.027
Cu	0.20
Mo	2.11
C	0.053
Fe	Balance

1.2 reagents and solutions preparation

Sulfuric acid, Sodium chloride 2-Thiophene carboxylic hydrazide **(TCH)**, 2-Thiophene carboxylic acid **(TCA)**, 3-Thiophene carboxaldhyde **(TCAL)**, 2-Acetyl thiophene**(AcT)**. The structure and some properties of the inhibitors used in this study are shown in figure 1. All chemicals purchased were used as received and

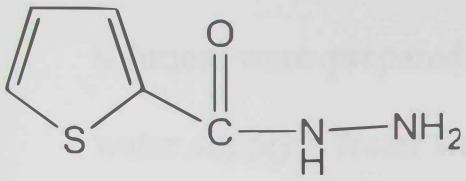

2-Thiophene carboxylic hydrazide

Solid	
m.p.	136-139 °C
NMR	2(2),479A
FT-IR	1(2),605B
TCH	

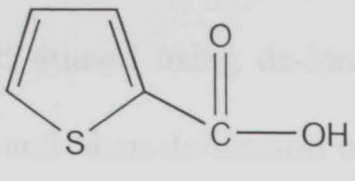

2-Thiophene carboxylic acid

Solid	
m.p.	127-130 °C
NMR	2(2),474D
FT-IR	1(2),600D
TCA	

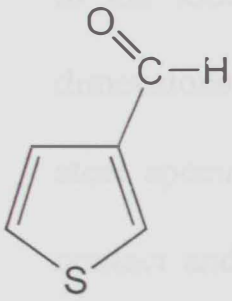

-Thiophene carboxaldehyde

Liquid	
.p.	86-87 °C/20 mm.
Density	1.28 g/mL
F_p	90 °C
TCAL	

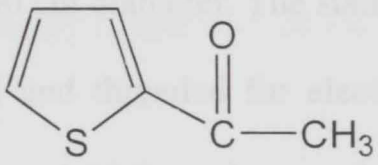

2-Acetyl Thiophene

Solid	
m.p.	10-11 °C
b.p.	214 °C
Density	1.168 g/mL
F_p	91 °C
NMR	2(2),471A
FT-IR	1(3),10472C
AcT	

Figure 1. List of Compounds Used as Inhibitors in the Present Study

were supplied by Aldrich Chem. Co (Wisconsim, USA). Test solution were prepared from stock and diluted using de-ionized water supply. Water was first distilled and then de-ionized using Millipore water purification system. The conductivity of water used in this study is 18.3 μS.

1.3 Electrode Mounting and Electrochemical Cells

AISI 316 stainless steel specimens were in the form of rods and sheets. Rod specimens were prepared and mounted according to the following steps: stainless steel rods were cut in the dimensions of 2.0 cm long and 0.60 cm diameter. The stainless steel specimen was then grooved and threaded for electrical contact and connection. A copper rod 12.0 cm long and 0.35 cm diameter was used for establishing electrical contact. The whole assemply was finally intersted in a glass tube 10.0 cm long and 0.8 cm inner diameter. Epoxy resin (Torr Seal , from Varian, MI, USA) was used to ensure the exposure of a determined apparent surface area of 0.283 cm^2. This specimen configuration was used for electrochemical measurements.

Flat specimen configuration was used for samples prepared for surface examination. In this setup, the stainless steel foils in the dimensions of 5 cm x 5 cm and 2 mm thick were cut and

mounted on a flat cell holder. The surface area exposed is either 1.0 cm^2 or 5.0 cm^2 according to the cell used.

Prior to each electrochemical measurement , the steel specimen subjected to surface experiments was prepared according to the following steps: the surface was polished mechanically using metallurgical papers of successive grades (120-600-1200 μm). The surface was then polished using alumina paste 0.3 μm dispersed on a soft cloth paper until a scratch-free surface is obtained. The surface was rinsed with distilled water, degreased in ethanol and was thoroughly rinsed with de-ionized water.

Two types of electrochemical cells were used in this investigatinon. A three-electrode one-compartment glass cell, with a saturated Ag/AgCl reference electrode and a platinum sheet (2 x 2 cm^2) counter electrode was used for the electrochemical measurements.

The second type of cells, is a one-compartment three electrode flat cell that was used to prepare the surface specimens.

Figure 2 shows diagram of the electrochemical cells used.

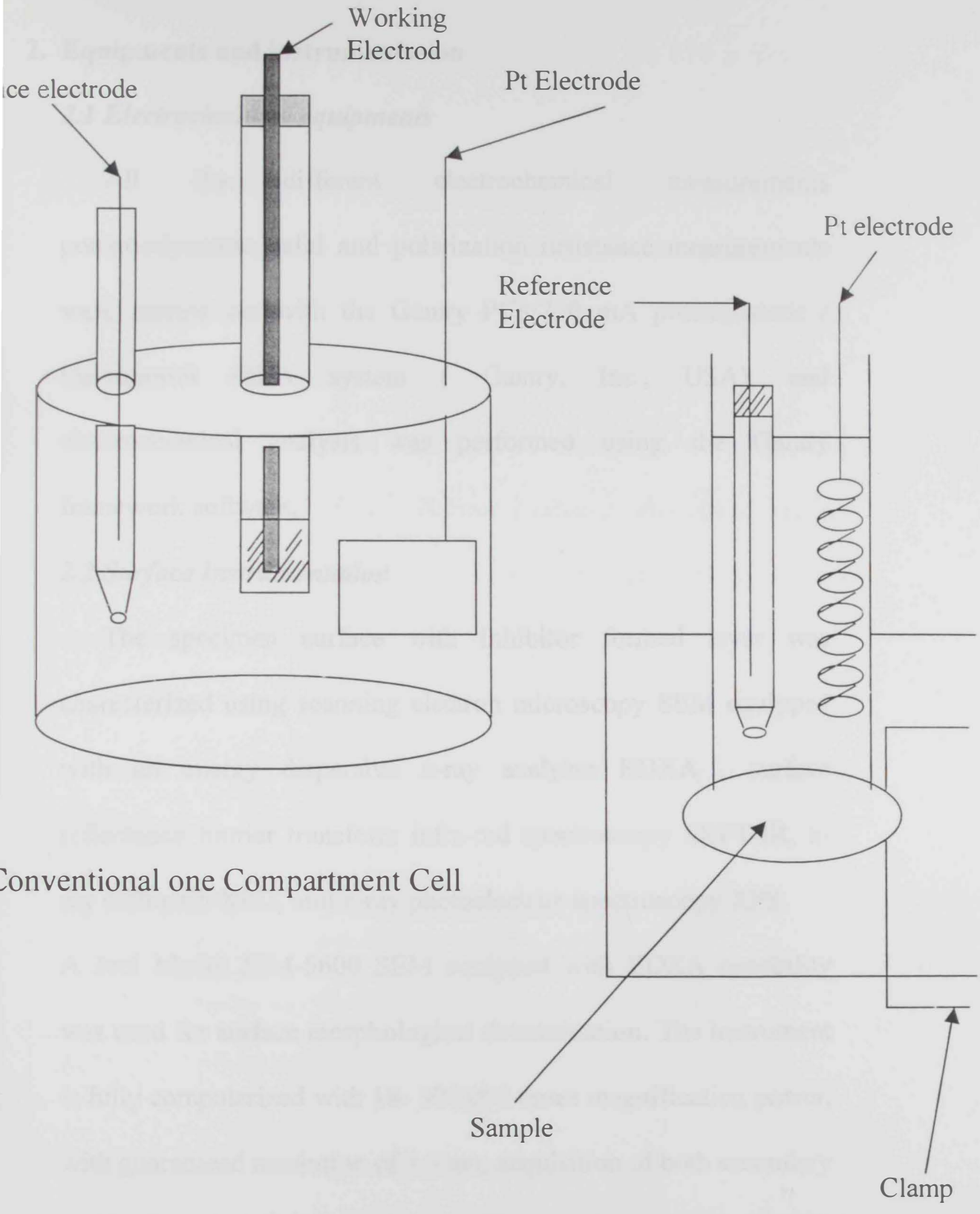

Conventional one Compartment Cell

Figure 2.b Flat Cell

2. Equipments and instrumentation

2.1 Electrochemical equipments

All the different electrochemical measurements potentiodynamic, tafel and polarization resistance measurements were carried out with the Gamry PC3/750 mA potentiostatic / Galvanostal /ZRA system (Gamry, Inc., USA), and electrochemical analysis was performed using the Gamry framework software.

2.2 Surface Instrumentation

The specimen surface with inhibitor formed layer was characterized using scanning electron microscopy SEM equipped with an energy dispersive x-ray analyzer EDXA , surface reflectance fourier transform infra-red spectroscopy SRFT-IR, x-ray diffractin XRD, and x-ray photoelectron spectroscopy XPS.

A Jeol Model JSM-5600 SEM equipped with EDXA capability was used for surface morphological determination. The instrument is fully computerized with 18- 300,000 times magnification power, with guaranteed resolution of 3.5 nm, acquisition of both secondary and back-scattered electron images. The samples were coated with a thin film of gold to eliminate the effect of charging during measurements. A Jeol JFC-1200 fine coater was used for this

purpose and a current of 20 mA was applied for 150 s coationg period.

3. Solutions preparation and solvents.

All solutions were prepared from reagent grade chemicals and de-ionized water. The 0.5 M H_2SO_4 was prepared by dilution from the stock concentrated sulfuric acid (5 M).

Different concentration of the inhibitors were prepared by dilution of the stock of 0.1 M of the inhibitor (table 2. shows the needed solvent to prepre the stock solution) ,and then diluted by de-ionized water to the different concentrations of $5x10^{-4}$ M, $1x10^{-3}$ M, $5x10^{-3}$ M, and $1x10^{-2}$ M.

Table 2 . A list of the inhibitors and suitable solvents for each inhibitor.

TCH	0.5 M H_2SO_4
TCA	7 ml ethanol and then diluted with 0.5 M H_2SO_4
TCAL	5 ml ethanol and then diluted with 0.5 M H_2SO_4
AcT	5 ml ethanol and then diluted with 0.5 M H_2SO_4

4. Electrochemical Measurements

All electrochemical measurements were performed at room temperature(ca. 25° C) except for those experiments concerning temperature coefficient. A three electrode cell was used for all measurements.

4. Electrochemical Measurements

All electrochemical measurements were performed at room temperature(ca. 25° C) except for those experiments concerning temperature coefficient. A three electrode cell was used for all measurements.

4.1 Potentiodynamic Polarization measurements

Table 3. shows the mesurements conditions for the potentiodynamic measurements. The potentiondynamic polarization measurements were performed to study the complete behavior of the current in the wide potential range scan. These measurements were carried for 316 stainless steel in presence and absence of the different inhibitors.

Table 3. Potentiodynamic Polarization experimental conditions

Initial Potential	-1 V vs. $E_{reference}$
Final Potential	1.5 V vs. $E_{reference}$
Scan Rate	5 mV/s
Initial Delay	1200 s

$E_{reference}$: vs. Ag/AgCl

4.2 Polarization Resistance measurements

Table 4 lists the experimental conditions for the polarization resistance experiments.

Table 4. Polarization Resistance experimental conditions

Initial Potential	-0.02 V vs. $E_{open\ curciut}$
Final Potential	0.02 V vs. $E_{open\ curciut}$
Scan Rate	1 mV/s
Initial Delay	300 s

4.3 Tafel measurements:

Table 5. Tafel measurement conditions

Initial Potential	-0.250 V vs. $E_{open\ curciut}$
Final Potential	0.250 V vs. $E_{open\ curciut}$
Scan Rate	1 mV/s
Initial Delay	300 s

4.4 EIS measurements

The specimen was left under open circuit conditions for 300 s. At this stage the open circuit potential, Eopen was determined. The onset potential of – 0.1 V and –0.2 V were chosen as the DC signal of EIS experiment.

Table 6. EIS experimental conditions

Frequency Range	0.02 – 5000 Hz
AC Potential	10 mV
DC Potential	-0.1 or-0.2 mV vs. $E_{open\ curciut}$
Initial delay	300 s
Inhibitor concs.	0, $5x10^{-4}$, $1x10^{-2}$ M
Electrolyte	0.5 M H_2SO_4

5. Surface characterization

A flat type three-electrode electrochemical cell, with saturated Ag/AgCl reference electrode and a platinum counter electrode, was used to prepare the sample. Surface area 5.3 cm^2 according to the cell used. The electrochemical cell was a pyrex glass cylinder with a flat circular piece of glass fused on each end. Two small holes on the top of the cylinder connected with two plastic tubes were used to accommodate the gas bubbler. A platinum sheet counter electrode of large area was housed inside the chamber. A cavity was left at the top of the chamber to be filled with the testing solution and to insert the reference electrode. The cavity is connected to the working electrode through a Luggin capillary tube (cf. Figure b).

Then a potentionstatic measurement was performed by applying a potential of 1.5 V for 10 minuntes vs. $E_{reference}$, then the sample was subject to the intended surface measurement.

Initial Potential	-0.5 V vs. $E_{reference}$
Initial Time	60 s
Final Potential	1.5 V vs. $E_{reference}$
Final Time	600 s
Limit I	250 A

.1 Scanning Electron Microscope SEM

Samples of 316 stainless steel investigated by SEM were in the form of sheets with surface area of 5.3 cm^2 . The samples were exposed to the different medium of :

a) 0.5 M H_2SO_4

b) 0.5 M H_2SO_4 + 10^{-2}M TCH

c) 0.1 M H_2SO_4 + 0.01 M NaCl

d) 0.1 M H_2SO_4 + 0.01 M NaCl + 0.01 TCH

.2 Surface Reflectance FT-IR Spectroscopy

Two 316 stainless steel samples were examined by FT-IR pectroscopy.

a) Unexposed sample .

b) And sample exposed to 0.1 M H_2SO_4 + 0.01 M TCH.

n order to examine the layer of the inhibitor built on the stainless steel urface.

RESULTS AND DISCUSSION

Evaluation of some thiophene derivatives for the inhibition of stainless steel:

Thiophene compounds possess aromatic molecules in which one carbon atom is replaced by a heteroatom, sulfur. The structure of the thiophene derivatives used in the present study is shown in figure 1. Thiophene compounds are used extensively in the preparation of several organic-based drugs [74], and recently in the preparation of organic conducting polymers [75]. The nature of substituent in the ring changes considerably the stability of the aromatic structure, the planarity of the ring, and consequently the electronic distribution around the atoms.

1- Electrochemical measurements:

1-a Potentiodynamic behavior investigation

However, thiophene compounds have not been investigated extensively for their potential application as corrosion inhibitors for metal or alloys. This part of the present work investigates the electrochemical behavior of stainless steel electrode in the presence of different concentrations of the above thiophene compounds in acidic and chloride-containing acidic solutions.

Potentiodynamic polarization experiments of stainless steel type 316 in 1.0 M H_2SO_4 at 25 °C in absence (a) and presence (b) of 2-

thiophene carboxylic hydrazide is depicted in Figure 2. The following observations could be drawn from the data shown in Figure 1

The general shape of the potentiodynamic curve in the absence and presence of the inhibitor is comparable.

However, the linear anodic and cathodic Tafel regions appeared extended over wider current range in the presence of the inhibitor when compared to that in the absence of the inhibitor.

The calculated corrosion potential, E_{corr}, in the case of the curve (b) in presence of the inhibitor is –299.2 mV with an associated corrosion current, i_{corr}, of 7.37 x 10^{-5} A.cm^{-2}. The corresponding values in the absence of the inhibitor are –1.0 mV and 1.385 x 10^{-3} A.cm^{-2}, respectively. The comparison of the values of E_{corr} and i_{corr} indicated that the addition of the 2-thiophene carboxylic hydrazide resulted in the shift of the corrosion potential to a negative value and a decrease in the corrosion current density.

The inhibitor appeared to be of the mixed type. This observation was withdrawn by comparing the values of the anodic and cathodic Tafel constants, β_a, β_c. The values are 153.7, 145.0 mV/decade, and 46.4, 86.0 mV/decade in absence and presence of the inhibitor, respectively. It was also concluded that the inhibitor acts as a mixed inhibitor for all

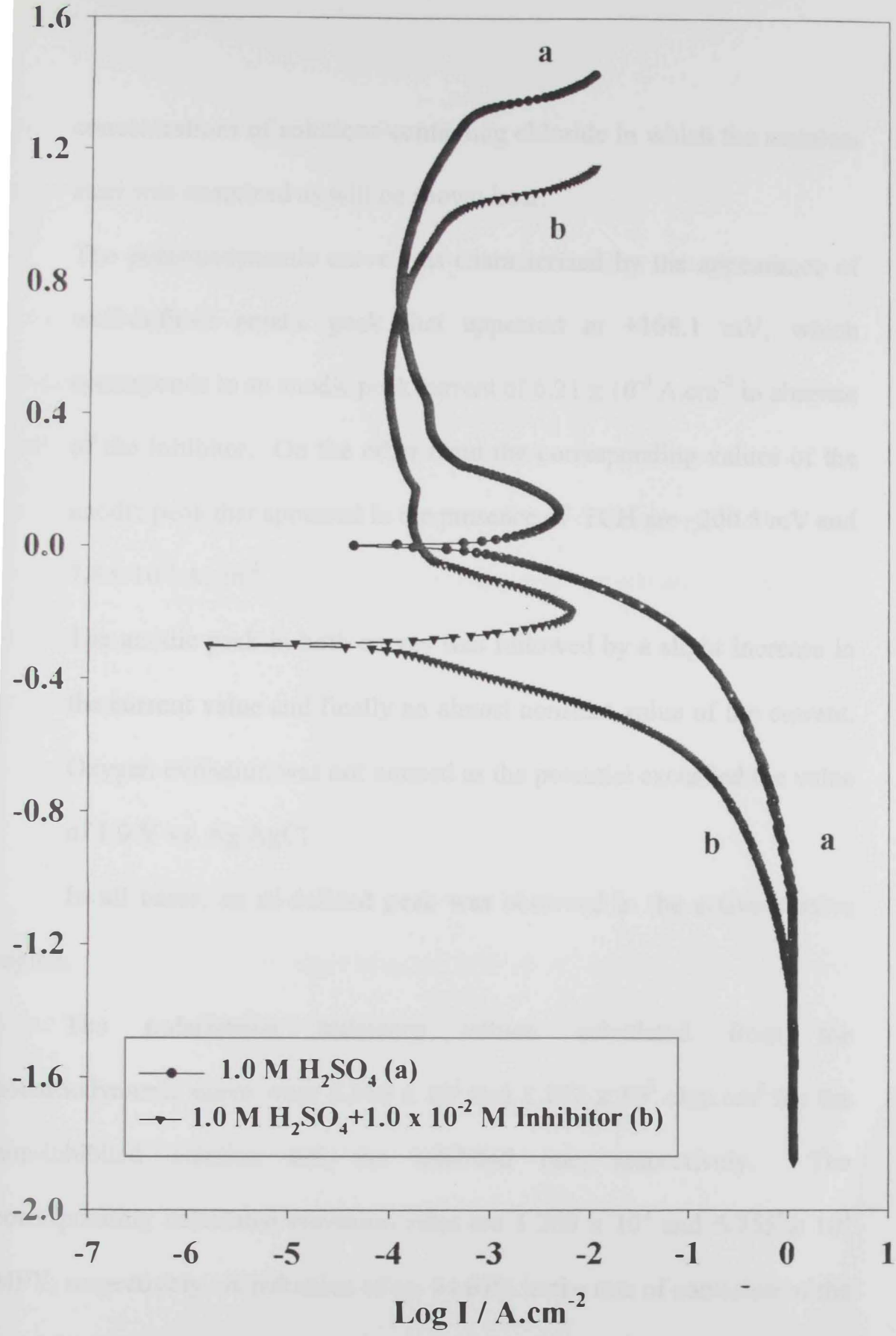

Figure 1 Potentiodynamic Polarization Curve of Stainless Steel Type 316 n 1.0 M H_2SO_4 in Presence and Absence of Thiophene Carboxylic Hydrazide

concentrations of solutions-containing chloride in which the stainless steel was examined as will be shown later.

The potentiodynamic curve was characterized by the appearance of well-defined anodic peak that appeared at +108.1 mV, which corresponds to an anodic peak current of 6.21×10^{-3} A.cm^{-2} in absence of the inhibitor. On the other hand the corresponding values of the anodic peak that appeared in the presence of TCH are –200.5 mV and 7.8×10^{-3} A.cm^{-2}.

The anodic peak in both curves was followed by a slight increase in the current value and finally an almost constant value of the current. Oxygen evolution was not noticed as the potential exceeded the value of 1.0 V vs. Ag/AgCl.

In all cases, an ill-defined peak was observed in the active-passive region.

The polarization resistance values, calculated from the potentiodynamic curve were 2.340×10^{1} and 1.777×10^{2} ohm.cm^{2} for the non-inhibited solution and the inhibited one, respectively. The corresponding calculated corrosion rates are 1.269×10^{3} and 6.755×10^{1} MPY, respectively. A reduction of ca. 94.67% in the rate of corrosion of the

nhibited stainless steel in the 1.0 M H_2SO_4 solution is therefore observed when compared to the non-inhibited one.

The presence of stainless steel 316 in sulfuric acid has evidently a detrimental effect on the integrity of the surface. The addition of 2-thiophene carboxylic hydrazide showed to minimize the corrosion rate of the steel. At this stage of the work, it was necessary to explore two factors: (i) the effect of addition of chloride ion to examine the inhibitory efficiency of the thiophene derivative in presence of an aggressive anion and (ii) the effect of changing the concentration of the inhibitors at fixed concentration of sulfuric acid.

1-b Effect of Adding Chloride Ions in Presence and Absence of the Inhibitor:

Sodium chloride with concentration of 0.01 M was added to the acidic solution to form a concentration ratio of H_2SO_4/NaCl of 10/1. The following treatment of the results is based on comparing the results obtained from the potentiodynamic experiments of the stainless steel in presence and absence of 1.0×10^{-2} M thiophene carboxylic hydrazide.

Potentiodynamic polarization experiments of stainless steel in 0.01 M NaCl/0.1 M H_2SO_4 at 25 °C in absence (a) and presence (b) of 1.0×10^{-2} M

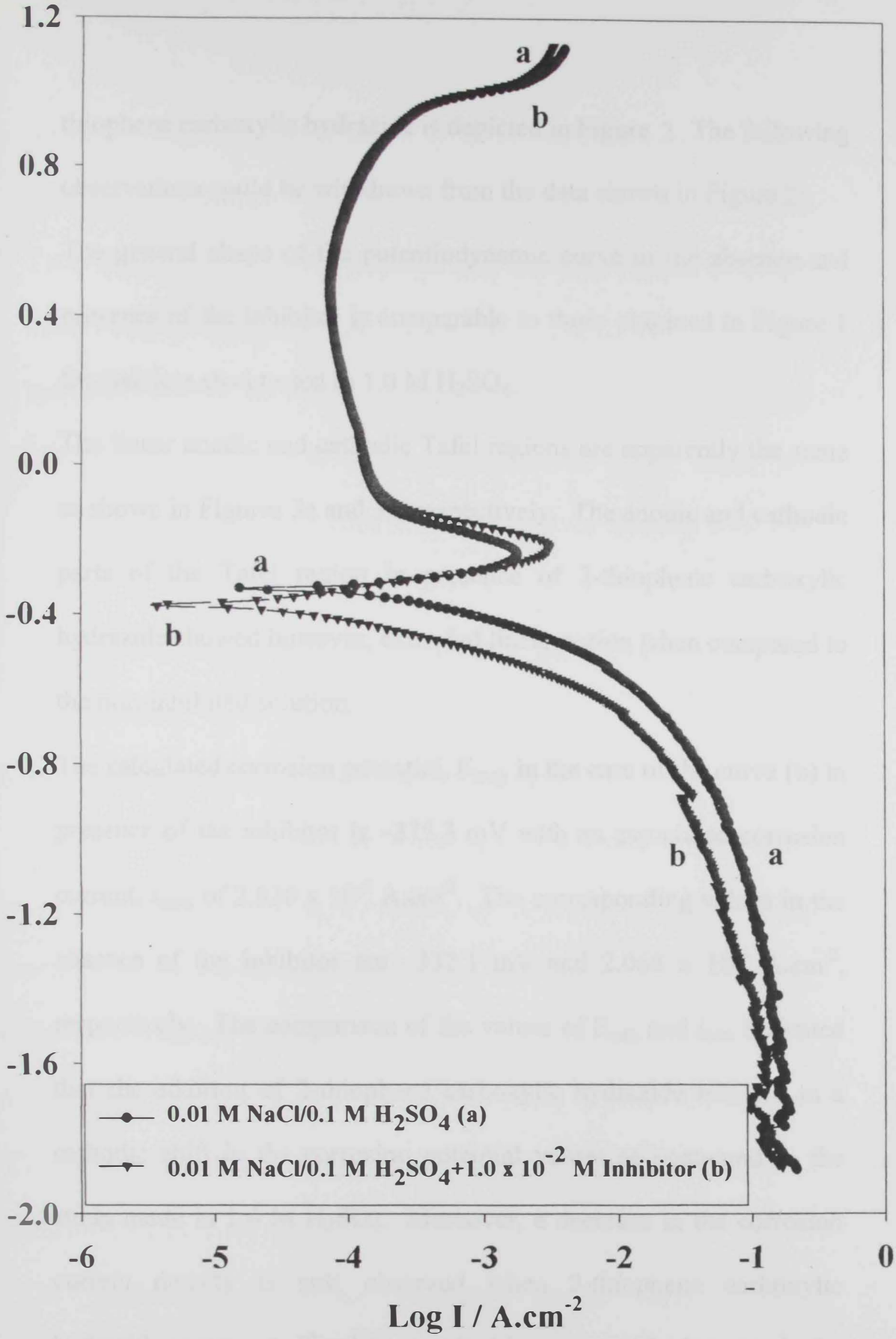

Figure 2 Potentiodynamic Polarization Curve of Stainless Steel Type 316 .01 M NaCl/0.1 M H_2SO_4 in Presence and Absence of Thiophene Carboxylic Hydrazide

thiophene carboxylic hydrazide is depicted in Figure 2. The following observations could be withdrawn from the data shown in Figure 2:

- The general shape of the potentiodynamic curve in the absence and presence of the inhibitor is comparable to those obtained in Figure 1 for stainless steel tested in 1.0 M H_2SO_4.
- The linear anodic and cathodic Tafel regions are apparently the same as shown in Figures 3a and 3b, respectively. The anodic and cathodic parts of the Tafel region in presence of 2-thiophene carboxylic hydrazide showed however, extended linear region when compared to the non-inhibited solution.
- The calculated corrosion potential, E_{corr}, in the case of the curve (b) in presence of the inhibitor is –375.3 mV with an associated corrosion current, i_{corr}, of 2.820 x 10^{-5} A.cm^{-2}. The corresponding values in the absence of the inhibitor are –332.1 mV and 2.068 x 10^{-4} A.cm^{-2}, respectively. The comparison of the values of E_{corr} and i_{corr} indicated that the addition of 2-thiophene carboxylic hydrazide resulted in a cathodic shift in the corrosion potential values as compared to the study made in 1.0 M H_2SO_4. Moreover, a decrease in the corrosion current density is still observed when 2-thiophene carboxylic hydrazide is present. The later resulted in a noticeable decrease in the

corrosion rate from 189.56 MPY to 25.85 MPY and an inhibition efficiency of 86.36 %.

Tafel slopes (β_c/β_a) for the cathodic and anodic processes exhibited lower values upon the addition of the 2-thiophene carboxylic hydrazide, namely, 83.4/65.7 mV/Decade in presence as compared to 119.5/82.0 mV/Decade in absence of inhibitor. The values are relatively lower than those cited in the literature for stainless steel 304 [76].

Electrode surface developed observable pits after polarization experiment.

Effect of Varying the Concentration of the Inhibitor

The effect of varying the concentration of the inhibitor with fixed ncentration of sulfuric acid, ca. 0.5 M, on the corrosion of stainless steel s examined in this section for two thiophene derivatives. The polarization ves for these solutions are shown in figures 4 and 5 in presence/absence 3-thiophene carboxyldehyde and 2-acetyl thiophene at room temperature °C), respectively. The following observations could be concluded when nparing the data shown in figures 3and 4:

The potentiodynamic curves exihibited distinct features when changing the type of inhibitor used. Thus, as the concentration of 3-

thiophene acetaldehyde in the medium increases the corrosion potential, E_{corr}, shifted to relatively higher cathodic values. On the other hand the corrosion potential remained basically constant in the case of using 2-acetyl thiophene.

An anodic peak is observed immediately after the extended anodic Tafel line for which the corresponding peak current and peak potential values changed upon changing the concentration of the inhibitor. In general, the peak current values shifted to lower values and that of the peak potential values shifted to relatively more positive values. These effects were more pronounced in the case of using 3-thiophene carboxaldehyde.

The inhibition efficiency increased as the concentration of the inhibitor increases. This is clearly shown when examining the values of the polarization resistance, R_p, and the corresponding corrosion rates calculated as depicted in tables 1 and 2, respectively. However, the inhibition efficiency for 3-thiophene carboxyldehyde is higher than that of 2-acetyl thiophene.

Again, it is important to notice that unexpectedly the values of the Tafel constants (β_a, and β_c), namely the anodic slope, are relatively lower than those cited in the literature [76]. Moreover, the addition

of the inhibitor to the medium changed both values of β_a, and β_c. This indicates that these inhibitors are of the mixed types as mentioned earlier in this section.

The potentiodynamic anodic plot is practically useful to determine important information such as: (i) the ability of the material to spontaneously passivate in the particular medium, (ii) the potential region over which the specimen remains passive, and (iii) the corrosion rate in the passive region. Anodic and cathodic Tafel slopes will be used to calculate the corrosion rate using the linear polarization method. The anodic or cathodic Tafel plots are described by the Tafel equation [4]:

$$\eta = \beta \log \frac{i}{i_{CORR}} \qquad (1)$$

Where,

η = overvoltage, or the difference between the potential of the specimen and the corrosion potential.

β = Tafel constant (slope).

i_{CORR} = current at overvoltage η.

Rearranging equation (1) gives:

$$\eta = \beta(\log i - \log i_{CORR}) \qquad (2)$$

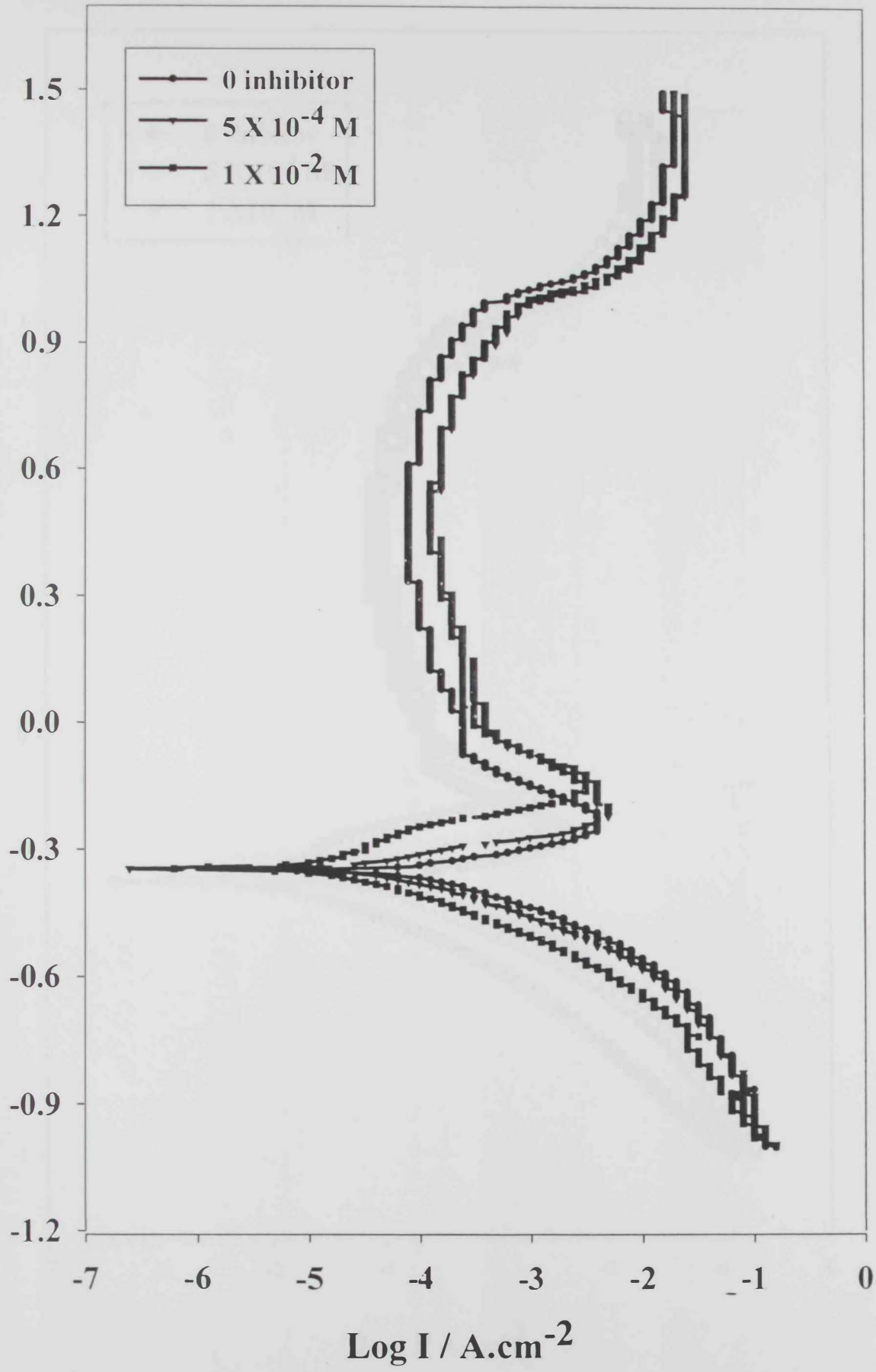

Figure 3 : Potentiodynamic curves for 316 stainless steel in absence and presence of 2-Thiophene acetyl

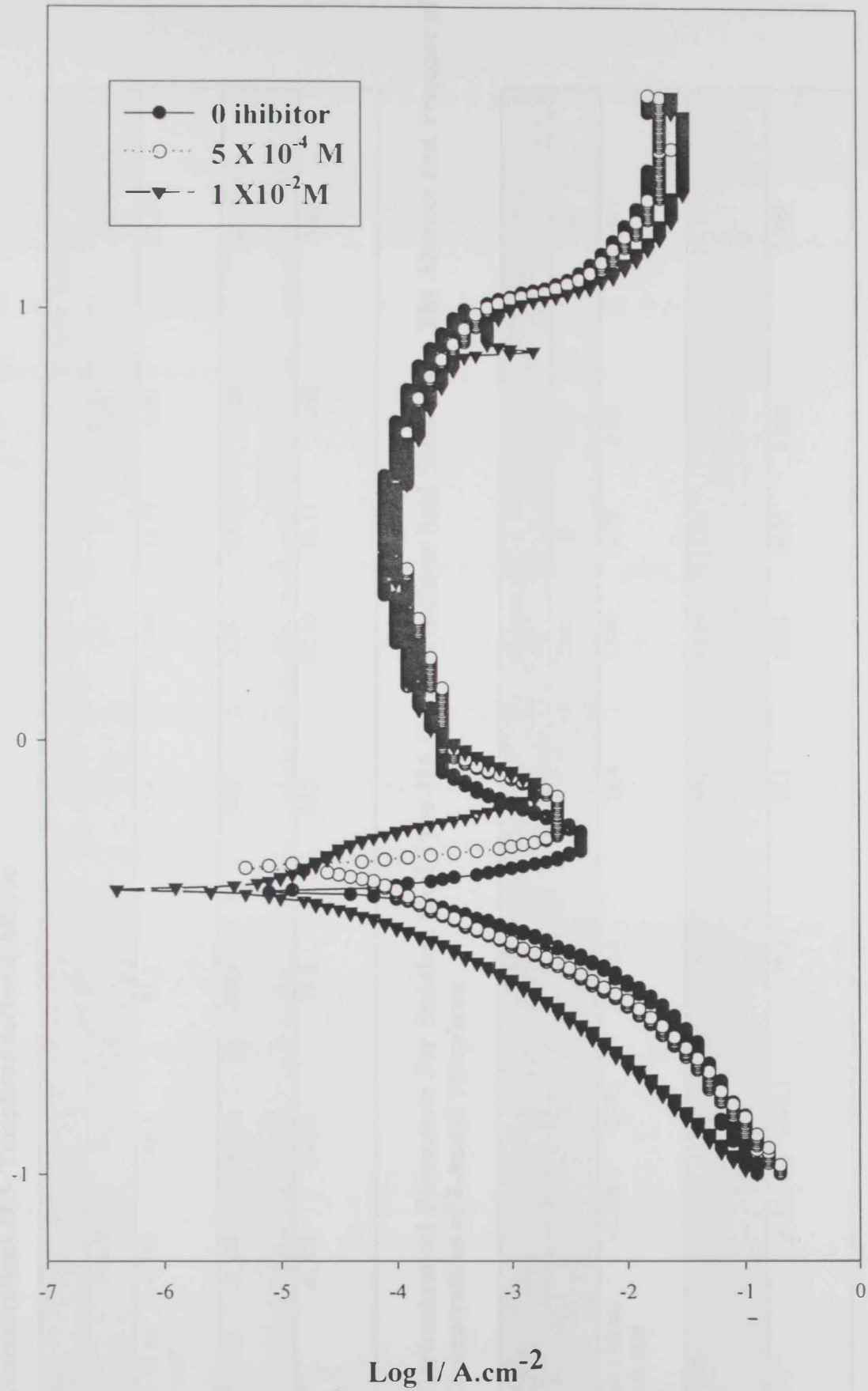

Figure 4: Potontiodynamic Curve of Stainless Steel Type 316 in 0.5 M H_2SO_4 in Presence and Absence of 3-Thiophene carboxaldhyde

Table 1. Electrochemical Parameters For Stainless Steel Type 316 in 0.5 M Sulfuric Acid Solutions in The Absence and Presence of Different Concentrations of 3- Thiophene carboxayldhyde

[Inhibitor] mol/L	E (mV)		β_c mV/Decade	β_a mV/Decade	R_p (ohm.cm^2) x 10^2		Corr. Rate (MPY)	
	Eoc(V)	E_{cor}			Tafel	B	Tafel	Tafel
5 ml ethanol + 45 ml 0.5sulfuric acid	-0.388	-348.1	88.1	55.4	1.640	14.78	0.90	82.541
5×10^{-4}	-0.362	-291.9	112.6	30.9	3.95	10.54	0.266	24.39
1×10^{-2}	-0.328	-343.5	78.6	99.8	32.39	19.11	0.058	5.404

Table 2. Electrochemical Parameters For Stainless Steel Type 316 in 0.5 M Sulfuric Acid Solutions in The Absence and Presence of Different Concentrations of 2-Acetyl Thiophene

[Inhibitor] mol/L	E (mV)		β_c mV/Decade	β_a mV/Decade	R_p (ohm.cm^2) x 10^2		Corr. Rate (MPY)	
	Eoc(V)	E_{cor}			Tafel	B	Tafel	Tafel
5 ml ethanol + 45 ml 0.5sulfuric acid	-0.388	-348.1	88.1	55.4	1.640	14.78	0.90	82.541
5×10^{-4}	-0.382	-345.1	76.2	56.3	4.336	14.07	0.32	29.723
1×10^{-2}	-0.371	-343.1	70.5	77.1	19.84	16.01	0.080	7.390

This equation has the form y = mx + b, so a plot of η vs. log i is a straight line with slope β. As could be noticed from equation (2), when η = 0 (at E_{CORR}), log i/i_{CORR} = 0, i/i_{CORR} = 1, and $i = i_{CORR}$. The anodic and cathodic Tafel constants are used to calculate the corrosion rate from polarization measurement data according to the following equations:

$$\frac{\Delta E}{\Delta i} = \frac{\beta_a \beta_c}{2.3(i_{corr})(\beta_a + \beta_c)} \qquad (3)$$

Where ΔE/Δi = slope of the polarization resistance plot, where ΔE is expressed in volts and Δi is expressed in μA. β_a, and β_c are anodic and cathodic Tafel constants, respectively. The values of the Tafel constants are determined from the Tafel plot. I_{corr} being the corrosion current in μA. Rearranging equation (3) yields:

$$i_{CORR} = \frac{\beta_a \beta_c}{2.3(\beta_a + \beta_c)} \frac{\Delta i}{\Delta E} \qquad (4)$$

Therefore, the corrosion current can be related directly to the corrosion rate through the following equation:

$$Corrsion\ rate(mpy) = \frac{0.13\, i_{corr}(E.W.)}{d} \qquad (5)$$

E.W. = equivalent weight of the corroding species, g.

d = density of the corroding species, g/cm^3.

i_{corr} = corrosion current density, $\mu A/cm^2$.

The inhibition efficiency (P)is given by the following relation:

$$P = \left(\frac{i_{corr(un.)} - i_{corr(inh.)}}{i_{corr(un.)}} \right) \times 100 \qquad (6)$$

d-d Effect of Varying the Concentration of Sulfuric Acid on the Efficiency of Inhibition

Polarization data for inhibited and uninhibited stainless steel 316 in 0.1 M, 0.5 M, and 1.0 M sulfuric acid solutions, are given in table 3. Anodic and cathodic Tafel slopes were reported in the range β_a/β_c = 121/87.5 to 169/106 [42, 44]. A slight difference is clearly observed in this study that indicates a change in the mechanism of inhibition for the thiophene derivatives when compared to those investigated previously.

As mentioned in preceding section, the thiophene derivatives appeared to act as mixed inhibitors. This observation was again proved when comparing the values of the anodic and cathodic Tafel constants (β_a/β_c) such as in the case of applying 2-thiophene carboxylic hydrazide (c.f. table 3). The values are: 58.3/106.2 mV/decade, and 88.9/76.9 mV/decade in absence and presence of 1.0 x 10^{-2} M 2-thiophene carboxylic hydrazide/0.1 M H_2SO_4, respectively. Two observations are worthwhile

mentioning: first, the values of the cathodic Tafel constant, β_c, calculated are generally smaller than those obtained for the uninhibited solutions in all concentrations H_2SO_4 studied. The values of the anodic Tafel constant, β_a, showed a general decrease in their values for the inhibited solutions with 2-thiophene carboxylic hydrazide compared to the uninhibited ones. Figure 5 shows the polarization curves for the inhibited stainless steel in different concentrations of sulfuric acid.

The polarization resistance values calculated from the potentiodynamic curve were $4.56 \times 10^2/5.39 \times 10^2$, $4.9 \times 10^3/2.70 \times 10^2$, $2.55 \times 10^1/2.68 \times 10^2$ ohms for the uninhibited solutions and the inhibited ones with different concentrations of H_2SO_4, respectively. The corresponding calculated corrosion rates are 0.834/0.772, 0.528/0.969, and 19.47/1.02 MPY, respectively. Again, a reduction of up to about 94.74% in the rate of corrosion of the inhibited stainless steel in the 1.0 M sulfuric acid solution is therefore observed when compared to the non-inhibited one. The corrosion rate observed in the more concentrated solution was however, relatively higher than those found in the less concentrated acid solution. Exception was observed in the case of H_2SO_4 with concentration of 0.5 M, in which the stainless steel surface exhibited a peculiar trend.

mol/L			mV/Decade	mV/Decade	(ohm.cm^2) X 10^2			
0.1 M H_2SO_4	-352.2	-348.5	106.2	58.3	4.57	16.36	0.358	0.834
0.1 M H_2SO_4 + 10^{-2} M TCH	-394.1	-403.5	76.9	88.9	5.39	17.92	0.331	0.772
0.5 M H_2SO_4	-214.1	-215.7	342.7	1013.0	49.03	111.3	0.226	0.528
0.5 M H_2SO_4 + 10^{-2} M TCH	-315.4	-323.8	78.7	38.7	2.70	144.1	0.416	0.967
1.0 M H_2SO_4	-15.6	-1.0	112.0	87.8	0.256	21.39	8.36	19.47
1.0M H_2SO_4 + 10^{-2} M TCH	-21.5	-17.1	104.5	36.9	2.68	11.72	0.440	1.026

Table 3 Electrochemical Parameters For Stainless Steel Type 316 in Different concentration of sulfuric acid in presence of 1X10^{-2} M TCH , Data Derived form Potentiodynamic measurements.

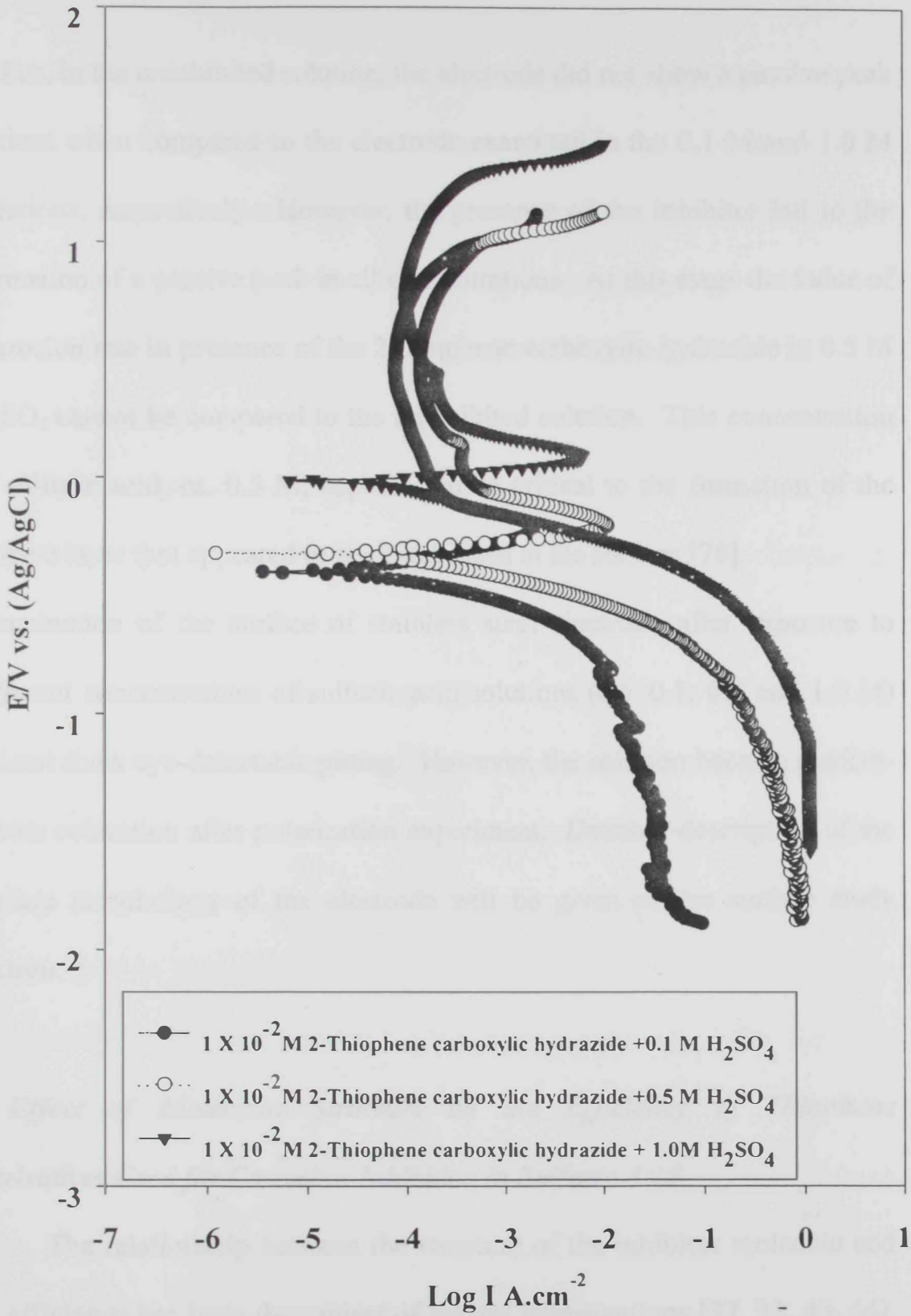

Figure 5. Potentiodynamic curves for 316 stainless steel in different acid concentrations in presence of 1 X 10^{-2} M 2-Thiophene carboxylic hydrazide

Thus, in the uninhibited solution, the electrode did not show a passive peak current when compared to the electrode examined in the 0.1 M and 1.0 M solutions, respectively. However, the presence of the inhibitor led to the formation of a passive peak in all concentrations. At this stage the value of corrosion rate in presence of the 2-thiophene carboxylic hydrazide in 0.5 M H_2SO_4 cannot be compared to the uninhibited solution. This concentration of sulfuric acid, ca. 0.5 M, appeared to be critical to the formation of the passive layer that appeared to be destabilized at the surface [78]. Examination of the surface of stainless steel electrode after exposure to different concentrations of sulfuric acid solutions (c.a. 0.1, 0.5 and 1.0 M) did not show eye-detectable pitting. However, the solution became reddish-brown coloration after polarization experiment. Detailed description of the surface morphology of the electrode will be given in the surface study section.

2 Effect of Molecular Structure on the Efficiency of Thiophene Derivatives Used for Corrosion Inhibition in Sulfuric Acid

The relationship between the structure of the inhibitor molecule and its efficiency has been the subject of several investigations [37, 38, 43, 44]. However, much less attention has been paid to the dependence of percentage

inhibition efficiency on the size and electronic distribution in the inhibitor molecule at the stainless steel surfaces. In this part of the present investigation, the candidate will attempt to answer few questions such as:

(i) What is the effect of changing the functional group in the side chain of the thiophene derivative on the percent inhibition efficiency?

(ii) What is the relation between the structure of the inhibitor molecules studied and their inhibition efficiencies?

(iii) What is the effect of changing the inhibitor on the mechanism of corrosion?

Figure 7 lists the compounds used in this study (cf. Figure 1 for structural formula). Energy minimization was used in order to display the compounds in three-dimensional format. Moreover, figure 6 reveals the electronic-density distribution profile for these compounds. From figures 1 and 6, one should be able to conclude the main criterion for the selection of the compounds studied that provided a number of variables. The variables considered in this study are:

(i) The effect of changing the position of substitution in the thiophene ring,

(ii) The change of type of substitution in the ring,

(iii) The change in the degree of functionality within the ring.

oth polarization resistance curves and Tafel plots for stainless steel in ılfuric acid in absence/presence of different thiophene derivatives with ifferent concentrations are given in figures 7a, 7b, 8a, 8b, 9a, 9b, 10a, and 0b, respectively. The electrochemical parameters derived from the above ıentioned polarization measurements are listed in tables 4a, 4b, 4c and 4d, espectively.

he data depicted in tables 4a-4d show that the inhibition efficiencies of ifferent thiophene derivatives is still pronounced even at relatively low oncentrations of the inhibitor used. However, the values of the inhibition fficiency increase as the concentration of sulfuric acid increases (as shown efore) and as the concentration of the inhibitor increases. It could be oticed that the values of the anodic and cathodic Tafel constants (β_a and $_c$), generally showed the same trend observed with 2-thiophene carboxylic ydrazide for all other inhibitors studied. The values of the anodic and athodic Tafel constants ($\beta_a$and β_c) generally decrease upon addition of ıhibitor and start to increase again with irregularity after a critical oncentration of the inhibitor is reached [36, 38]. It is recognized that the ıhibitors that shift the entire current-potential curves towards more negative athodic) values are cathodic-type inhibitors while those that shift the urves in the anodic direction are anodic-type inhibitors [79].

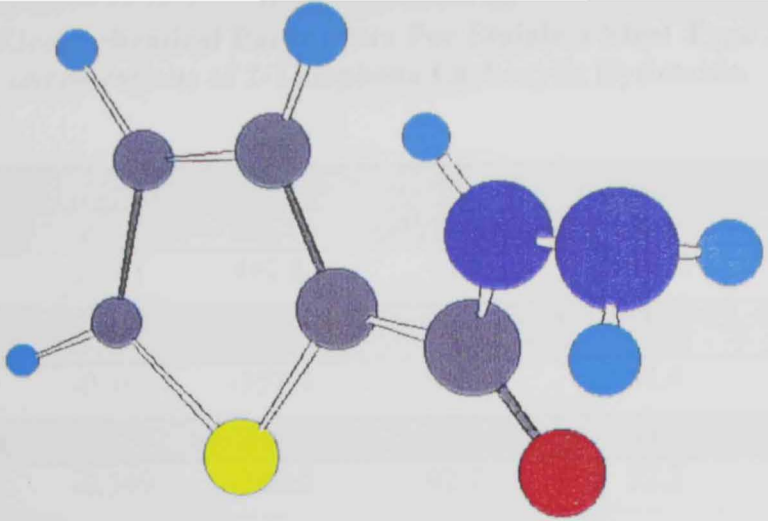

TCH

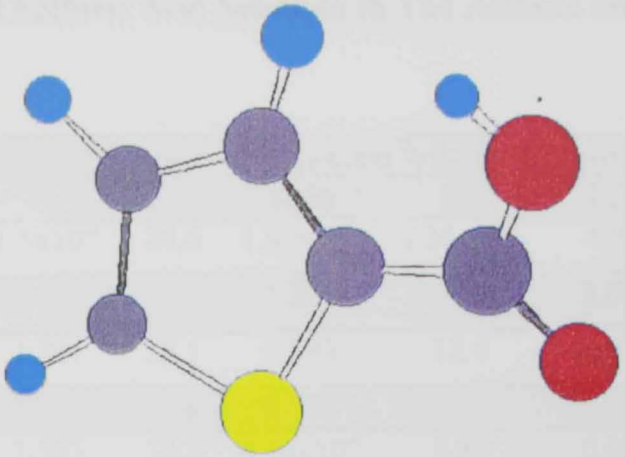

TCA

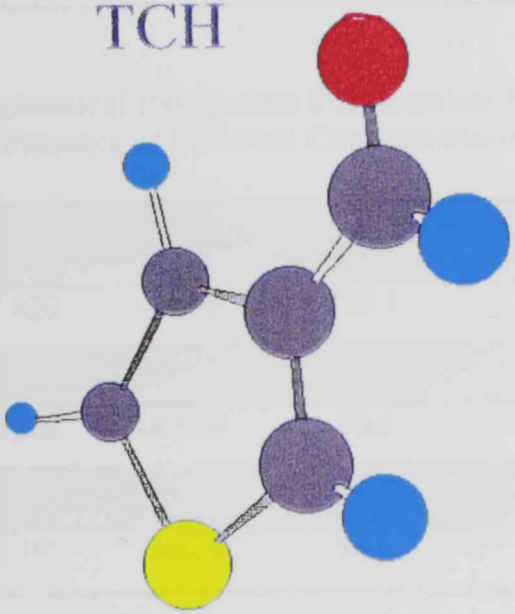

TCAL

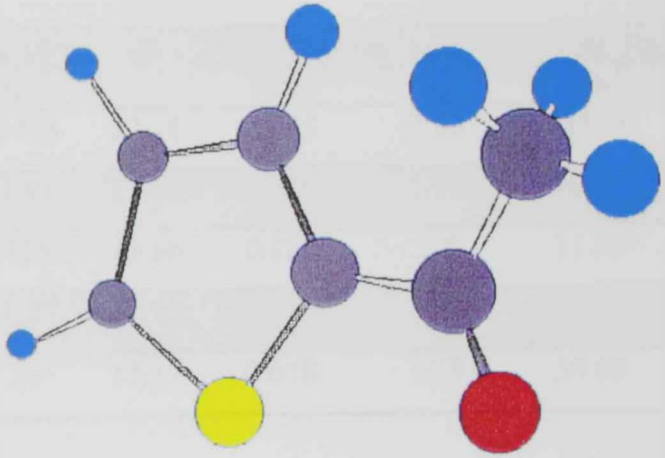

AcT

Figure 6. Conformation of Inhibitors

Table 4a Electrochemical Parameters For Stainless Steel Type 316 in 0.5 M Sulfuric Acid Solutions in The Absence and Presence of Different Concentrations of 2-Thiophene Carboxylic Hydrazide.

[Inhibitor]*	E (mV)		β_c	β_a	R_p (ohm.cm^2) x 10^2		B	I_{corr} (A.cm^{-2}) x 10^{-4}		Corr. Rate (MPY)	
mol/L	E_{oc}	E_{cor}	mV/Decade	mV/Decade	Tafel	R_p		Tafel	R_p	Tafel	R_p
0	0.461	462.8	117	109.6	$1.27x10^{-3}$	$1.3x10^{-3}$	24.6	$1.92x10^{3}$	$1.36x10^{3}$	4480	4185
$5 x 10^{-4}$	-0.359	-353.9	92.6	58.7	1.174	1.187	15.6	1.328	13.1	3.092	30.63
$1 x 10^{-3}$	-0.367	-357.4	86.6	58.4	1.684	1.241	15.1	0.899	12.4	2.093	28.35
$5 x 10^{-3}$	-0.359	-340.3	92.2	49.7	1.93	1.141	14.0	0.723	12.3	1.685	28.7
$1 x 10^{-2}$	-0.349	-349.0	92.7	52.2	17.7	1.531	14.5	$8.16x10^{-4}$	8.85	0.002	20.62

Table 4b Electrochemical Parameters For Stainless Steel Type 316 in 7 ml ethanol and diluted with 43ml Sulfuric Acid Solutions in The Absence and Presence of Different Concentrations of 2-Thiophene Carboxylic acid.

[Inhibitor]*	E (mV)		β_c	β_a	R_p (ohm.cm^2) x 10^2		B	I_{corr} (A.cm^{-2}) 10^{-4}		Corr. Rate (MPY)	
mol/L	Eoc(V)	E_{cor}	mV/Decade	mV/Decade	Tafel	R_p		Tafel	R_p	Tafel	R_p
0	-0.420	-419.6	120.1	88.9	0.8269	0.3458	22.18	2.684	7.53	245.96	690.68
$5 x 10^{-4}$	-0.396	-414.3	81.6	54.4	6.87	.9042	15.48	0.206	1.93	18.89	264.12
$1 x 10^{-3}$	-0.382	-406.0	80.6	46.9	10.1	1.416	13.66	0.126	1.8	11.59	168.64
$5 x 10^{-3}$	-0.404	-417.6	83.5	60.1	1.65	0.8077	16.49	0.920	3.24	84.32	295.627
$1 x 10^{-2}$	-0.385	-396.9	78.0	55.5	2.27	1.39	15.17	0.618	3.28	56.68	171.77

Table 4c Electrochemical Parameters For Stainless Steel Type 316 in 5 ml ethanol and diluted with 0.5 M Sulfuric Acid Solutions in The Absence and Presence of Different Concentrations of 3- Thiophene carboxaldehyde.

Inhibitor]*	E (mV)		β_c	β_a	R_p (ohm.cm^2) x 10^2		B	I_{corr} (A.cm^{-2}) x 10^{-4}		Corr. Rate (MPY)	
mol/L	E_{oc}	E_{cor}	mV/Decade	mV/Decade	Tafel	R_p		Tafel	R_p	Tafel	R_p
0	-0.404	-386.2	127.0	131.3	0.76	1.098	28.06	3.683	2.37	337.58	217.4
5×10^{-4}	-0.391	-366.7	93.8	38.3	4.353	1.252	11.82	0.262	2.08	24.03	190.67
1×10^{-3}	-0.387	-365.3	83.3	42.9	3.23	1.896	12.3	0.380	1.37	34.87	125.96
5×10^{-3}	-0.358	-336.4	77.6	28.3	16.4	4.771	9.016	0.0548	0.54	5.028	50.059
1×10^{-2}	-0.346	-335.6	81.3	40.3	22.8	8.38	11.7	0.0511	0.31	4.689	28.496

Table 4d Electrochemical Parameters For Stainless Steel Type 316 in 5 ml ethanol and diluted with 0.5 M Sulfuric Acid Solutions in The Absence and Presence of Different Concentrations of 2-Acetyl Thiophene.

[Inhibitor]*	E (mV)		β_c	β_a	R_p (ohm.cm^2) x 10^2		B	I_{corr} (A.cm^{-2}) x 10^{-4}		Corr. Rate (MPY)	
mol/L	E_{oc}	E_{cor}	mV/Decade	mV/Decade	Tafel	R_p		Tafel	R_p	Tafel	R_p
0	-0.381	-386.2	127	131.3	0.761	1.098	28.0	3.68	2.37	337.5	217.4
5×10^{-4}	-0.3915	-369.7	96.4	55.2	1.998	1.30	15.2	0.762	2.00	69.9	183.617
1×10^{-3}	-0.3919	-369.7	93.8	48.9	1.663	1.347	13.9	0.839	1.93	76.9	177.299
5×10^{-3}	-0.3909	-354.4	109.3	53.2	2.093	1.44	15.5	0.742	1.8	68.0	165.393
1×10^{-2}	-0.3859	-343.9	97.7	65.1	5.573	2.3	16.9	0.304	1.13	27.9	103.642

On the other hand, mixed-type inhibitors cause a shift in the cathodic Tafel lines towards more negative values and the current-potential curves near the free corrosion potential towards less cathodic potentials. In this respect, Tafel results for TCH showed a dramatic shift of the entire potential-current curves towards more cathodic values upon addition of the inhibitor. On the other hand, values of the corrosion potential, E_{corr}, showed slight shift towards more anodic values upon increasing the concentration of TCH while the corresponding corrosion current, i_{corr}, decreased towards much lower values (cf. figure 7a and table 4a). Moreover, the values of the anodic Tafel constant, β_a, decreased from a value of 109.6 mV/Decade for the uninhibited solution to a value of ~50.0 mV/Decade at higher concentrations of TCH. The corresponding values of the cathodic Tafel constant, β_c, showed a change in value from 117.0 mV/Decade to a value around 92.7 mV/Decade for all concentration studied of TCH. Polarization resistance data are depicted in figure 7b, and the corresponding electrochemical parameters are given in table 4a for TCH. Examination of figure 7b and table 4a revealed that the polarization resistance increased dramatically upon the addition of the inhibitor and resulted in a slight increase in the slope of the polarization resistance curve upon increasing the concentration of the inhibitor in solution.

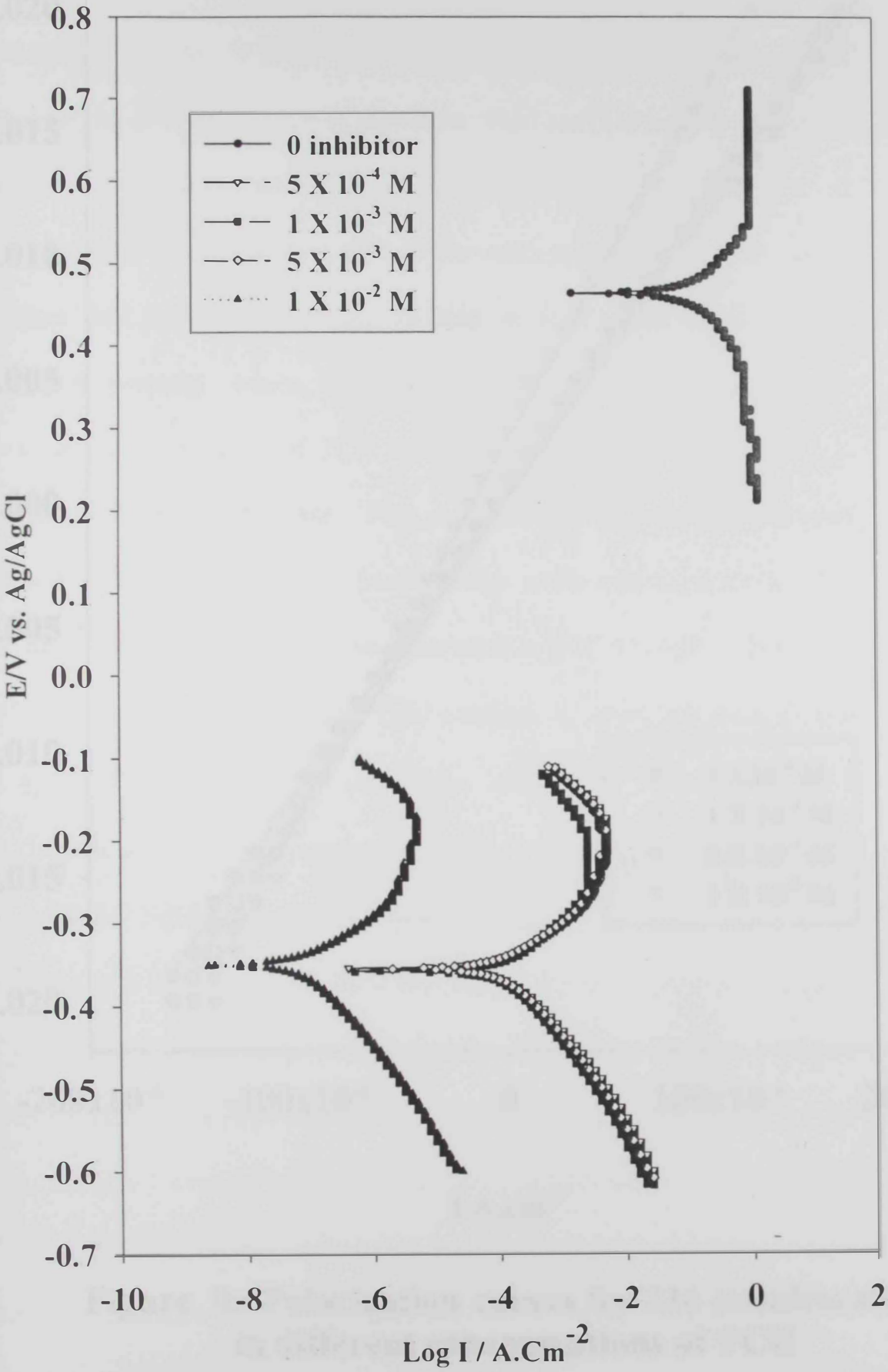

Figure 7a. Tafel curves for 316 stainless steel in 0.5M of sulforic acid in absence and presence of thiophene carboxylic hydrazide

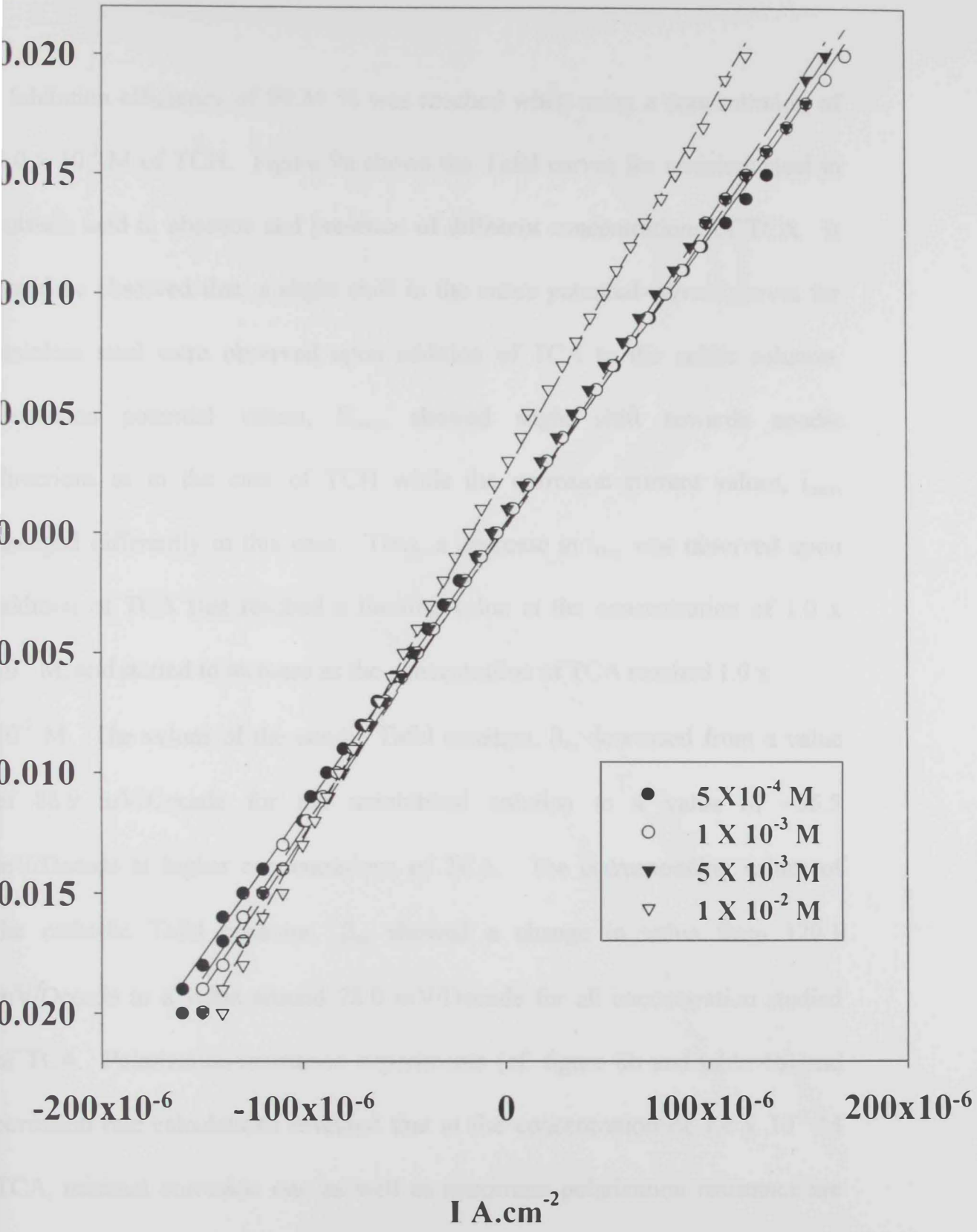

Figure 7b: Polarization curves for 316 stainless steel in different concentrations of TCH

Inhibition efficiency of 99.34 % was reached when using a concentration of .0 x 10^{-2} M of TCH. Figure 9a shows the Tafel curves for stainless steel in ulfuric acid in absence and presence of different concentrations of TCA. It could be observed that, a slight shift in the entire potential-current curves for tainless steel were observed upon addition of TCA to the acidic solution. Corrosion potential values, E_{corr}, showed slight shift towards anodic directions as in the case of TCH while the corrosion current values, i_{corr}, changed differently in this case. Thus, a decrease in i_{corr} was observed upon addition of TCA that reached a limiting value at the concentration of 1.0 x 0^{-3} M, and started to increase as the concentration of TCA reached 1.0 x 10^{-2} M. The values of the anodic Tafel constant, β_a, decreased from a value of 88.9 mV/Decade for the uninhibited solution to a value of ~55.5 mV/Decade at higher concentrations of TCA. The corresponding values of he cathodic Tafel constant, β_c, showed a change in value from 120.1 mV/Decade to a value around 78.0 mV/Decade for all concentration studied of TCA. Polarization-resistance experiments (cf. figure 8b and table 4b) and corrosion rate calculations revealed that at the concentration of 1.0 x 10^{-3} M TCA, minimal corrosion rate as well as maximum polarization resistance are achieved. This interesting observation could be explained on the basis that a critical concentration of TCA is reached in solution that caused optimal

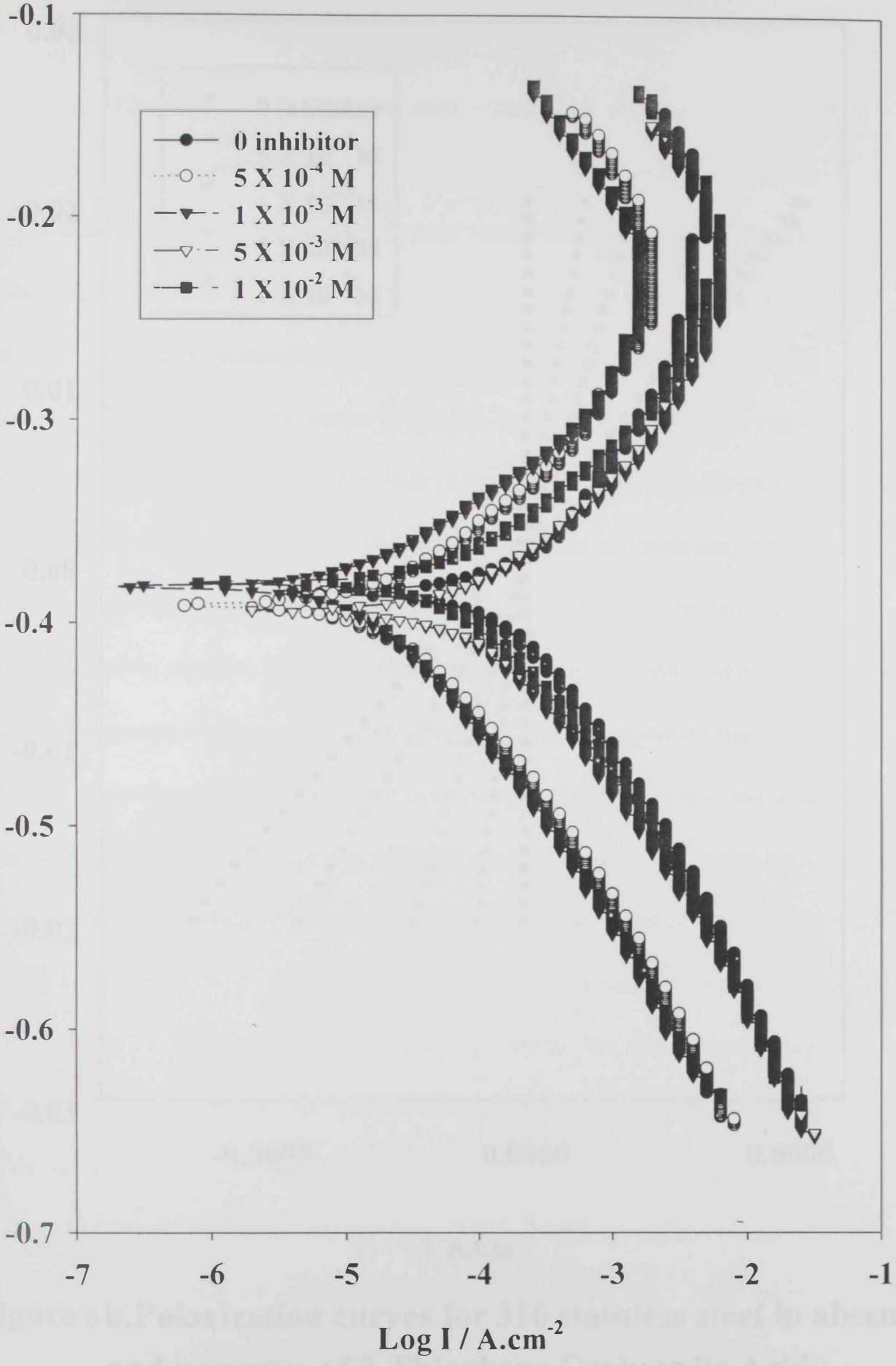

Figure 8a: Tafel curves for 316 stainless steel in 0.5 M of sulfuric acid in absence and presence of 2-Thiophene carboxylic acid

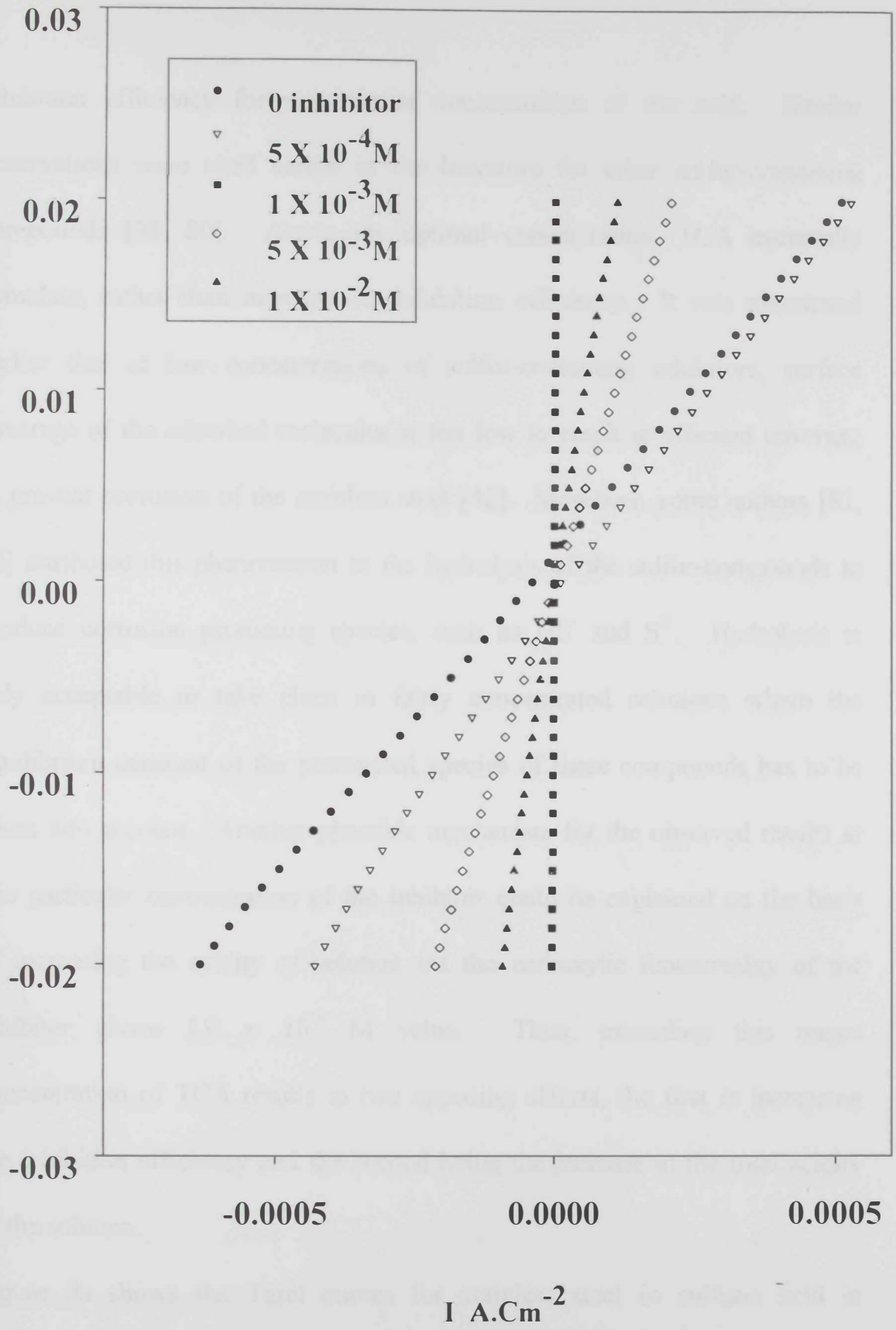

Figure 8 b.Polarization curves for 316 stainless steel in absence and presence of 2-Thiophene Carboxylic Acid

nhibition efficiency for a particular concentration of the acid. Similar bservations were cited earlier in the literature for other sulfur-containing ompounds [38, 80]. Above the optimal concentration, TCA eventually timulate, rather than increase the inhibition efficiency. It was mentioned arlier that at low concentrations of sulfur-containing inhibitors, surface overage of the adsorbed molecules is too low to result in efficient coverage o prevent corrosion of the stainless steel [42]. Moreover, some authors [81, 2] attributed this phenomenon to the hydrolysis of the sulfur-compounds to roduce corrosion promoting species, such as HS^- and S^{2-}. Hydrolysis is nly acceptable to take place in fairly concentrated solutions where the quilibrium constant of the protonated species of these compounds has to be aken into account. Another plausible mechanism for the observed results at his particular concentration of the inhibitor could be explained on the basis f increasing the acidity of solution via the carboxylic functionality of the nhibitor above 1.0×10^{-3} M value. Thus, exceeding this magic concentration of TCA results in two opposing effects, the first is increasing he inhibition efficiency and the second being the increase in the total acidity f the solution.

Figure 9a shows the Tafel curves for stainless steel in sulfuric acid in absence and presence of different concentrations of TCAL. E_{corr} values

how similar trend as that observed in the case of TCA. However, the trend bserved for the Tafel constants displayed some differences. On the other and, the values of i_{corr} exhibited a gradual decrease in value with increase in oncentration of the inhibitor. Thus, the values of the anodic Tafel constant, β_a, decreased from a value of 131.3 mV/Decade for the uninhibited solution o a value of ~ 40.3 mV/Decade at higher concentrations of TCAL. The orresponding values of the cathodic Tafel constant, β_c, showed a change in alue from 127.0 mV/Decade to a value around 81.3 mV/Decade for all oncentration studied of TCAL (cf. table 4c). Polarization resistance neasurements data are depicted in figure 9b. The data clearly exhibited an xpected trend of increase in the slope of the E-I with increase in the oncentration of the inhibitor added. Figure 11a depicts the data obtained or the Tafel measurements at stainless steel in sulfuric acid in absence and resence of different concentrations of AcT. The corresponding lectrochemical data are displayed in table 4d. As could be noticed from igure 10a, the entire potential-current curves are shifted towards more nodic values. Moreover, both anodic and cathodic Tafel constants showed hanges towards relatively lower values upon addition of AcT and upon ncreasing its concentration.

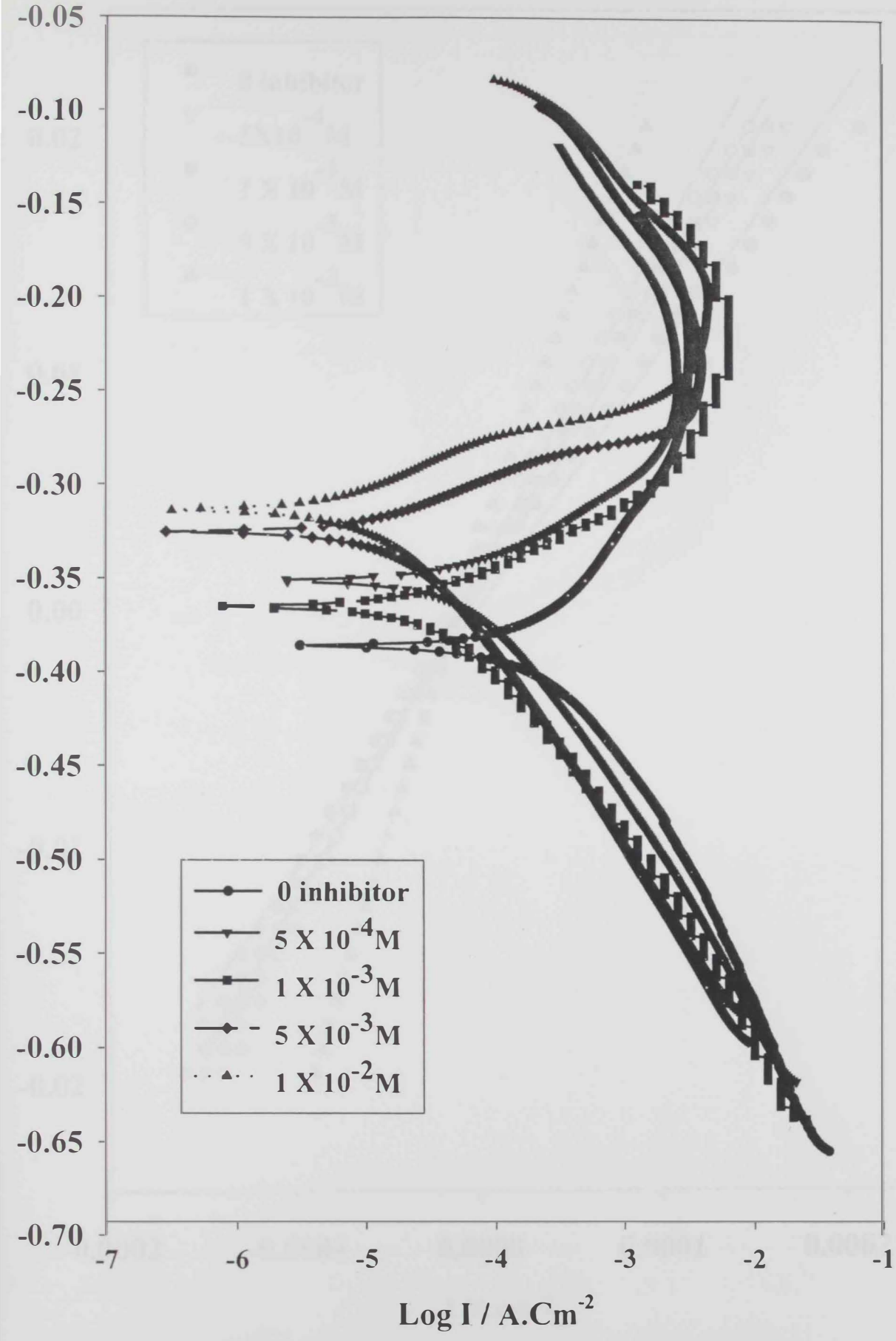

Figure 9 a.Tafel curves for stainless steel 316 in 0.5M sulforic in presence and absence of thiophene carboxaldehyde

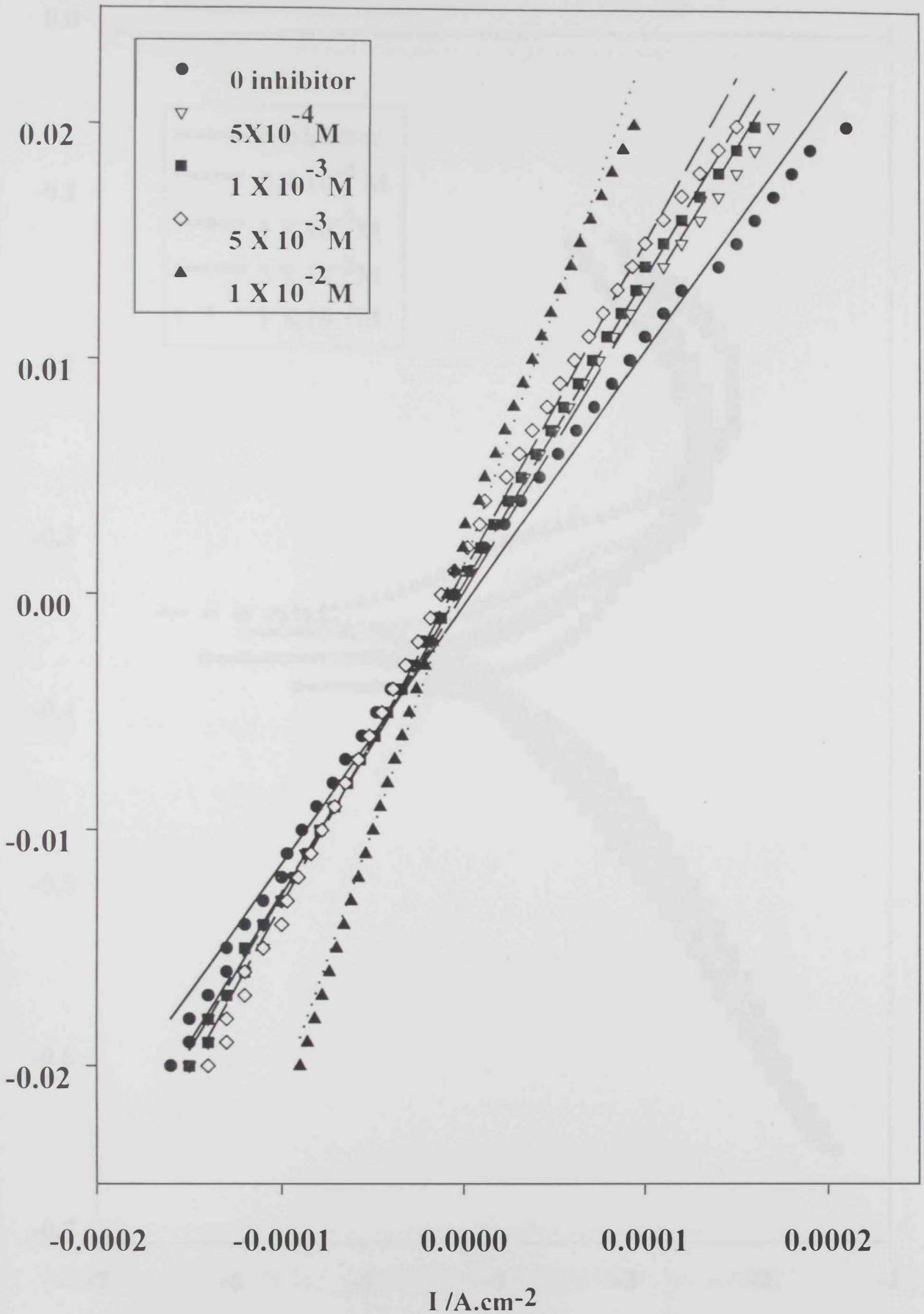

Figure 9 b. Stainless Steel 316 in 0.5 M Sulfuric Acid in Presence and Absence of 3-Thiophene Carboxaldehyde

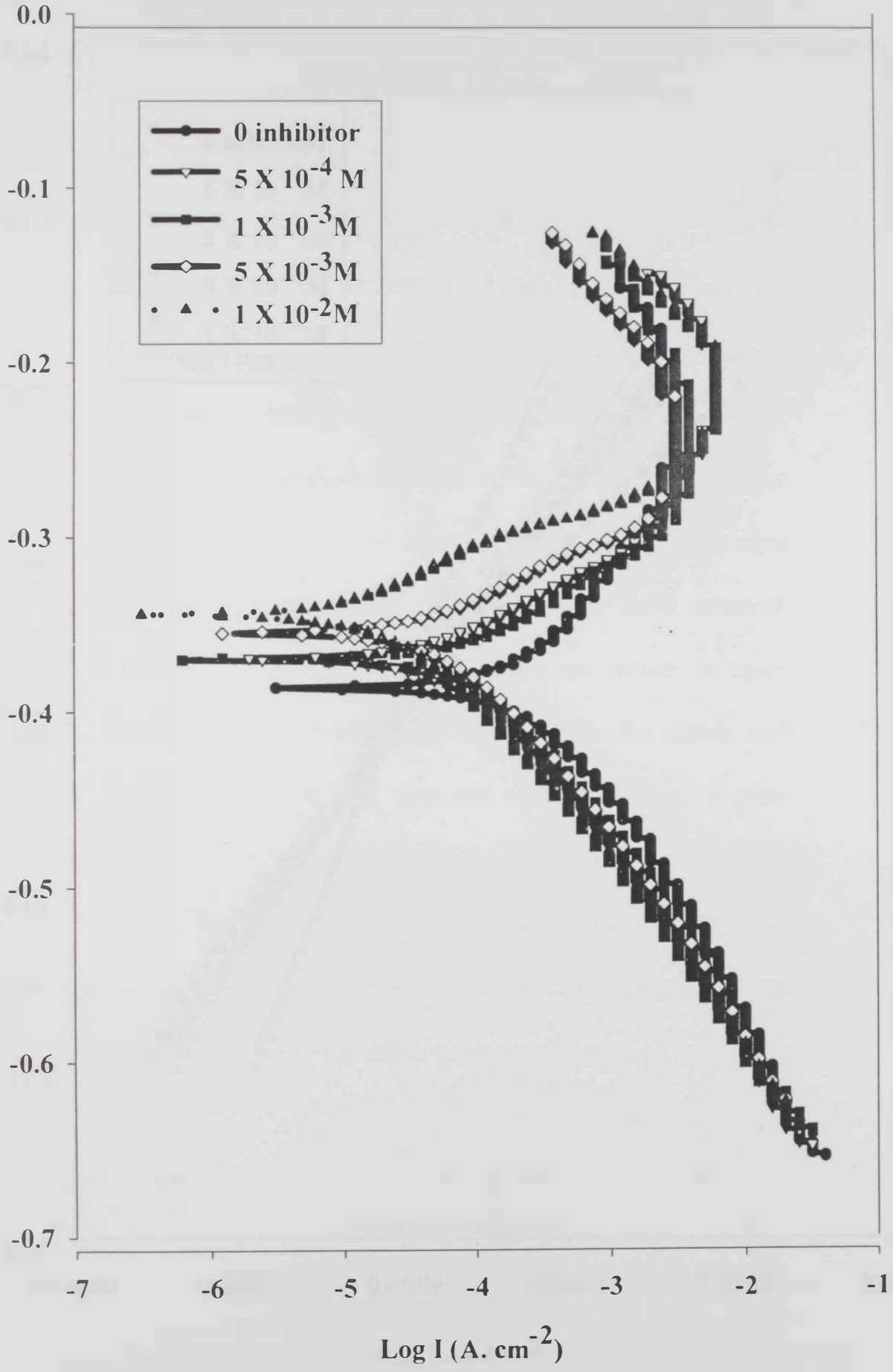

Figure 10a: Tafel curves for 316 in 0.5 M sulforic acid in absence and present of 2-Acetyl Thiophene

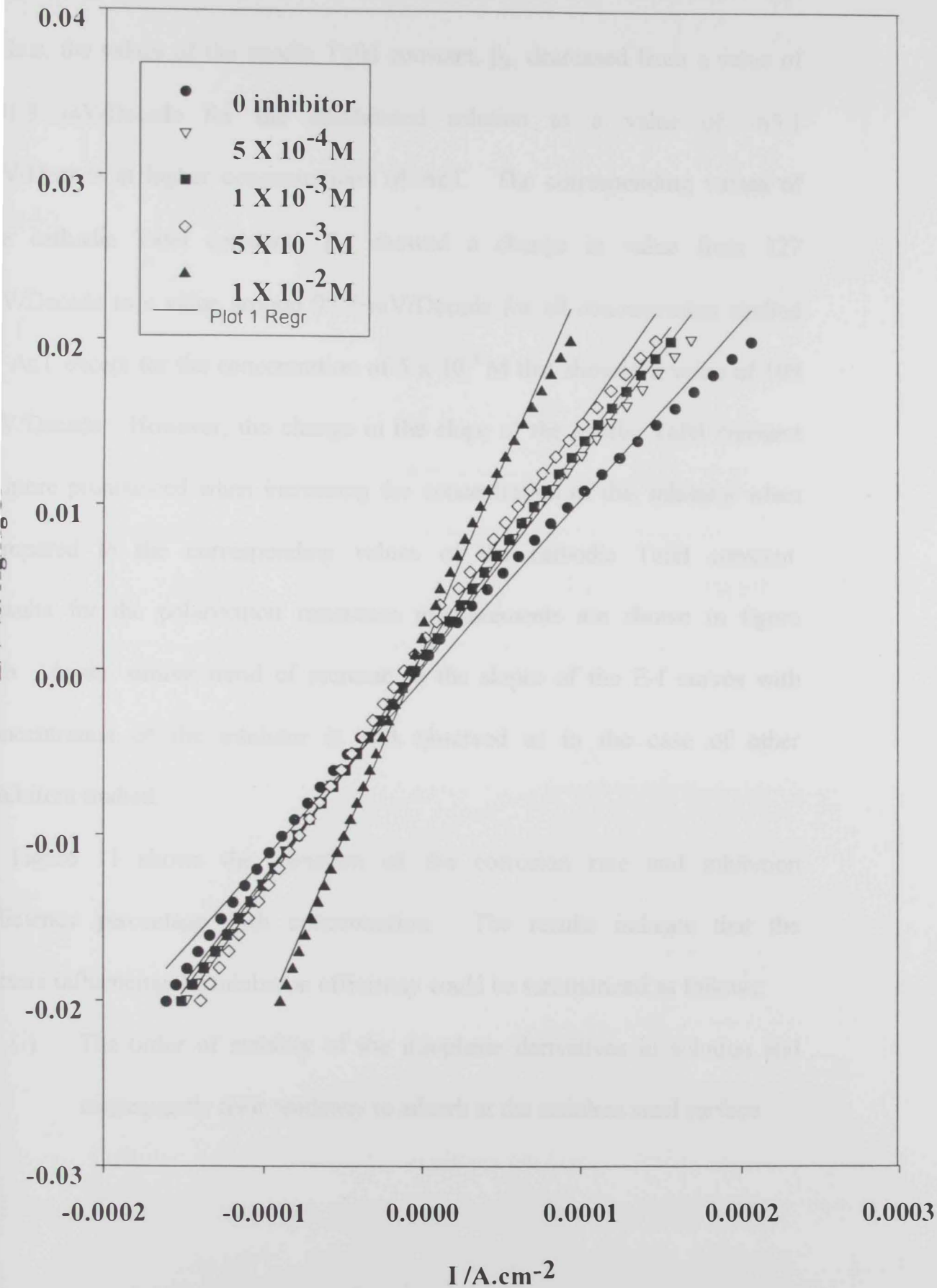

Figure 10b. Polarization curves for 316 in 0.5 M sulforic in presence and absence of acetyl thiophene

Thus, the values of the anodic Tafel constant, β_a, decreased from a value of 1.3 mV/Decade for the uninhibited solution to a value of ~65.1 V/Decade at higher concentrations of AcT. The corresponding values of e cathodic Tafel constant, β_c, showed a change in value from 127 V/Decade to a value around 97.7 mV/Decade for all concentration studied AcT except for the concentration of 5×10^{-3} M that showed a value of 109 V/Decade. However, the change in the slope of the anodic Tafel constant more pronounced when increasing the concentration of this inhibitor when mpared to the corresponding values of the cathodic Tafel constant. esults for the polarization resistance measurements are shown in figure b. Again, similar trend of increase in the slopes of the E-I curves with ncentration of the inhibitor is still observed as in the case of other hibitors studied.

Figure 11 shows the variation of the corrosion rate and inhibition fficiency percentage with concentration. The results indicate that the ctors influencing the inhibition efficiency could be summarized as follows:

(i) The order of stability of the thiophene derivatives in solution and consequently their tendency to adsorb at the stainless steel surface.

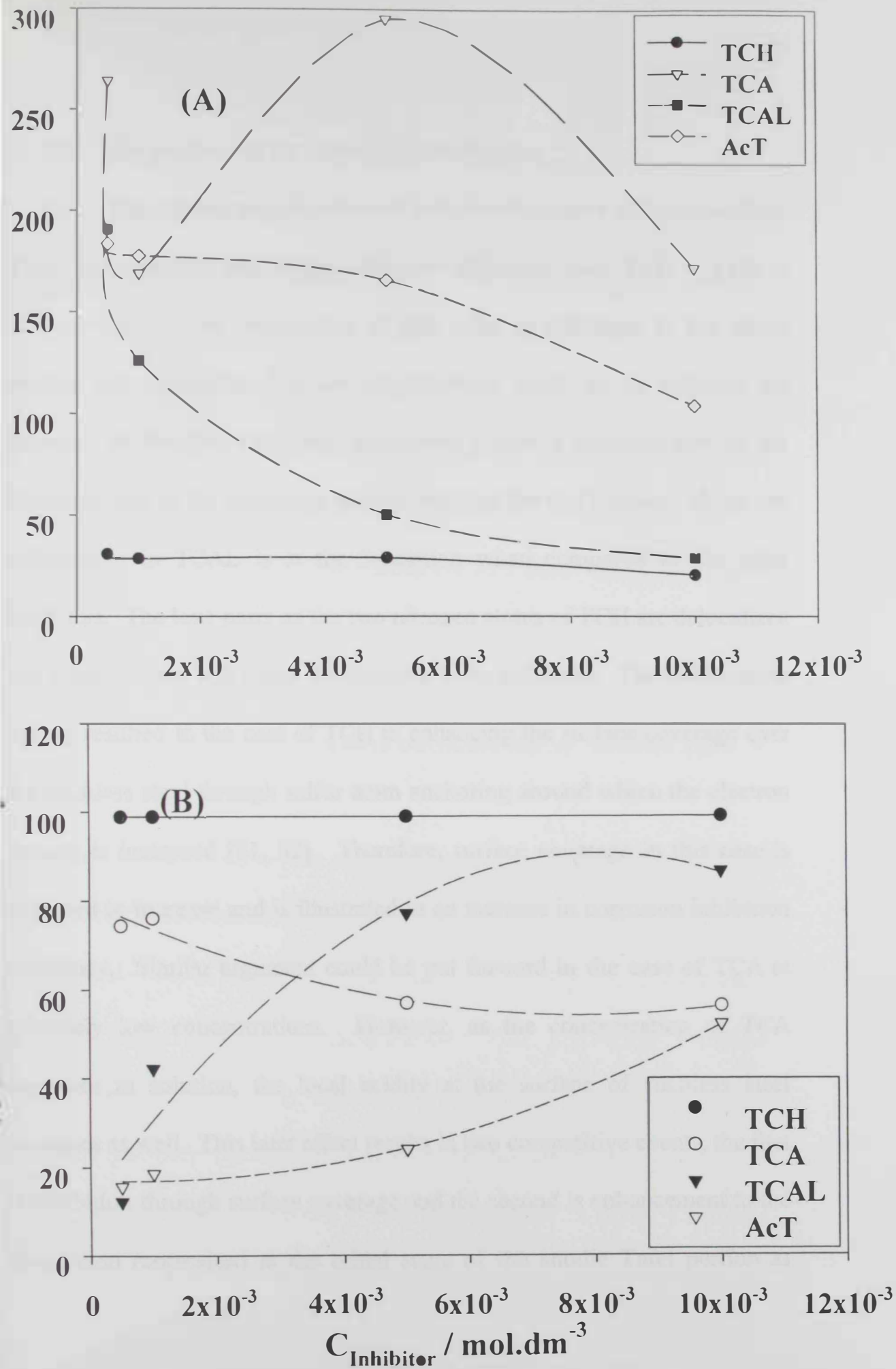

Figure 11. Variation Rate and % Inhibition Effeciency

(ii) The position of the substitution on the ring.

(iii) The number and the nature of substituent (degree of functionality).

Thus, the order of percentage inhibition efficiency was TCH > TCA > TCAL > AcT. The explanation of this order in reference to the above factors and molecular structure consideration could be as follows: the structure of the four thiophene derivatives posses a common part of the structure, that is the thiophene moiety attached the C=O group. However, substitution in TCAL is at the 3-position when compared to the other inhibitors. The lone pairs on the two nitrogen atoms of TCH are delocalized and consequently will cause the structure to be stabilized. The stabilization energy resulted in the case of TCH in enhancing the surface coverage over the stainless steel through sulfur atom anchoring around which the electron density is increased [81, 82]. Therefore, surface coverage in this case is expected to increase and is illustrated in an increase in corrosion inhibition efficiency. Similar argument could be put forward in the case of TCA at relatively low concentrations. However, as the concentration of TCA increases in solution, the local acidity at the surface of stainless steel increases as well. This later effect results in two competitive events, the first is inhibition through surface coverage and the second is enhancement to the dissolution (corrosion) at the initial stage of the anodic Tafel portion as

ndicated in the I-E curve. The results indicated that TCAL exhibited a egular increase in the percentage of inhibition efficiency that reached a table value at the higher concentration. The leveling in the inhibition fficiency could be explained from the fact of the possible formation of thin olymeric layer at the surface of the stainless steel due to the polymerization f TCAL [83]. On the other hand, AcT exhibited the least percentage in nhibition efficiency. This could be explained in terms of the lack of resence of lone pairs on the methyl group for AcT when compared to other ompounds.

- Temperature Coefficient of Corrosion Inhibition of Stainless Steel by hiophene Carboxaldehyde

The corrosion of stainless steel 316 in 0.5 M H_2SO_4 in absence and resence of different concentrations of thiophene carboxaldehyde (5.0 x 0^{-4}–1.0 x 10^{-2} M) at different temperatures (25–40 °C) was studied using afel and linear polarization experiments. The percentage inhibition fficiency was calculated using equation (6). Figure 12 shows the plot of the rotection efficiency against the logarithm of concentration of TCAL at ifferent temperatures. Inspection of the data depicted in figure 12 reveals at the extent of protection efficiency increases with the concentration of

the inhibitor as mentioned before. On the other hand, it was found that the inhibition protection efficiency decreases with increasing the temperature. Moreover, it could be noticed that the curves possess a characteristic s-shaped isotherms for some concentrations of the acid used, that indicate an adsorption mechanism for the inhibition process. General irregularity could be observed at some concentrations for different temperatures. The studied inhibitor is a five-member heterocycle ring with either half-chair or envelope-like structures [84, 85] with the most probable structure in the half-chair form. The adsorption may be mainly via the lone-pair of the sulfur-atom in the ring while the rest of the molecule covers the surface in the case of TCAL. Some interaction of the electron cloud of the ring could also be expected along with water displacement from the surface as indicated previously by Hubbard et al. [86]. The resulting mode of coverage of the inhibitor to the surface would be an anchor (through the sulfur atom) and a blanket (from the rest of the molecule). Different adsorption isotherms were suggested in the literature [85 – 87] and were tested for their fit to the experimental data. The degree of coverage, θ, at constant potential is given by the following relation [88, 89]:

$$\theta = 1 - \frac{i_c}{i_a} \qquad (7)$$

Table 5a. **Electrochemical Parameters For Stainless Steel Type 316 in 0.5 M Sulfuric Acid Solutions in The Absence and Presence of Different Concentrations of 2-Thiophene Carboxaldehyde at 25° C.**

[Inhibitor]*	E (mV)		β_c	β_a	R_p (ohm.cm^2) x 10^2		B	I_{corr} (A.cm^{-2}) x 10^{-4}		Corr. Rate (MPY)	
mol/L	E_{oc}	E_{cor}	mV/Decade	mV/Decade	Tafel	R_p		Tafel	R_p	Tafel	R_p
0	-0.404	-386.0	127	131.3	0.76	1.098	28.06	3.683	2.37	337.588	217.4
5×10^{-4}	-0.368	-339.4	93.8	38.3	2.53	1.252	11.82	0.262	2.08	24.03	190.67
1×10^{-3}	-0.387	-365.3	86.8	40.2	3.069	1.896	12.3	0.388	1.37	35.642	125.96
5×10^{-3}	-0.358	-336.4	77.6	28.3	16.4	4.771	9.016	0.0548	0.54	5.028	50.059
1×10^{-2}	-0.346	-335.6	81.3	40.3	22.8	8.38	11.7	0.0511	0.31	4.689	28.496

Table 5b. **Electrochemical Parameters For Stainless Steel Type 316 in 0.5 M Sulfuric Acid Solutions in The Absence and Presence of Different Concentrations of 2-Thiophene Carboxaldehyde at 30° C**

[Inhibitor]*	E (mV)		β_c	β_a	R_p (ohm.cm^2) x 10^2		B	I_{corr} (A.cm^{-2})x 10^{-4}		Corr. Rate (MPY)	
mol/L	Eoc(V)	E_{cor}	mV/Decade	mV/Decade	Tafel	R_p		Tafel	R_p	Tafel	R_p
0	-0.327	-325.5	78.1	40.1	1.11	1.241	11.5	1.16	2.10	103.95	192.5
5×10^{-4}	-0.336	-321.7	90.1	38.2	2.49	1.137	11.6	0.467	2.29	42.82	210.0
1×10^{-3}	-0.335	-310.5	87.1	30.5	3.09	1.550	9.82	0.316	1.68	29.02	154.1
5×10^{-3}	-0.313	-283.1	101.0	20.4	3.56	2.80	7.37	0.206	0.923	18.90	84.65
1×10^{-2}	-0.297	-274.8	94.5	28.8	7.92	5.773	9.59	0.119	0.54	10.90	41.3

Table 5c. Electrochemical Parameters For Stainless Steel Type 316 in 0.5 M Sulfuric Acid Solutions in The Absence and Presence of Different Concentrations of 2-Thiophene Carboxaldehyde at 35° C.

[Inhibitor]* mol/L	E (mV)		β_c mV/Decade	β_a mV/Decade	R_p (ohm.cm^2) x 10^2		B	I_{corr} (A.cm^{-2})		Corr. Rate (MPY)	
	Eoc(V)	E_{cor}			Tafel	R_p		Tafel x 10^{-4}	R_p x 10^{-4}	Tafel	R_p
0	-0.340	-334.2	111.3	85.3	0.866	0.628	20.3	2.4	4.14	221.8	380.2
5 x 10^{-4}	-0.816	-796.1	89.0	33.3	1.046	0.916	10.5	1.005	2.84	92.14	260.6
1 x 10^{-3}	-0.811	-794.7	93.2	32.1	1.295	0.847	10.3	0.800	3.07	73.38	281.6
5 x 10^{-3}	-0.326	-297.2	87.5	38.5	27.16	14.92	11.6	0.427	1.74	39.17	160.1
1 x 10^{-2}	-0.312	-289.8	80.7	33.0	27.35	20.31	19.1	0.371	1.28	34.06	117.6

Table 5d. Electrochemical Parameters For Stainless Steel Type 316 in 0.5 M Sulfuric Acid Solutions in The Absence and Presence of Different Concentrations of 2-Thiophene Carboxaldehyde at 40° C.

[Inhibitor]* mol/L	E (mV)		β_c mV/Decade	β_a mV/Decade	R_p (ohm.cm^2) x 10^2		B	I_{corr} (A.cm^{-2}) x 10^{-4}		Corr. Rate (MPY)	
	E_{oc}	E_{cor}			Tafel	R_p		Tafel	R_p	Tafel	R_p
0	-0.350	-343.8	92.0	54.4	1.145	0.985	14.8	1.296	2.64	118.7	242.2
5 x 10^{-4}	-0.344	-322.9	97.2	43.3	1.250	1.077	13.0	1.040	2.419	95.30	221.6
1 x 10^{-3}	-0.331	-313.3	82.0	31.9	3.634	1.549	9.98	0.274	1.682	25.14	154.1
5 x 10^{-3}	-0.325	-298.7	90.2	24.29	2.047	2.044	8.3	0.404	1.275	37.04	116.8
1 x 10^{-2}	-0.300	-275.5	96.3	20.30	5.365	3.566	7.28	0.136	0.730	12.61	66.96

Where i_a, i_c are the corrosion currents of uninhibited and inhibited experiments, respectively.

As was indicated above, the inhibition efficiency increases with concentration, however shows irregularities at some concentrations with temperature as indicated in figure 12. The latter is confirmed by inspecting the values of the Tafel constants listed in table 5a, 5b, 5c, and 5d, respectively. More interestingly, the values of the cathodic Tafel constant (β_c) that corresponds to hydrogen evolution in absence of inhibitor, decreased noticeably as the temperature increases from 25 to 30 °C. The value of β_c starts to increase again as the temperature increases above 30 °C. Bockris et al. [90], formalized a mechanism for hydrogen evolution reaction as β_c decreases with temperature. In this case, the mechanism seems to work similarly for lower temperatures and changes as the temperature increases. On the other hand, corresponding values of β_a showed similar trend as those for β_c. The relatively lower values found in this study for the stainless steel compared to those found for mild steel [91] and iron [92], are due to less impurities present in stainless steel. Effective inhibition efficiency is, therefore, more pronounced at lower temperatures. The calculated protection efficiencies when using 5.0×10^{-3} M TCAL are 77.2, 56.0, 51.7, 57.9 % in 0.5 M H_2SO_4 at 25, 30, 35, and 40 °C, respectively.

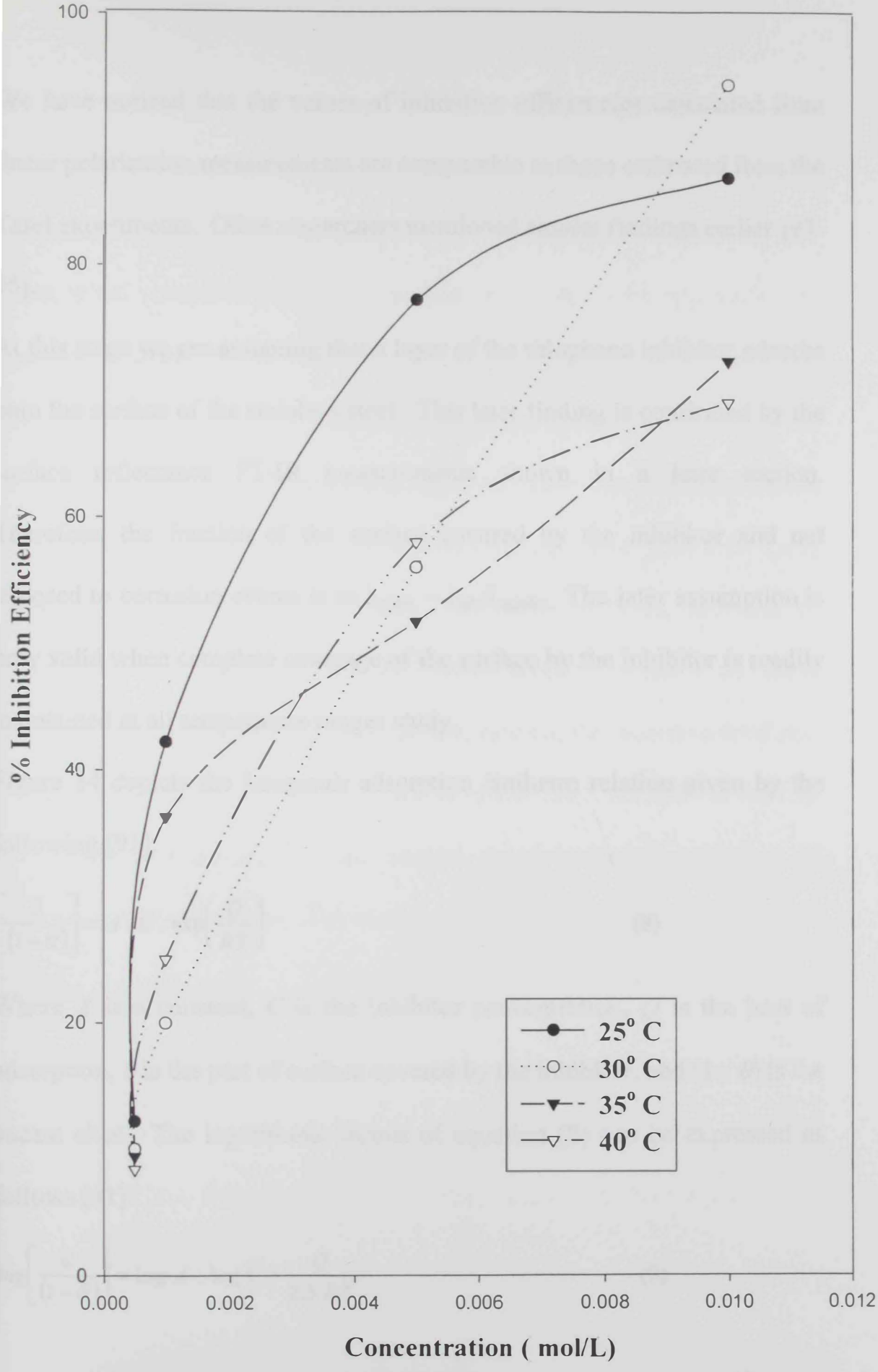

Figure 12. Inhibition effeiciency for different concentration of TCAL at different temperature

We have noticed that the values of inhibition efficiencies calculated from linear polarization measurements are comparable to those estimated from the Tafel experiments. Other researchers mentioned similar findings earlier [93-95].

At this stage we are assuming that a layer of the thiophene inhibitor adsorbs onto the surface of the stainless steel. This later finding is confirmed by the surface reflectance FT-IR measurements shown in a later section. Therefore, the fraction of the surface covered by the inhibitor and not exposed to corrosion events is to $i_{uninh.} - i_{inh.}/i_{uninh.}$. The later assumption is only valid when complete coverage of the surface by the inhibitor is readily maintained at all temperature ranges study.

Figure 14 depicts the Langmuir adsorption isotherm relation given by the following [91]:

$$\left[\frac{\theta}{(1-\theta)}\right] = A \,.\, C \,.\, \exp\left(\frac{Q}{RT}\right) \qquad (8)$$

Where A is a constant, C is the inhibitor concentration, Q is the heat of adsorption, θ is the part of surface covered by the inhibitor, and $(1 - \theta)$ is the vacant sites. The logarithmic format of equation (8) can be expressed as follows [91]:

$$\log\left[\frac{\theta}{(1-\theta)}\right] = \log A + \log C + \frac{Q}{2.3\,RT} \qquad (9)$$

Thus, a plot of log [$\theta/(1-\theta)$] vs. log C should yield a straight line. As could be noticed from figure 14 that as the temperature reaches 40 °C, the change in surface coverage with change in temperature differs in magnitude and extent when compared to lower temperatures. A direct application of Langmuir equation (9) is to plot values of log [$\theta/(1-\theta)$] vs. 1/T at given concentration values. The heat of adsorption could be estimated for different concentrations as depicted in figure 15. The heats of adsorption are -83.18, -60.34, -131.63, and -116.47 for 5.0×10^{-4}, 1.0×10^{-3}, 5.0×10^{-3}, and 1.0×10^{-2} M inhibitor, respectively. On the other hand, the heat of adsorption could be estimated from the relation between the rate of corrosion and the inverse of temperature [91]. In this method, the total measured rate of corrosion could be expressed as the sum of two rates, the first for the rate of uninhibited reaction, and the second for the rate of corrosion of completely covered surface. The expression of these two rates is [91]:

$$\frac{-d[Fe]}{dt} = K_1(1-\theta) + K_2\theta \qquad (10)$$

Where K_1 and K_2 are the rate constants of the two processes, respectively. In most of our discussion, we will be considering the Langmuir model of adsorption. Thus, from substituting for the values of θ from equation (8) into equation (10), we obtain:

$$\frac{-d[Fe]}{dt} = \frac{K_1}{1 + ACe^{Q/RT}} + \frac{K_2 ACe^{Q/RT}}{1 + ACe^{Q/RT}} \qquad (11)$$

n equation (11), the activation energy should increase as the extent of nhibition increases. This is related to the term $A.C.e^{Q/RT}$, and when the surface is inhibited, C is equal to zero. Upon rearrangement of equation (11), where K_1 and K_2 are replaced by their exponential forms:

$$\frac{-d[Fe]}{dt} = \frac{K_1' e^{-E_1/RT}}{1 + ACe^{Q/RT}} + \frac{K_2' ACe^{Q/RT - E_2/RT}}{1 + ACe^{Q/RT}} \qquad (12)$$

In the later case, the activation energy for the corrosion process should be equal to E_1. Moreover, as the extent of inhibition increases, and θ becomes large, the activation energy increases to equal (E_1+Q). At very large values for θ the activation energy is equal to E_2. If we assume intermediate coverage by the inhibitor to the stainless steel surface and adopting the Langmuir model, the activation energy of adsorption could be determined. In this respect, a plot of the rate of corrosion versus 1/T as depicted in figure 15 would allow the calculation of activation energy of adsorption. The activation energy is then plotted versus the inhibitor concentration as shown in figure 16. The maximum value shown in figure 16 corresponds to the value of (E_1+Q) that is equal to 110 kJ.mol^{-1} for 3 x 10^{-3} mol.

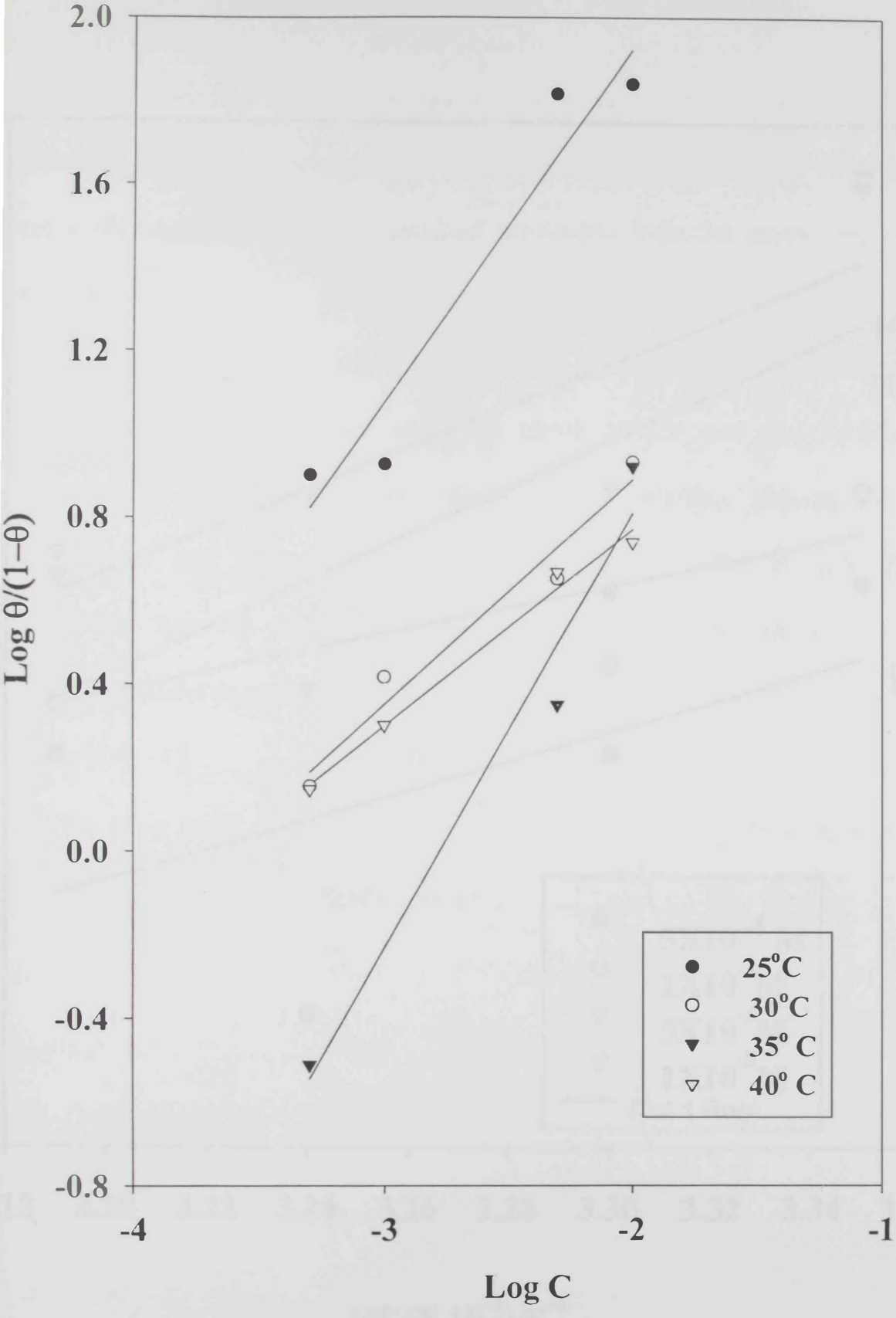

Figure 13. Plot of Log θ/(1–θ) vs. Log C for 316 stainless steel in presence of TCAL in 0.5 M H_2SO_4

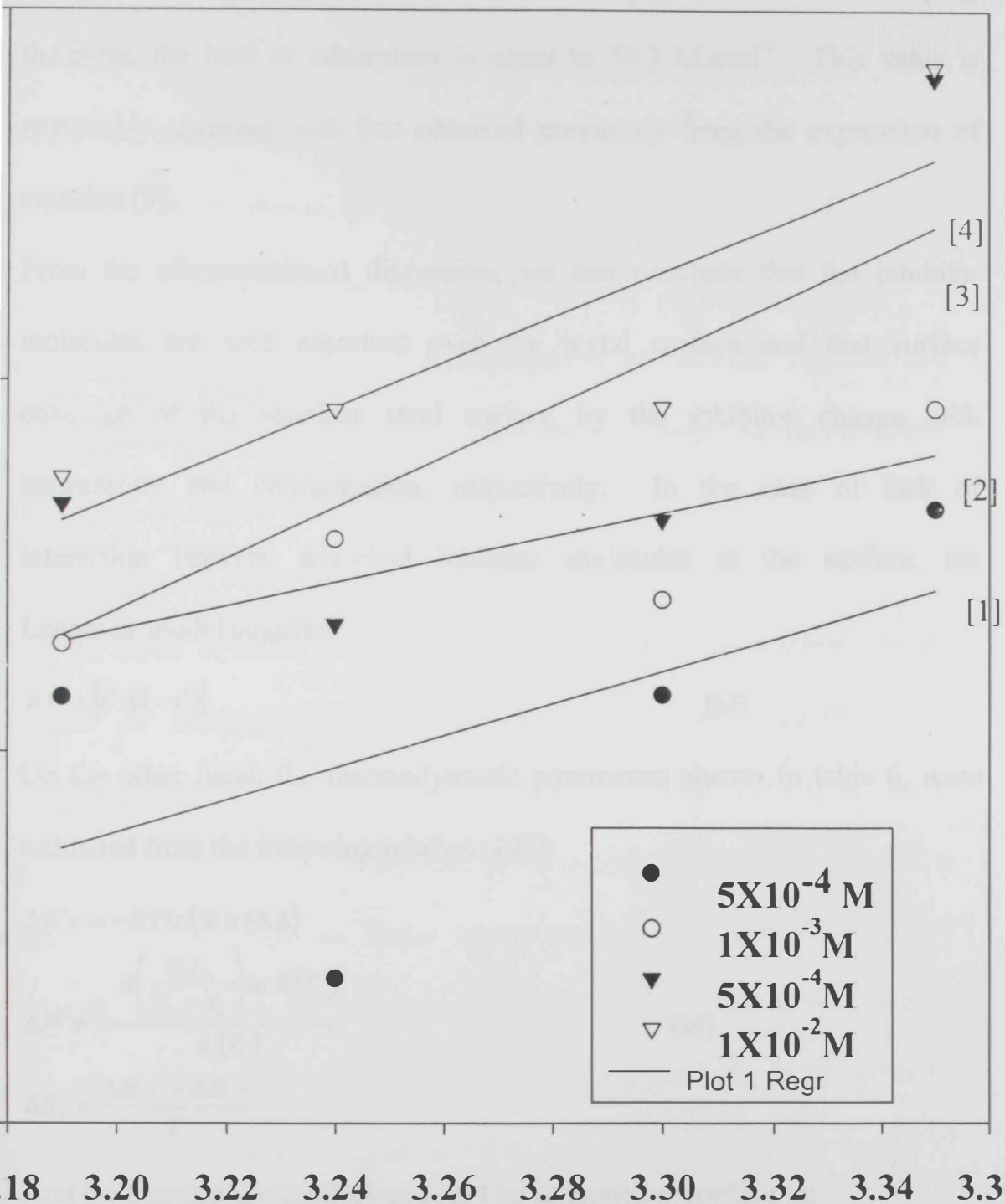

Fig 14: Plots of Log(θ/1-θ) vs. 1/T at different concentratations of 3-Thiophene carboxaldyde (1) 5 X 10^{-4}, (2) 1X 10-3, (3) 5 X 10^{-3}, (4) 1 X 10^{-2} in 0.5 M sulfuric acid

If the E_1 for the uninhibited reaction is equal to 7.64 $kJ.mol^{-1}$ [96], therefore, the heat of adsorption is equal to 59.7 $kJ.mol^{-1}$. This value is reasonably agreeing with that obtained previously from the expression of equation (9).

From the aforementioned discussion, we can conclude that the inhibitor molecules are well adsorbed over the metal surface and that surface coverage of the stainless steel surface by the inhibitor change with temperature and concentration, respectively. In the case of lack of interaction between adsorbed inhibitor molecules at the surface, the Langmuir model suggests:

$$KC = [\theta/(1-\theta)] \qquad (13)$$

On the other hand, the thermodynamic parameters shown in table 6, were estimated from the following relations [91]:

$$\Delta G^{\circ}_{T} = -RT\ln(K \times 55.5)$$

$$\Delta H^{\circ}_{T} = \frac{R\left(\frac{T_1 T_2}{T_2 - T_1}\right)\ln K(T_2)}{K(T_1)} \qquad (14)$$

$$\Delta S_{T} = \frac{\Delta H^{\circ}_{T} - \Delta G^{\circ}_{T}}{T}$$

And the temperature coefficient could be estimated according to:

$$\Delta G^{\circ} = \Delta H^{\circ} - ZFT\left(\frac{dE}{dT}\right) \qquad (15)$$

$$E_{eff} = -2.3 * 8.314 * \frac{d \log i}{d \log \frac{1}{T}} \qquad (15b)$$

As indicated in the values calculated in table 6, the enthalpy of adsorption, $\Delta H°$, entropy of adsorption, $\Delta S°$, and free energy of adsorption, $\Delta G°$, are all negative. The negative value of $\Delta H°$ indicates the adsorption process is exothermic. On the other hand, the magnitude of $\Delta S°$ and $\Delta G°$ indicate that replacement process took place during the adsorption of the inhibitor molecules at the surface of the stainless steel [97].

1- Electochemical Impedance Spectroscopy (EIS)

The corrosion behavior of stainless steel 316, in acidic solution in the presence of 2-thiophene carboxylic acid and 2-acetyl thiophene with different concentrations was investigated by the EIS method at room temperature. The locus of Nyquist plots is regarded as one part of a semicircle. The equivalent circuit model employed for this system is as previously reported in the literature [98] and shown in figure 17. Nyquist plots of stainless steel 316 in inhibited and uninhibited acidic solutions containing various concentrations of TCAL and AcT are shown in figures 17 and 18. As could be noticed the impedance diagrams obtained are not perfect semicircles, and this could be attributed to frequency dispersion as indicated earlier [99]. The equivalent circuit to which the data were fitted is

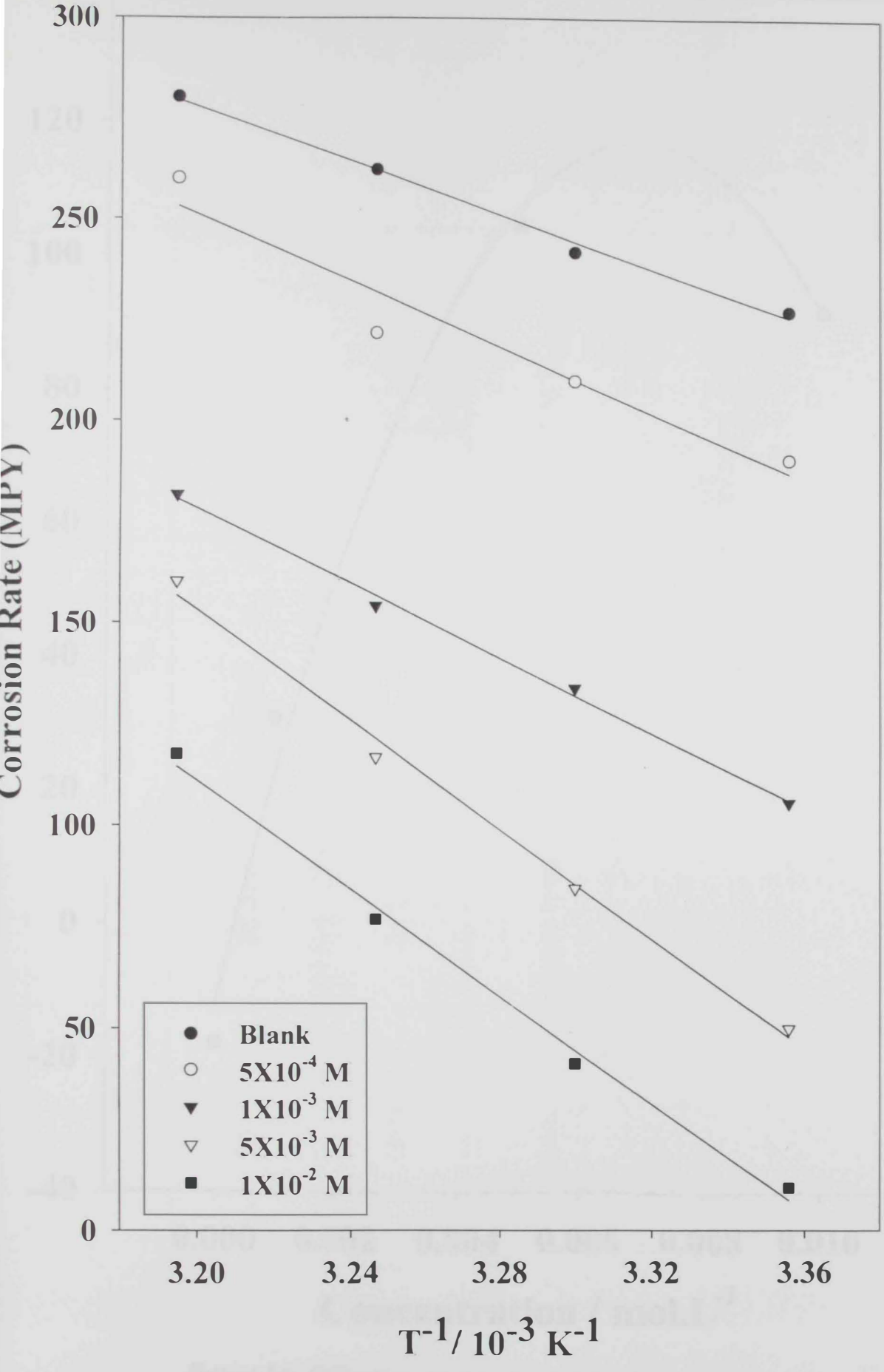

Figure 15. Arrhenius plots of Inhibited Corrrosion Rate for 3-Thiophene carboxaldehyde

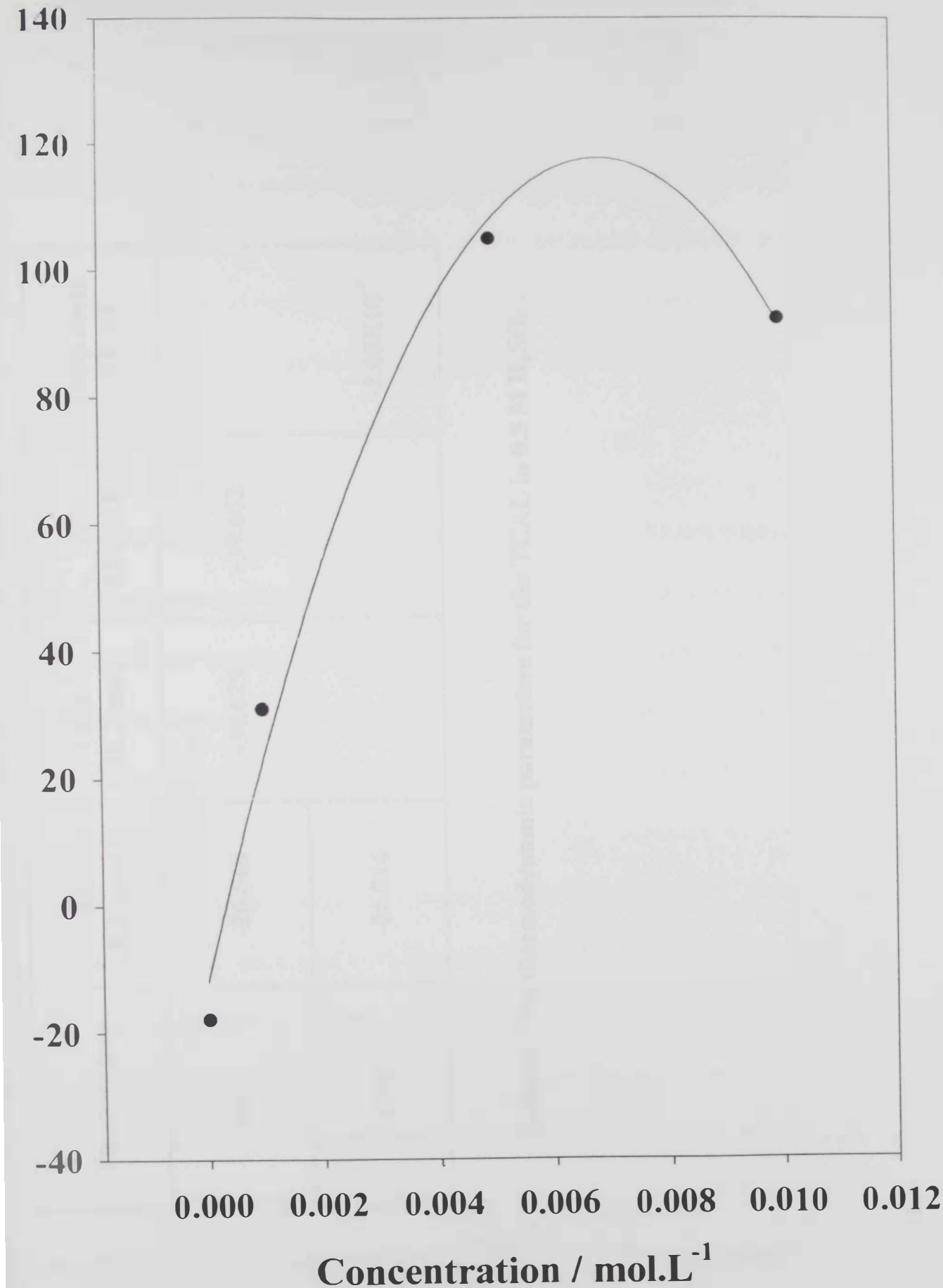

figure 16. Effective energy for inhibition corrosion of stainless steel in 0.5 M H_2SO_4 and TCAL

Tmeperature	ΔG (KJ/moml)	ΔH (KJ/mol)	ΔS (J/mol.K)	Temp.coeff. .dE/dT
30° C	-26.610	-38.625	-39.652	
40°C	-26.214			$-2.05X10^{-7}$

Table 6: The thermodynamic parameters for the TCAL in 0.5 M H_2SO_4 .

nown in figure 19. The charge-transfer resistance, R_t, values could be alculated from the difference in impedance at lower and higher frequencies. o obtain the double layer capacitance (C_{dl}), the frequency at which the naginary component of the impedance is maximum (-Imag max) is found nd C_{dl} values could be calculated from the equation [99]:

$$f(-\mathrm{Imag\ max}) = \frac{1}{2\pi C_{dl} R_t} \qquad (16)$$

could be noticed from the data of figures 19 and 20 that the impedance emicircle size depends on type and concentration of the inhibitor used. The resence of the semicircle in the impedance diagrams indicated that, the orrosion of stainless steel 316 is, controlled by a charge transfer process. ables 7 and 8 depict the impedance parameters obtained by line fitting to ne semicircle. The charge transfer resistance (R_{ct}) increases as the oncentration of the inhibitor increases for the two inhibitors studied. Also, ne double layer (C_{dl}) decreases with increase in the concentration of the nhibitor. This decrease is due to adsorption of inhibitor on the metal urface causing a change of the double layer structure as indicated earlier 100]. When comparing the inhibition efficiencies obtained from testing nethods used in this study, it can be concluded that there is a fair agreement etween the obtained results from EIS and other d.c techniques. Again, it

could be noticed that 2-acetyl thiophene showed higher inhibition efficiency at lower concentrations when compared to 2-thiophene carboxylic that showed relatively higher inhibition efficiency for higher concentrations. In summary, all electrochemical techniques used in this study showed comparable trend in inhibition efficiency and that the formation of stable film through chemical/physical adsorption on stainless steel surface is responsible for the observed corrosion inhibition of the thiophene derivatives studied. It is worthwhile to mention that inhibition efficiency was calculated from EIS measurements as indicated in tables 7 and 8 using the following relation [100]:

$$p = \frac{R_{ct(uninh.)}^{-1} - R_{ct(inh.)}^{-1}}{R_{ct(uninh.)}^{-1}} \times 100 \qquad (17)$$

Where p is the inhibition efficiency, $R_{ct(uninh.)}$ and $R_{ct(inh.)}$ are the charge transfer resistance values without and with inhibitor, respectively. We have followed the progress of R_{ct} and C_{dl} with immersion time and noticed that without the inhibitor, R_{ct} decreases with immersion time, whereas C_{dl} increases. Both R_{ct} and C_{dl} change trend to the opposite direction in presence of inhibitor. Again, we can conclude that the change in R_{ct} and C_{dl} values is due to the gradual replacement of water molecules on the metal surface, decreasing the extent of dissolution reaction.

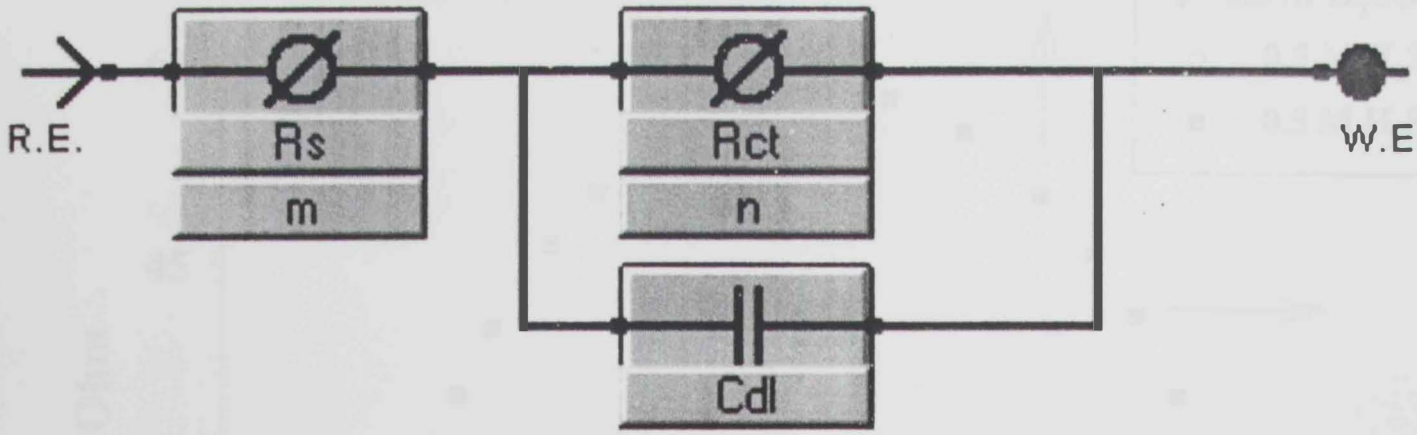

Figure [17] Equivalent Circuit Used in Data Fitting for the Corrosion of SS 316 in 0.5 M Sulfuric Acid in Presence of Thiophene Derivative Inhibitors

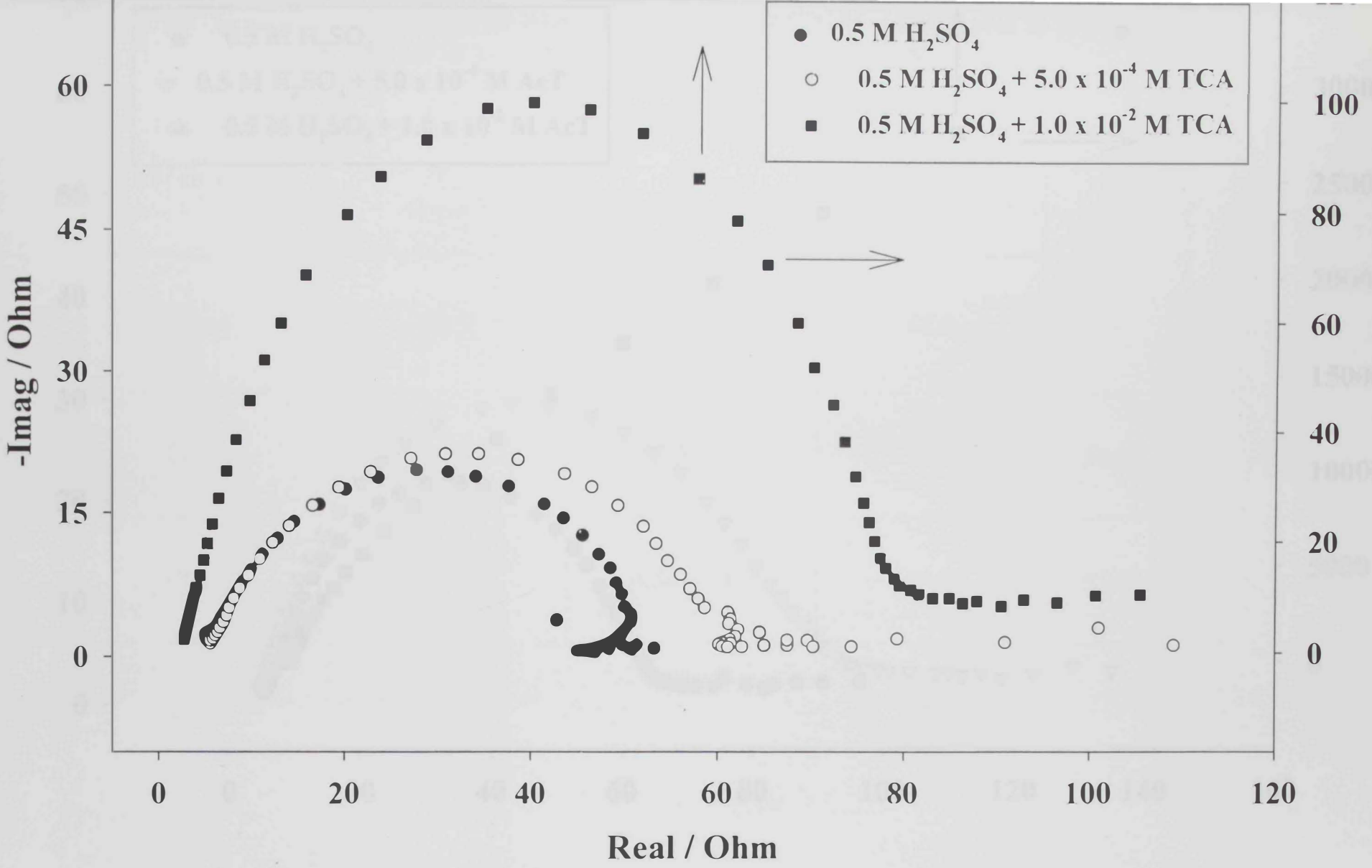

Figure 18 Nyquist Diagrams for Stainless Steel 316 in 0.5 M H_2SO_4 in Different Concentrations of 2-Thiophene Carboxylic Acid

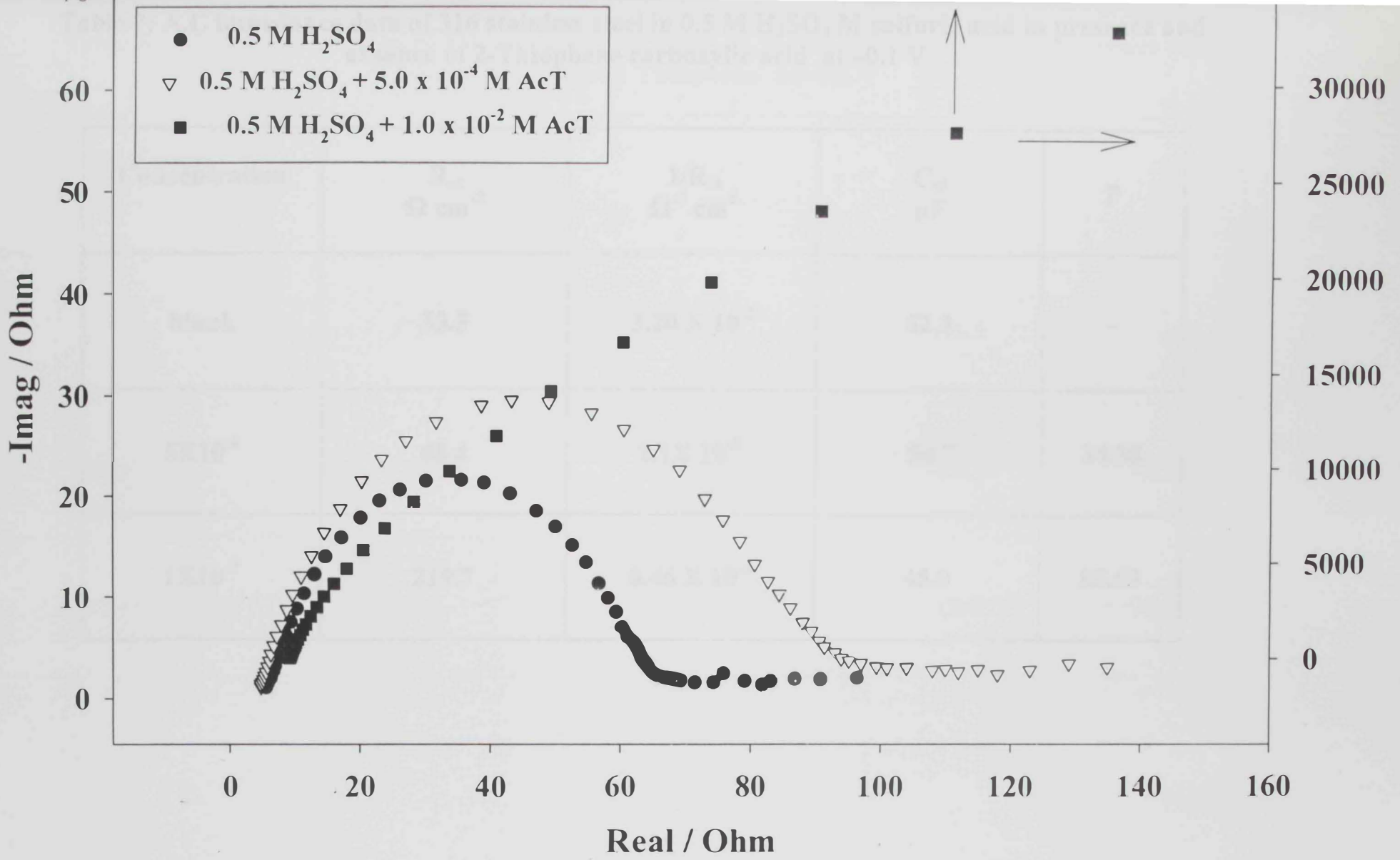

Figure 19. Nyquist Diagrams for Stainless Steel 316 in 0.5 M H_2SO_4 in Different Concentrations of 2-Acetyl Thiophene

Table 7: A.C impedance data of 316 stainless steel in 0.5 M H_2SO_4 M sulfuric acid in presence and absence of 2-Thiophene carboxylic acid at –0.1 V

Concentration	R_{ct} $\Omega\ cm^{-2}$	$1/R_{ct}$ $\Omega^{-1}\ cm^{2}$	C_{dl} μF	P
blank	30.5	3.20×10^{-2}	62.3	-
$5X10^{-4}$	48.4	$2.1X\ 10^{-2}$	54.7	34.38
$1X10^{-2}$	219.7	0.46×10^{-3}	45.0	85.63

Table 8: A.C impedance data of 316 stainless steel in 0.5 M H_2SO_4 M sulfuric acid in presence and absence of 2-Acetyl Thiophene at –0.1 V

Concentration	R_{ct} $\Omega\ cm^{-2}$	$1/R_{ct}$ $\Omega^{-1}\ cm^{2}$	C_{dl} μF	p
blank	52.2	0.0392	58.6	-
$5X10^{-4}$	52.8	0.0189	41.3	51.78
$1X10^{-2}$	102.4	0.00976	18.6	75.08

5- Surface Measurements

5-a Scanning Electron Microscopy

Figure 20 shows the surface features of stainless steel 316 exposed to 0.5 M H_2SO_4 with and without 2-thiophene carboxylic hydrazide for 10 minutes. Figure 20.a shows extensive corrosion in 0.5 M H_2SO_4. Figure 20.b exhibits the effect of 1.0×10^{-3} M 2-thiophene carboxylic hydrazide in 0.5 M H_2SO_4. The specimen surface is nearly intact as even the original polishing scratches are seen after the exposure. Few pits are visible on the specimen surface after exposure to a 0.01 M NaCl-containing 0.5 M H_2SO_4 in absence of inhibitor as shown in figure 20.b. Energy dispersive x-ray analyses (EDAX) were performed on the exposed stainless steel samples. The data are depicted in figures 21a and 21b for a sample exposed to 0.5 M H_2SO_4 and to 0.5 M H_2SO_4 + 1.0×10^{-3} M 2-thiophene carboxylic hydrazide, respectively. Several important observations could be noticed from the data of figure 21:

(i) The general features of the spectra are similar in both cases, where the stainless steel is only exposed to the sulfuric acid solution and that containing the inhibitor.

(ii) The amount of iron, nickel and molybdenum were affected when comparing the two graphs. Thus, the amount of iron,

nickel and molybdenum decreased in case of sample exposed to inhibitor-containing solution, whereas the amount of chromium increases.

(iii) A sulfur peak clearly appeared in the case of sample exposed to the thiophene carboxylic hydrazide sample.

The decrease in the amount of iron, nickel and molybdenum and the increase in the amount of chromium indicated that the dissolution of stainless steel is inhibited. Moreover, the appearance of the sulfur peak could be attributed to the adsorption of 2-thiophene carboxylic hydrazide moiety at the stainless steel surface. This assumption was confirmed by the data obtained from surface reflectance FT-IR measurements.

5-b Surface Reflectance FT-IR

Surface reflectance FT-IR experiments were conducted on specimens that were exposed to 0.5 M H_2SO_4 and compared to stainless steel sheets exposed to 0.5 M H_2SO_4 + 1.0 x 10^{-3} M 2-thiophene carboxylic hydrazide. One important goal for this experiment is to ensure whether the inhibitor adsorbs to the surface of the metal substrate after exposure and thorough washing. Thus, figure 22 shows the data obtained by reflectance from the surface of the stainless steel (displayed in red) and that obtained from a

conventional transmission experiment of the 2-thiophene carboxylic hydrazide (displayed in blue). Region A is characterized by a strong "two-band" signal in the region 3100-3500 cm^{-1} that is characteristic of primary amines stretch [101]. Regions B and C are characteristics of the aromatic C-H stretch and bending bands of the thiophene ring at 1414 cm^{-1} and 1075 cm^{-1}, respectively. A rather weak band appeared at 1660 cm^{-1} that is thought to be due to the carbonyl group in the amide linkage -C=O-NH. At this stage, we can conclude that the inhibitor is adsorbed to the surface of the substrate via the thiophene sulfur electron lone-pair, and those of the oxygen and the nitrogen atoms of the amide link. The presence of a thin oxide layer at the surface of the stainless steel is inevitable as indicated in the SEM micrographs depicted in figures 20.a and 20.b.

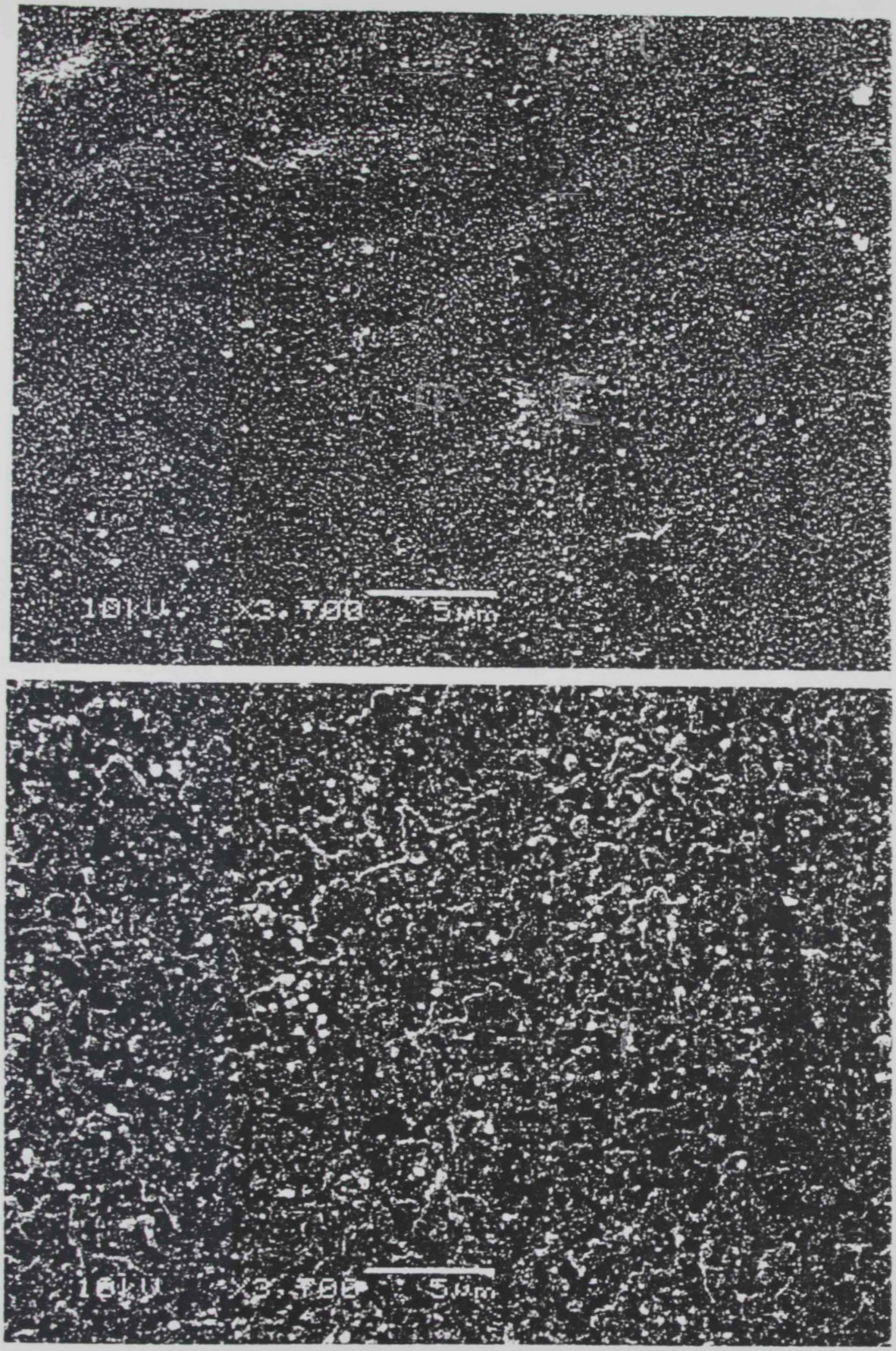

Figure 20.a showes the surfaces of stainless steel 316 exposed to 0.5 M H_2SO_4 with and without TCH

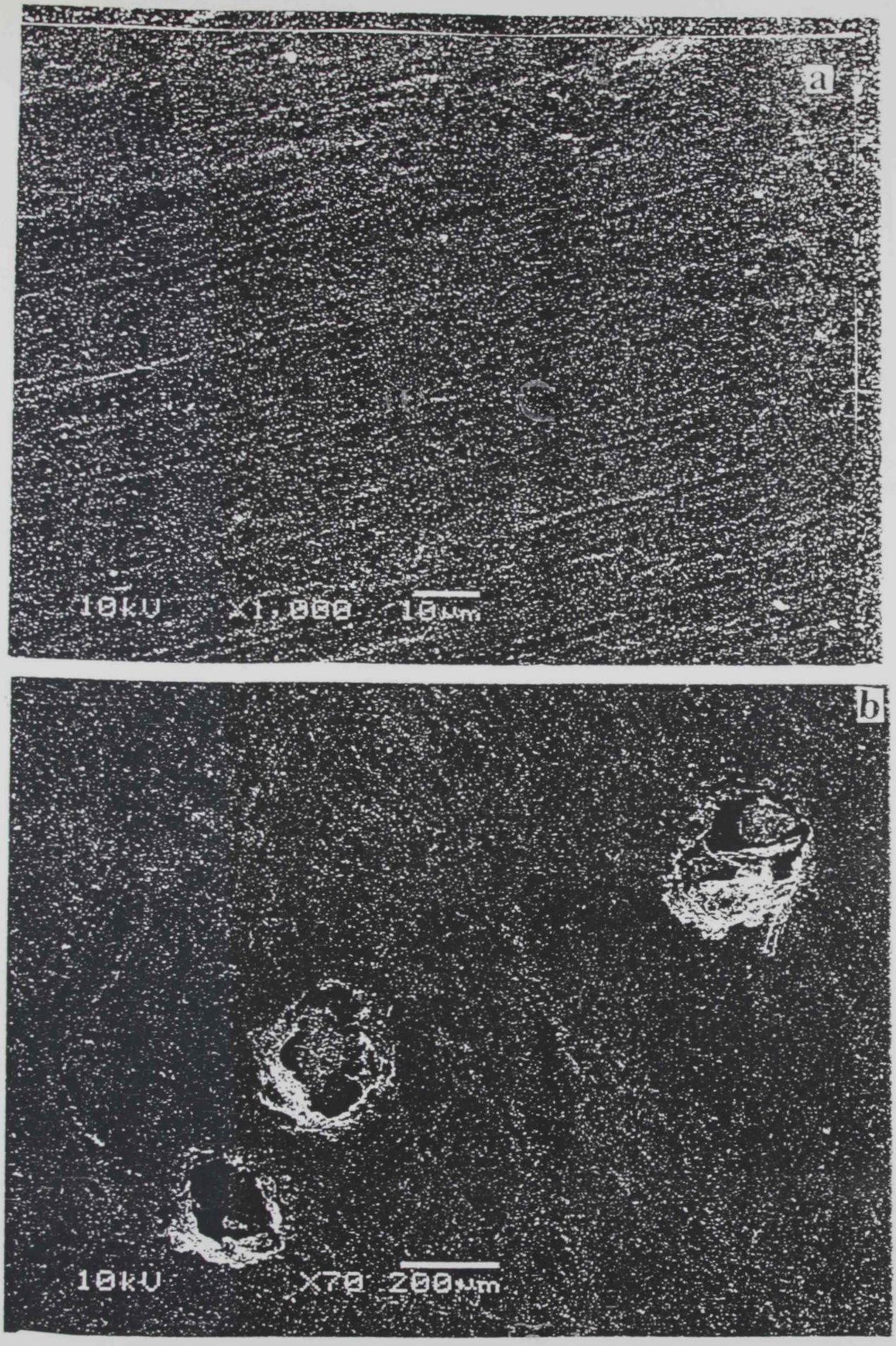

Figure 20.b Surface of stainless steel 316 exposed to 0.1 M H_2SO_4 and TCH in absence (a) and presence (b) of chloride ions

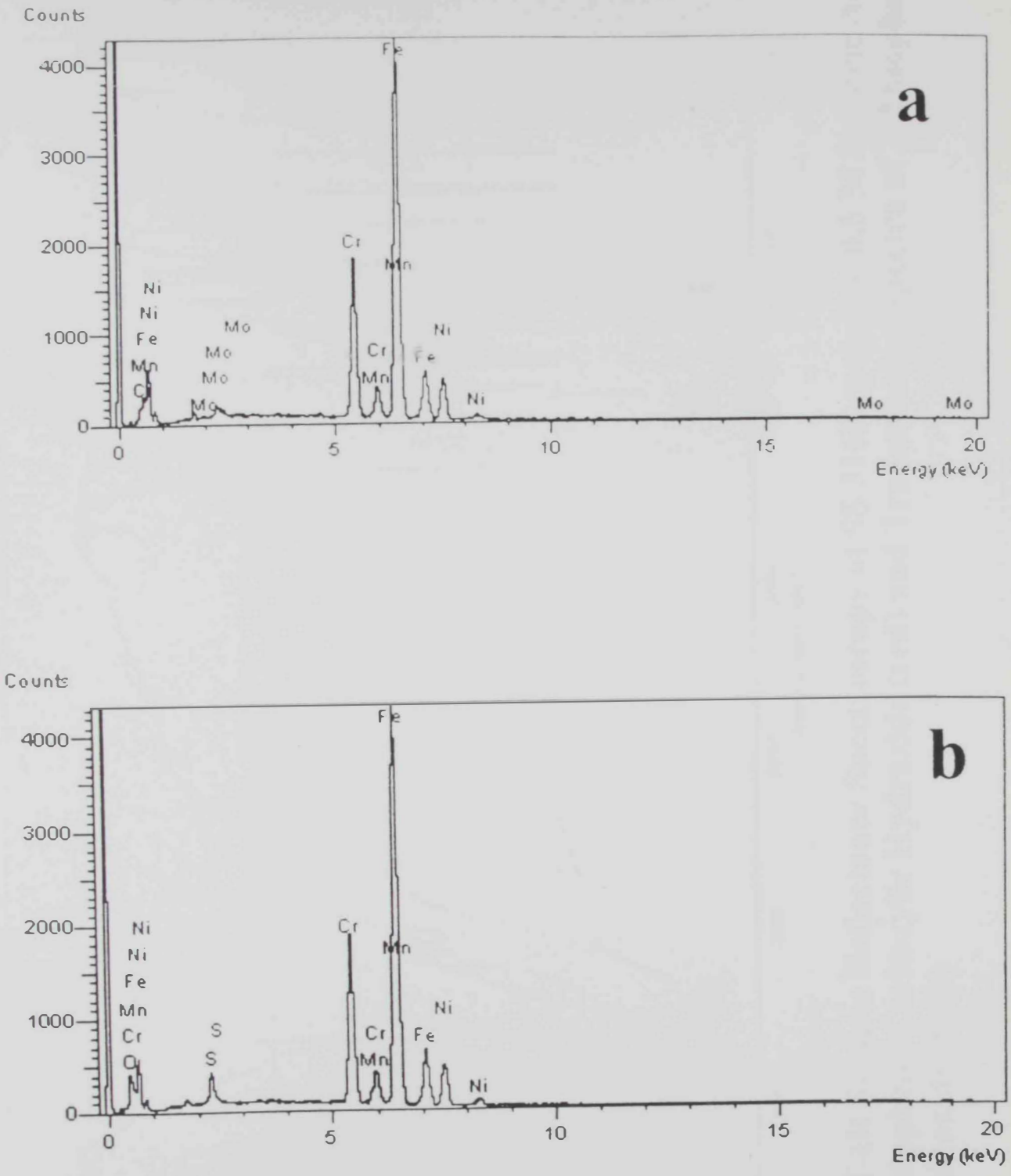

Figure 21. EDAX of SS 316 in 0.5 M sulfuric acid(a) and to 0.5 M sulfuric + 0.001 M 2-thiophene carboxylic hydrazide(b)

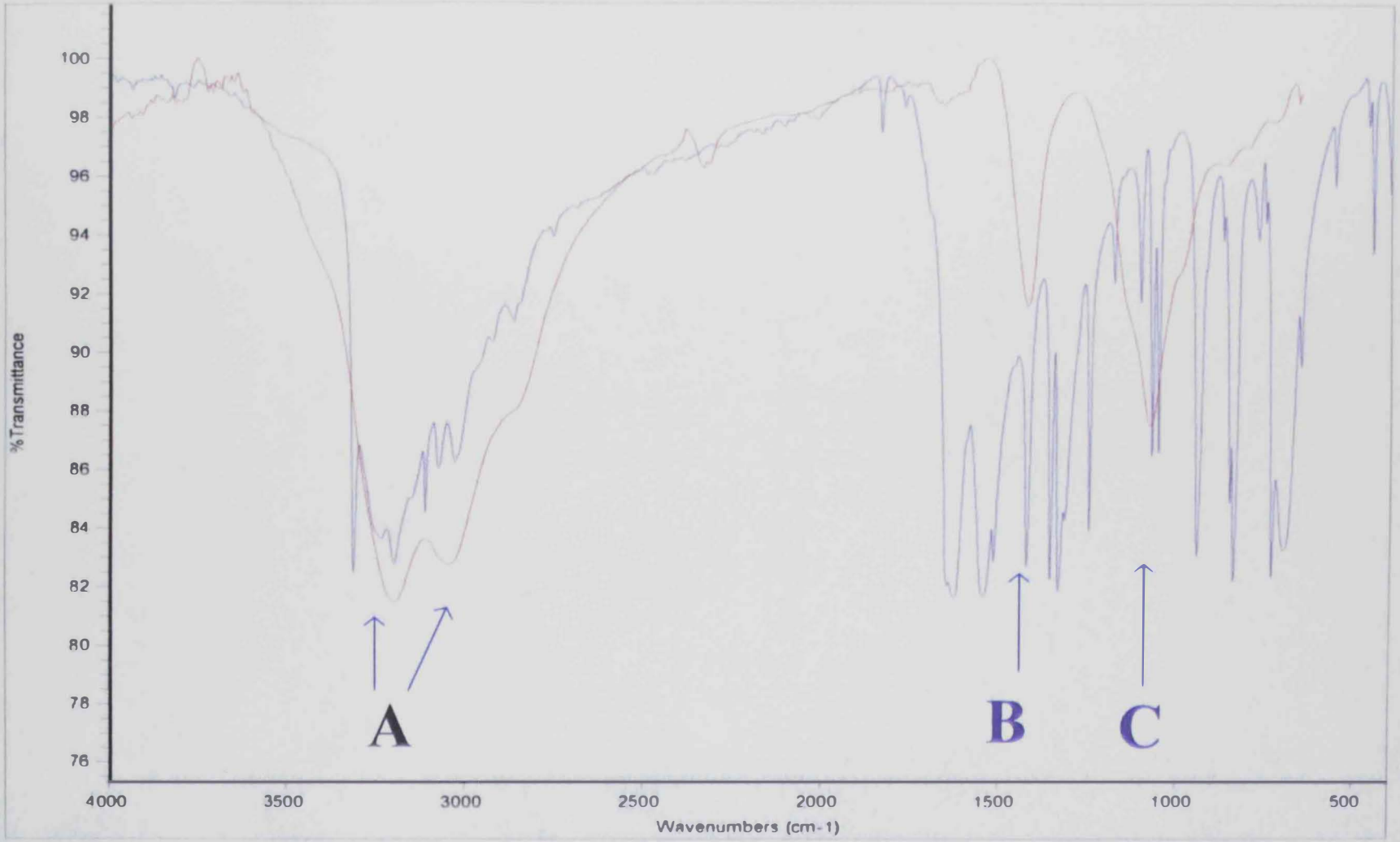

Figure 22 FT-IR Surface Reflectance Spectroscopy at SS 316Exposed to 0.5 M Sulfuric Acid + 0.001 M 2-Thiophene Carboxylic Hydrazide (red) and Transmission Spectra of 2-Thiophene Carboxylic Hydrazide (blue)

CONCLUSIONS

Conclusions

The present work studied the corrosion behavior of stainless steel type 316 in acidic medium. The inhibitory effect and efficiencies of different thiophene derivatives were evaluated on the electrochemical behavior of stainless steel type 316 in acidic medium. The effect of adding chloride to the acid medium was also studied. The inhibitors studied showed distinct inhibition efficiencies depending on the molecular and configurational states of the inhibitor. The inhibitors appeared to be of the mixed type. This conclusion was achieved by comparing the change in the values of the anodic and cathodic Tafel slopes. Inhibition efficiencies of ca. 97% were realized using these inhibitors in 0.5 M H_2SO_4. The presence of chloride ions in the acid medium was found to be detrimental and initiated pitting to the surface of the alloy. The application of thiophene carboxylic hydrazide hindered the formation of pits on the surface of stainless steel. Increasing the concentration of the inhibitor caused a gradual decrease in the rate of corrosion. Opposite effect was observed on rate of corrosion by increasing the concentration of H_2SO_4. The order of increasing the percentage of inhibition efficiency was 2-thiophene carboxylic hydrazide > 2-Thiophene carboxylic acid > 3-thiophene carbxaldhyde > 2-acetyl thiophene. This sequence was explained in terms of the order of stability

of the thiophene derivatives in solution and consequently their tendency to adsorb at the stainless steel surface, the position of the substitution on the ring, and the number and nature of substituent. On the other hand, increasing the temperature resulted in a decrease in the inhibition efficiencies. Heat of adsorption was calculated as –38.625 $kJ.mol^{-1}$ for thiophene carboxaldehyde. The negative values calculated for $\Delta H°$ indicates that the adsorption process is exothermic. Moreover, the magnitudes of $\Delta S°$ and $\Delta G°$ indicate that a replacement process took place during the adsorption of the inhibitor molecules at the surface of the stainless steel.

Surface measurements indicated that the surface of the stainless steel is protected in presence of the inhibitor in aggressive medium. Also, surface reflectance FT-IR indicated that the inhibitor adsorbs effectively at the surface of stainless steel.

REFERENCES

References

1- Dillon, C.P., Corrosion Control in the Chemical Process Industries. McGraw-Hill, New York, NY, **1986.**

2- Streicher, M.A., "Stainless Steels. Past, Present and Future." Proceedings, *Stainless Steels '77*, sponsored by Climax Molybdenum Company and AMAX Nickel, Division of AMAX, Inc., London, England, September 26-27, **1977.**

3- Binder, W.D. and Brown, C.M. *Proc. Am. Soc. Test. Mater.*, Vol. 46, p. 593, **1946.**

4- Sedriks, A. John, "*Corrosion of Stainless Steels*", Corrosion Monograph Series (sponsored by the Electrochemical Society), John Wiley & Sons, Inc. **1996.**

5- Bundy, K.J., "Corrosion and other electrochemical aspects of biomaterials" *Crit. Rev. Biomed. Eng.*, 22, 139, **1994.**

6- C. Wagner; and W. Traud, *Zeit. Electrochem.*, 44, **1938.**

7- Landolt, D. in "Corrosion Mechanisms in Theory and Practice," P. Marcus; and J. Oudar, eds., Marcel Dekker, Inc., New York, **1995.**

8- Stern, M.; and Geary, L. *J. Electrochem. Soc.*, 104, 56, **1957.**

9- Stern, M.; and Weisert, E. D., *Proc. ASTM*, 59, 1280, **1959.**

10- Leidheiser, H. Jr., ed., Corrosion Control by Organic Coatings, NACE, **1981.**

11- Dickie, R.A.; and Floyd, F.L. eds., "Polymeric Materials for Corrosion Control"; American Chemical Society, **1986.**

12- Leidheiser, H. Jr., *"Corrosion Mechanisms"* F. Mansfeld,ed., Marcel Dekker, New York, **1987.**

13- A.J. Kinloch, *"Adhesion 3,"* K.W. Allen, ed., Applied Science, London, **1979.**

14- Feser, R., Ph.D. thesis, University of Clausthal-Zellerfeld, **1990.**

15- Feser ,R. and Stratmann, M., *Werkstoffe Korros.*, 42, 187, **1991.**

16- Leidheiser, H. Wang .Jr., W. and Igetoft, L. , " Mechanism for the cathodic delamination of organic coatings from a metal surface", *Proc. Org. Coat.*, 11, 19, **1983.**

17- Koehler, E.L., *Proc. 4th Int. Congr. On Metallic Corrosion*, p. 736, **1972.**

18- Hammond, J.S. , Holubka, J.W. and Dickie, "Surface analysis of interfacial chemistry in corrosion-induced paint adhession loss" ,R.A., *J. Coat. Technol.*, 51, 45, **1979.**

19- stratmann, M., *Adv. Mater.*, 2, 191, **1990.**

20- Ishida, H. , "Review of recent progress in the studies of molecular and microstructure of coupling agents and their functions in composites, coatings and adhesive joints", *Polym. Compos.*, 5, 101, **1984.**

21- Mittal, ed., "*Silanes and Other Coupling Agents*," VSP, **1992.**

22- Lipkowski and Ross, P. eds., "Adsorption of Molecules at Metal Electrodes," Verlag Chemie, Weinheim, **1992.**

23- Schmitt, " Application of inhibitors for acid media", *Br. Corros. J.*, 9, 165, **1984.**

24- Rozenseld, I. L.,, *corrosion inhibition*, McGraw-Hill, New York, **1981.**

25- Tarvin, M.E. and Miksic, B.A., *Corrosion*, New Orleans, paper no. 344, **1989.**

26- Lorentz, W.J. and Mansfeld, F., International Conference on Corrosion Inhibition, NACE, **1987.**

27- Bockris ,J.O.M. and Swinkels, R.A.J., *J. Electrochem. Soc.*, 111, 736, **1964**.

28- Vetter, K.J. and Schultze, J.W., *J. Electroanal. Chem.*, 121, 67, **1974.**

29- Schultze, J. W. and Koppitz, K.D., *Electrochim. Acta*, 21, 327, **1976**.

30- Hackerman, N. and Hard, R.M., *1st. Int. Congr. Met. Corros.*, Butterworths, London, **1962**.

31- Fujimoto, S. , Yamada, T. and T. Shibata, T., "Improvement of pitting corrosion resistance of type 304 stainless steel by modification of passive film with ultraviolet light irradiation" *J. Electrochem. Soc.*, 145, L79, **1998**.

32- Aballe, A., Bethencourt, M., Botana, F.J., Marcos, M., Perez, J., Rodriguez, M.A., *Rev. Metal. (Madrid)*, 33, 363, 1997.

33- Barkleit, G., Schneider F., and Mummert, K., *Mater. Corros.*, 48, 822, **1997**.

34- Luo, H. , Guan, H., Y.C., and Han, K.N., "Corrosion inhibition of mild steel by Aniline and alkylaminesin acidic solutions" *Corrosion*, 54(9), 721-731, **1997.**

35- Foad El Sherbini,E.E., " Sulphamethoxazole as an effective inhibitor for the corrosion of mild steel in 1.0M HCl solution" , *Mater.Chem.Phys.*, 61, 223-228, **1999**.

36- Ebenso, E.E., Ekpe, U.J., Ita, B.I., Offiong, O.E.,Ibok, U.J.,"Effect of molecular structure on the efficiency of amides and thiosemicarbazones used for corossion inhibition of mild steel in hydrochloric acid" , *Mater.Chem.Phys.*, 60, 79-90, **1999**.

37- Bentiss, F.; Traisnel, M; and Lagrenee, M., " The Substituted 1,3,4-oxadiazoles: a New Class of Corrosion Inhibitors of mild steel in acidic media," *Corros. Sci.*, 42, 127-146, **2000**.

38- Ateya, B. G.; El-Anadouli, B. E.; and El-Nizamy, F. M. A., "Corrosion Inhibition and Adsorption Behavior of Some Thioamides on Mild Steel in Sulfuric Acid," *Bull. Chem. Soc. Jpn.*, 54, 3157-3161, **1981**.

39- Singh, I. , Inhibition of steel corrosion by thiourea , *Corrossion*, 49(6), 473-478,**1993**.

40- Stoyanova, A.E., Soklova, E.I., and Raicheva, S.N., The inibition of mild steel corrosion in 1 M HCl in the presence of linear and cyclic

thiocarbamides-effect of concentration and temperature of the corrosion medium on their protective action, *Corr. Sci.*,39 (9), 1595-1604, **1997**.

41- Ita, B.I., Offiong, O.E. , "Corrosion inhibitory properties of 4-phenylsemicarbazide and semicarbazide on mild steel in hydrochloric acid", *Mater. Chem. Phys*, 59, 179-184, **1999**.

42- Cheng, X. L.; Ma, H. Y.; Chen, S. H.; Yu, R.; Chen, X.; and Yao, Z. M., "Corrosion of Stainless Steel in Acid Solutions with Organic Sulfur-Containing Compounds," *Corros. Sci.*, 41, 321-333, **1999**.

43- Quraishi, M. A.; Wajid Khan, M. A.; Muralidharan, S.; and Venkatakrishna Iyer, S., "Influence of Substituted Benzothiazoles on Corrosion in Acid Solution," *J. Appl. Electrochem.*, 26, 1253-1258, **1996**.

44-Agrawal, R.; and Namboodhiri, T. K. G., "The Inhibition of Sulfuric Acid Corrosion of 410 Stainless Steel by Thiourea," *Corros. Sci.*, 30(1), 37-52, **1990**.

45- Hong, T. and Nagumo, M., "The effect of chloride concentration on early stages of pitting for type 304 stainless steel revealed by the AC impedance method" , *Corr. Sci.*, 39(2), 285-293, **1997**.

46- M.S Mord, "Influence of propargyl alcohol on the corrosion behavior of mild steel in H_3PO_4 solutions", *Mater. Chem. Phys*, 60, 188-195, **1999**.

47- E. E. Foad El sherbini, "Effect of some ethoxylated fatty acids on the corrosion behavior of mild steel in sulphuric acid solution", *Mater. Chem. Phys.*, 60, 286-290, **1990**.

48- Lemaitre, C., *NATO ASI Ser.*, Modelling aqueous corrosion , Ser. E (266), **1994**.

49- Chen, X. ; Zhang, M. ;Xu, Y. , "Corrosion inhibition of sodium dodecyl benzene sulfonate for stainless steel" , *Bejing Haugong Xueyuan Xueboe, Ziran Kexueban*, 21(2) , 75-81 , **1994**.

50- Lemaitre, C.; Baroux, B.; Beranger, G., "Chromate as a pitting corrosion inhibitor: stochastic study", *Werkst. Korros.*, 40(4), 229-236, **1989**.

51- Dhirendra, "Theoritical analysis of the effects of alloying elements on distribution functions of passivity breakdown", *Korrosion*, 18(2), 79-83, **1987**.

52- Crolet, J.L, Bonis, M. R., "Experience in the use of 13 Cr tubing in corrosive CO_2 fields", *SPE. Prod. Eng.*, 1(15), 344-350, **1986**.

53- Makhlouf, M. Th., Wahdan, M.H., "Thermodynamic parameters of synergistic effect of some thiols and halide ions on the acid corrosion of mild steel" , *Pol. J. Chem.*, 69(7) , 1072-1079, **1995**.

54- Wistrom, R.E.; Duquette, D. J., "Comparison of the effect alloyed molybdenum and aqueous molybdate on the pitting resistance of iron-chromium alloys" , *Report from Energy Res. Abstr.*, 11(16), **1986**.

55- Carroll, W. M. ; Howley, M. B., "The influence of temperature, applied potential , buffer and inhibitor addition on the passivation behavior of a commercial grade 316L steels in aqueous halide solutions", *Corr. Sci.*, 30(6/7), 643-655, **1989**.

56- Zhan, G. ; Yuau,X. ; Wei, B.; Qiu,Y. ;Yu,M., "Inhibition study of inhibitor BMAT on the corrosion of stainless steel in hydrochloric acid pickling" , *Nanjing Hauagong Daxue Xuebo*, 17(4), 22-26, **1995**.

57- Lu, Y.C; Ives, M. B., "Electrode reaction inhibition by surface modification and localized corrosion resistance of stainless steels in aqueous solution", *Eur. Fed. Corros.*, 168-172, **1994**.

58- E.A Abd Elmguid ; V.K Gouda; N. A. Mahmoud, "Pitting corrosion behavior of type SUS904L and SUS316L stainless steels in chloride solutions", *Mater. Trans.*, 35(10), 699-702, **1994**.

59- Ohsawa, Shigeki; Meguri, Kazuko; Takedo, Makoto; Saito, Kazue, "Effect of GEDTA acid on corrosion inhibition of stainless steel", *Ibaraki Daigaku Kogakubu Kenku Shusho*, 38, 1-11 , **1990**.

60- Ohashi, K. ; Honda, T. ; Kashimure, E. ; Furutani, Y. , "Effect of dissolved oxygen on corrosion of ferrous materials in high temperature pure water", *Boshoku Gijutsu*, 37(4) ,198-204, **1988**.

61- Newman, R.C.; Shaharabi, T., "The effect of alloyed nitrogen or dissolved nitrate ions on the anodic behavior of austenitic stainless steel in hydrochloric acid", *Corros. Sci.*, 27(8), 827-838, **1987**.

62- Dawson, J. L.; Ferreira, M. G. S., "Crevice corrosion of 316 stainless steel in 3% sodium chloride solution", *Corros. Sci.*, 26(12), 1027-1040, **1986**.

63- Habeed, Hassan S.; Nassior, Huda, Yas, J., Abbas F.; Hammo, Bushra B., "A study on the inhibition efficiency of organic inhibitors in different concentration of sulfuric acid using stainless steel types 316L and 316 MA in the temperature range 25-65 degree.C", *J. Pet. Res.*, 5 (1), 133-142, **1986**.

64- Trabanelli, G., Frinani, A., Zucchi, F., Zucchini, M., "The inhibition of the intergranular corrosion of a sensitized stainless steel in hot acidic solutions", *Z. Phys. Chem.*, 264(4), 813-826, **1983**.

65- Fouda, A. S., "Influence of some thiophene derivatives on the corrosion of iron in nitric acid solution". *I. Indian Chem. Soc.* , 65, 476-478, **1988**.

66- Gomma, G.K, Issa, R.M., ElBaradie, H. Y. , Sokry, H.E., "Adsorption of organic acids on low carbon steel", *I. Indian Chem. Soc.*, 70(1), 131-134, **1993**.

67- Pakhomov, V.S.; Parshin, A. G., "Peculiarities of metal corrosion under heat transfer conditions", *Zashch. Met.*, 27(4), 652-657, **1991**.

68- DeBerry, D.W.; Viehbeck, A., " Inhibition of pitting corrosion of AISI 304L stainless steel by surface active compounds", *Corrsoion (houston)*, 44(5) , 299-305, **1988**.

69- Trabanelli, G.; Frignani, A.; Monticelli,C., "Inhibition of the intergranular corrosion of a sensitized stainless steel in hot, dilute sulfamic acid solutions", *Int. Corros. Conf. Ser.*, NACE-7(Corros. Inhib.), 73-78, **1988**.

70- Trabanelli, G.; Frignani, A; Zucchi, F., "Use of the low strain rate technique for studying stress corrosion cracking inhibition by organic inhibitors", *Corros. Conf. Ser.*, 68-72, **1988**.

71- Koenig, W.; Friedrich, J., "The significance of the anodic coating formation for the electrochemical dissolution", *Ind. Anz*, 111(37), 38-39, 1989.

72- Trabanelli, G; Zucchi, F.; Brunoro, G., "Inhibition of corrosion resistant alloys in hot hydrochloric acid solutions", *Werkst. Korros.*, 39(12), 589-594, **1988.**

73- Marques, Ademir Azevedo, *Braz. Pedido PI.* , 4 pp.

74- Ilies, M.; Supuran, C.T.; Scozzafava, A.; Casini, A.; Mincione, F.; Menabuoni, L.; Caproiu, M.T.; Maganu, M.; and Banciu, M.D., "Carbonic anhydrase inhibitors: Sulfonamides incorporating furan-, thiophene- and pyrrole-carboxamido groups possess strong topical intraocular pressure lowering properties as aqueous suspensions," *Bioorg. & Medicin. Chem.*, 8 (8), 2145-2155, **2000.**

75- Naudin, E.; El Mehdi, N.; Soucy, C.; Breau, L.; and Belanger, D., "Poly(3-arylthiophenes): Synthesis of monomers and spectroscopic and electrochemical characterization of the corresponding polymers," *Chem. Mater.*, 13 (2), 634-642, **2001.**

76- Singh, A.; and Chaudhary, R.S., "Dithizone and thiosemicarbazide as inhibitors of corrosion of type 304 stainless steel in 1.0 M sulphuric acid solution," *Bri. Corr. J.*, 31 (4), 300-304, **1996.**

77- Pourbaix, M., "Lectures on Electrochemical Corrosion," Plenum Press, New York, **1973**, p. 252.

78- Attrens, A.; Baroux, B.; and Mantel, M., "The Secondary Passive Film for Type 304 Stainless Steel in 0.5 M Sulfuric Acid," *J. Electrochem. Soc.*, 144(11), 3697-3704, **1997.**

79- Ammar, I. A.; and El-Khorafi, F., " Adsorbability of thiourea on iron cathods", *Werkst. Korros.*, 702, **1973.**

80- Pillai, K. C.; and Narayan, R., " Inhibitoin of corrosion of iron in acids by thiourea and derivatives ", *J. Electrochem. Soc.*, 125(9), 1393-1397, **1978.**

81- Streitwieser,Jr. A., "Molecular Orbital Theory for Organic Chemists," Wiley, New York, p. 43, **1961.**

82- Hackerman, N.; and Makrides, A. C., *Ind. Eng. Chem.*, 46, 523-....., **1954**.

83- Skotheim, T. A. (ed.), "Handbook of Conducting Polymers," Marcel Dekker, New York, **1986**.

84- Caigman, G. A.; Metcalf, S. K.; and Holt, E. M., "Thiophene Substituted Dihydropyridines," *J. Chem. Cryst.*, 30, 415-422, **2000**.

85- Gibson, D. H.; He, H. Y.; and Mashuta, M. S., "Synthesis and Characterization of Chair and Boat Forms of fac-Re(CO)(3)(P-3)(X)[P-3=eta(2)-CH3C(CH2PPh2)(3), X = Br, Cl]," *Organo-metallics*, 20, 1456-1461, **2001**.

86- Ren, D. X.; and Hubbard, A. T., "Influence of pH on the Packing Density of (4-pyridyl)-Hydroquinone Molecules Adsorbed at a Platinum(111) Thin-Layer Electrode," *J. Coll. Interf. Sc.*, 202, 89-94, **1998**.

87- Mills, P.; Korlann, S.; Bussell, M. E.; Reynolds, M. A.; Ovchinnikov, M. V.; Angelici, R. J.; Stinner, C.; Weber, T.; and Prins, R., "Vibrational Study of Organometallic Complexes with Thiophene Ligands: Models for Adsorbed Thiophene on Hydrodesulfurization Catalysts," *J. Phys. Chem. (A)*, 105, 4418-4429, **2001**.

88- Ammar, I. A.; and Darwish, S., *Corros. Sci.*, 7, 679, **1967**.

89- Fisher, H., "*Ann. Univ. Ferrara, Sez*, 1960, Suppl. No. 3," p.1, **1961**.

90- Bockris, J. O. M.; and Drazis, D., *Electrochim. Act.*, 4, 325, **1961**.

91- Gomma, G. K.; and Wahdan, M. H., "Temperature Coefficient of Corrosion Inhibition of Steel by Adenine," *Bull. Chem. Soc. Jpn.*, 67, 2621-2626, **1994**.

92- Kelly, E. J., *J. Electrochem. Soc.*, 112, 124, **1965**.

93- Juiyuan, Z., "Proc. Int. Congr. Met. Corros.," Madras, India, Abstr., p. 111, **1987**.

94- Devarajan, G.; and Balakrishnan, K., *Bull. Electrochem.*, 3, 213, **1987**.

95- Roy, S. C.; Roy, S. K.; and Sicar, S. C., " Critiqe of inhibition evoluation by polarization measurements" *Br. Corros. J.*, 23, 2, **1988**.

96- Olenl, R. L.; and Ray, H. M., "21st Conference, National Association of Corrosion Engineers," St. Louis, Missouri, March 15-19, **1965**, Abstr., p. 252.

97- Cabello, C. I.; Botto, I. L.; and Thomas, H. J., "Anderson Type Heteropolyoxomolybdates in Catalysis: 1.$(NH_4)_3[CoMo_6O_{24}H_6]$ center Dot $7H_2O$/Gamma-Al_2O_3 as Alternative of Co-Mo/Gamma-Al_2O_3 Hydrotreating Catalysts," *Appl. Cataly. (A)*, 197, 79-86, **2000**.

98- Mansfeld, F.; Kending, M. W.; and Lorenz, W. J.,*J. Electrochem. Soc.*, 132, 290, **1985**.

99- Mansfeld, F.; Kending, M. W.; and Tsai, S., *Corrosion*, 37, 301, **1982**.

100- Szklarska-Smialowska, Z., "Electrochemical and Optical Techniques for the Study of Metallic Corrosion," Kluwer Academic, the Netherlands, p. 545, **1991**.

101- Jones, Jr. M., in "Organic Chemistry," W. W. Norton & Company, New York, pp. 651-656, **2000**.

أظهرت النتائج تباين في تأثير كل من المثبطات المختلفة اعتمادا على الشكل الجزيئي والكثافة الإلكترونية حول ذرة الكبريت في حلقة الثايوفين. معطية الترتيب التالي لكفاءة المثبطات ٣-٢-thiophene carboxylic acid > ٢-thiophene carboxylic hydrazide > ٢-acetyl thiophene > ٢-thiophene carboxaldehyde

يتبع نظام الامتزاز لهذه المثبطات نموذج لانجمير. كما تم حساب معاملات الديناميكا الحراريه، واستنتج ان هذه المثبطات تكون طبقة رقيقه على سطح الفولاذ تحميه من التآكل في الوسط الحمضي من خلال الامتزاز عن طريق ذرة الكبريت ويكون بقية الجزئ غطاء على سطح الفولاذ.

كما برهنت طريقة المسح السطحي الانعكاسي بالاشعة تحت الحمراء على امتزاز هذه المثبطات على سطح الفولاذ المقاوم للصدأ. و أظهرت نتائج الميكروسكوب الالكتروني المسحي أن وجود هذه المثبطات يحمي سطح الفولاذ ضد التآكل في حال وجوده في وسط يحتوي على أيون الكلوريد في حمض الكبريتيك .

-

المـلخـــــــص

يدخل الفولاذ في صناعة السيارات والصناعة الالكترونية وتطبيقات أخرى . ويعتبر عنصري الحديد والكروم من المكونات الرئيسية الداخلة في تكوينه اذ تتراوح نسبتيهما بين60 -75% و 10ـ 25% لكل منهما على التوالي كما توجد بعض العناصر الأخرى بنسب مختلفة كالنيكل ، الكوبالت، الموليبديونم ، المنجنيز والكربون. أحد أهداف هذه الرسالة هو استخدام قياسات كهروكيميائية وسطحية لدراسة سلوك الفولاذ من نوع 316 (نسبة العناصر الداخلة في تركيبه موجودة في جدول (1)) في الوسط الحمضي في وجود و عدم وجود مشتقات مختلفة لمركب الثايوفين. كما توجد أهداف أخرى كدراسة تأثير أيون الكلورايد في الوسط الحمضي على سلوك تآكل الفولاذ وحساب كفاءة المثبطات المستخدمة وتحديد المعامل الحراري وطبيعة الامتزاز لهذه المثبطات على سطح الفولاذ.

تم استخدام طرق كهروكيميائية مختلفة كطريقة تغير الجهد مع الزمن (البوتنشوديناميكا)، وطريقة تافل ومقاومة الاستقطاب لتقييم تأثير المثبطات على تآكل الفولاذ 316.

كما تم استخدام تحاليل سطحيه لمعرفة شكل والتركيب الكيميائي للسطح كجهاز الميكروسكوب الالكتروني للمسح السطحي، وطريقة القياس السطحي الانعكاسي باستخدام الاشعة تحت الحمراء وطريقة القياس التشتتي باستخدام أشعة اكس.

لجـــــنة الإشـــــــراف على الأطروحة

أ.د راشد عبد الرحمن السعيد

أستاذ الكيمياء الفيزيائية

قسم الكيمياء

كلية العلوم

جامعة الإمارات العربية المتحدة

د. أحمد جلال حلمي

أستاذ مساعد في الكيمياء الفيزيائية وكيمياء المواد

قسم الكيمياء

كلية العلوم

جامعة الإمارات العربية المتحدة

تقييم أداء بعض المثبطات العضوية لتآكل الفولاذ غير القابل للصدأ باستخدام طرق كهروكيميائية وسطحية مختلفة

أطروحة مقدمة إلى

عمادة الدراسات العليا
جامعة الإمارات العربية المتحدة

مريم حسن سعيد الحسن

لمتطلبات الحصول على درجة الماجستير

في

علوم وهندسة المواد

٢٠٠١